Climate Summary Report

Tribe:
Nez Perce Tribe

Area of Interest:
Indian Claims Commission
Territory

Annual Average Temperature

Average daily temperature from
January to December.

Emissions	Time	Value	Change
Historical	1990	42.6 °F	
Low	2010-2039	45.2+/-0.7 °F	+2.5 °F
Low	2040-2069	47.2+/-1.2 °F	+4.5 °F
Low	2070-2099	48.2+/-1.4 °F	+5.6 °F
High	2010-2039	45.5+/-0.7 °F	+2.9 °F
High	2040-2069	48.7+/-1.4 °F	+6.1 °F
High	2070-2099	52.3+/-2.0 °F	+9.7 °F

Data Source: MACAv2-METDATA

Jun.-Aug. Maximum Temperature

Average daily maximum temperature from June to August.

Emissions	Time	Value	Change
Historical	1990	75.1 °F	
Low	2010-2039	78.3+/-0.9 °F	+3.1 °F
Low	2040-2069	80.7+/-1.5 °F	+5.5 °F
Low	2070-2099	81.9+/-1.7 °F	+6.8 °F
High	2010-2039	78.7+/-0.9 °F	+3.6 °F
High	2040-2069	82.7+/-1.8 °F	+7.6 °F
High	2070-2099	87.2+/-2.6 °F	+12.1 °F

Data Source: MACAv2-METDATA

Warm Days (above 86°F (30°C))

Average number of days each year in which the daily maximum temperature is above 86°F (30°C).

Emissions	Time	Value	Change
Historical	1990	16.6 days	
Low	2010-2039	26.9+/-2.8 days	+10.2 days
Low	2040-2069	36.3+/-5.5 days	+19.7 days
Low	2070-2099	42.4+/-6.7 days	+25.7 days
High	2010-2039	28.6+/-2.8 days	+11.9 days
High	2040-2069	45.0+/-6.8 days	+28.3 days
High	2070-2099	66.1+/-10.8 days	+49.5 days

Data Source: MACAv2-METDATA

Freeze Free Days

Average number of days each year when the minimum daily temperature remains above freezing at 32°F (0°C).

Emissions	Time	Value	Change
Historical	1990	175.2 days	
Low	2010-2039	198.7+/-7.6 days	+23.5 days
Low	2040-2069	216.6+/-13.0 days	+41.4 days
Low	2070-2099	227.6+/-16.0 days	+52.4 days
High	2010-2039	201.6+/-8.4 days	+26.4 days
High	2040-2069	230.5+/-15.5 days	+55.3 days
High	2070-2099	262.8+/-18.6 days	+87.6 days

Data Source: MACAv2-METDATA

Annual Precipitation

Total precipitation from January to December.

Emissions	Time	Value	Change
Historical	1990	34.1 in	
Low	2010-2039	35.4+/-1.3 in	+1.3 in
Low	2040-2069	35.5+/-1.1 in	+1.4 in
Low	2070-2099	36.0+/-1.6 in	+1.9 in
High	2010-2039	34.9+/-1.1 in	+0.7 in
High	2040-2069	35.9+/-1.6 in	+1.8 in
High	2070-2099	37.1+/-1.9 in	+3.0 in

Data Source: MACAv2-METDATA

Oct.-Mar. Precipitation

Total precipitation from October to March.

Emissions	Time	Value	Change
Historical	1990	20.9 in	
Low	2010-2039	21.8+/-0.7 in	+0.9 in
Low	2040-2069	22.1+/-0.8 in	+1.2 in
Low	2070-2099	22.4+/-1.0 in	+1.5 in
High	2010-2039	21.5+/-0.9 in	+0.5 in
High	2040-2069	22.3+/-1.0 in	+1.4 in
High	2070-2099	23.6+/-1.0 in	+2.7 in

Data Source: MACAv2-METDATA

Apr.-Sept. Precipitation

Total precipitation from April to September.

Emissions	Time	Value	Change
Historical	1990	13.2 in	
Low	2010-2039	13.5+/-0.8 in	+0.3 in
Low	2040-2069	13.4+/-0.9 in	+0.2 in
Low	2070-2099	13.6+/-1.1 in	+0.4 in
High	2010-2039	13.4+/-0.6 in	+0.2 in
High	2040-2069	13.6+/-1.1 in	+0.4 in
High	2070-2099	13.5+/-1.4 in	+0.3 in

Data Source: MACAv2-METDATA

Apr. 1st Snow

	Amount of water contained in the snowpack on April 1st.

Emissions	Time	Value	Change
Historical	1990	13.6 in	
Low	2010-2039	12.0+/-0.8 in	-1.6 in
Low	2040-2069	10.6+/-0.7 in	-3.0 in
Low	2070-2099	9.4+/-1.1 in	-4.2 in
High	2010-2039	12.0+/-0.8 in	-1.7 in
High	2040-2069	9.6+/-1.4 in	-4.0 in
High	2070-2099	6.1+/-1.6 in	-7.5 in

Data Source: VIC-MACAv2-LIVNEH

May 1st Snow

	Amount of water contained in the snowpack on May 1st.

Emissions	Time	Value	Change
Historical	1990	11.5 in	
Low	2010-2039	9.1+/-1.0 in	-2.4 in
Low	2040-2069	7.5+/-0.7 in	-4.0 in
Low	2070-2099	5.8+/-1.1 in	-5.7 in
High	2010-2039	9.0+/-0.9 in	-2.5 in
High	2040-2069	6.2+/-1.2 in	-5.3 in
High	2070-2099	3.0+/-1.0 in	-8.5 in

Data Source: VIC-MACAv2-LIVNEH

Jul.-Sept. Soil Moisture

Average amount of water contained in the upper meters of soil from July to September.

Emissions	Time	Value	Change
Historical	1990	20.7 in	
Low	2010-2039	19.4+/-0.4 in	-1.3 in
Low	2040-2069	18.7+/-0.5 in	-2.0 in
Low	2070-2099	18.4+/-0.7 in	-2.3 in
High	2010-2039	19.5+/-0.5 in	-1.2 in
High	2040-2069	18.2+/-0.7 in	-2.6 in
High	2070-2099	17.1+/-1.1 in	-3.6 in

Heat Accumulation (above 32°F (0°C))

Measure of the heat accumulation in plants, calculated as the annual daily sum of degrees in which the average daily temperature exceeds 32°F (0°C), an important temperature threshold for species in achieving different phases in their life cycles. This metric is also called the cumulative degree days.

Emissions	Time	Value	Change
Historical	1990	4750.4 GDD (°F)	
Low	2010-2039	5450.9+/-190.0 GDD (°F)	+700.5 GDD (°F)
Low	2040-2069	6017.4+/-361.4 GDD (°F)	+1267.0 GDD (°F)
Low	2070-2099	6354.4+/-442.5 GDD (°F)	+1604.0 GDD (°F)
High	2010-2039	5544.3+/-196.3 GDD (°F)	+793.9 GDD (°F)
High	2040-2069	6492.4+/-436.4 GDD (°F)	+1741.9 GDD (°F)
High	2070-2099	7649.1+/-667.4 GDD (°F)	+2898.7 GDD (°F)

Heat Accumulation (above 40°F (3°C))

Measure of the heat accumulation in plants, calculated as the annual daily sum of degrees in which the average daily temperature exceeds 40°F (3°C), an important temperature threshold for species in achieving different phases in their life cycles. This metric is also called the cumulative degree days.

Emissions	Time	Value	Change
Historical	1990	3456.2 GDD (°F)	
Low	2010-2039	4052.2+/-164.1 GDD (°F)	+596.0 GDD(°F)
Low	2040-2069	4538.0+/-315.2 GDD (°F)	+1081.7 GDD(°F)
Low	2070-2099	4829.0+/-382.5 GDD (°F)	+1372.8 GDD(°F)
High	2010-2039	4132.4+/-167.7 GDD (°F)	+676.1 GDD(°F)
High	2040-2069	4956.6+/-382.4 GDD (°F)	+1500.4 GDD(°F)
High	2070-2099	5978.7+/-604.1 GDD (°F)	+2522.5 GDD(°F)

Data Source: MACAv2-METDATA

Heat Accumulation (above 45°F (5°C))

Measure of the heat accumulation in plants, calculated as the annual daily sum of degrees in which the average daily temperature exceeds 45°F (5°C), an important temperature threshold for species in achieving different phases in their life cycles. This metric is also called the cumulative degree days.

Emissions	Time	Value	Change
Historical	1990	2726.8 GDD (°F)	
Low	2010-2039	3255.2+/-146.8 GDD (°F)	+528.4 GDD(°F)
Low	2040-2069	3689.1+/-282.8 GDD (°F)	+962.3 GDD(°F)
Low	2070-2099	3947.7+/-340.7 GDD (°F)	+1220.9 GDD(°F)
High	2010-2039	3327.6+/-149.4 GDD (°F)	+600.8 GDD(°F)
High	2040-2069	4068.5+/-343.6 GDD (°F)	+1341.7 GDD(°F)
High	2070-2099	4993.4+/-553.0 GDD (°F)	+2266.6 GDD(°F)

Data Source: MACAv2-METDATA

Heat Accumulation (above 50°F (10°C))

Measure of the heat accumulation in plants, calculated as the annual daily sum of degrees in which the average daily temperature exceeds 50°F (10°C), an important temperature threshold for species in achieving different phases in their life cycles. This metric is also called the cumulative degree days.

Emissions	Time	Value	Change
Historical	1990	1321.4 GDD (°F)	
Low	2010-2039	1694.6+/-109.0 GDD (°F)	+373.1 GDD(°F)
Low	2040-2069	2010.3+/-209.9 GDD (°F)	+688.9 GDD(°F)
Low	2070-2099	2196.3+/-250.2 GDD (°F)	+874.9 GDD(°F)
High	2010-2039	1749.1+/-109.2 GDD (°F)	+427.6 GDD(°F)
High	2040-2069	2298.9+/-256.0 GDD (°F)	+977.4 GDD(°F)
High	2070-2099	3003.7+/-430.5 GDD (°F)	+1682.2 GDD(°F)

Data Source: MACAv2-METDATA

Growing Season Length

Average number of consecutive days each year when the minimum daily temperature remains above freezing at 32°F (0°C).

Emissions	Time	Value	Change
Historical	1990	95.2 days	
Low	2010-2039	120.4+/-9.6 days	+25.2 days
Low	2040-2069	138.8+/-16.1 days	+43.6 days
Low	2070-2099	140.6+/-18.2 days	+45.4 days
High	2010-2039	124.0+/-10.8 days	+28.8 days
High	2040-2069	152.2+/-18.3 days	+57.0 days
High	2070-2099	175.3+/-22.5 days	+80.1 days

Data Source: MACAv2-METDATA

Data Sources:

MACAv2-METDATA: MACAv2-METDATA: downscaled climate data from CMIP5 bias corrected to climate observations from METDATA dataset.

VIC-MACAv2-LIVNEH: VIC-MACAv2-LIVNEH: modeled hydrology data using the VIC hydrology model forced with climate data from MACAv2-LIVNEH bias corrected to climate observations from LIVNEH dataset.

IN THE MATTER OF APPLICATION)	
FOR PERMIT 77-14378 AND)	
APPLICATIONS FOR TRANSFER)	**PRELIMINARY ORDER**
85396, 85397, AND 85398, AND)	**APPROVING APPLICATIONS**
APPLICATION FOR EXCHANGE)	
85538 IN THE NAME OF PERPETUA)	
<u>RESOURCES IDAHO, INC.</u>)	

BACKGROUND

On October 8, 2021, Perpetua Resources Idaho, Inc. ("Perpetua") filed Application for Permit 77-14378 and Applications for Transfer 85396, 85397, and 85398 with the Idaho Department of Water Resources ("Department"). On November 15, 2021, Perpetua filed Application for Exchange 85538 and an amendment for Application 85398 with the Department. On November 18, 2021, Perpetua filed an amendment for Application 77-14378. USDA Forest Service ("USFS"), Nez Perce Tribe ("NP Tribe"), Save the South Fork Salmon, Inc. ("SSFS"), and Idaho Conservation League ("ICL") filed separate protests against all five applications.

On August 19, 2022, the hearing officer for the Department issued an *Interlocutory Order Deciding Questions of Law* ("Interlocutory Order") specific to Application 77-14378. The Interlocutory Order rejected one of the water sources proposed on Application 77-14378 but did not change the quantity of water sought or the other water sources described in the application.

On March 1, 2023, Perpetua and the USFS filed a *Stipulation and Joint Motion to Approve Settlement and Dismiss Protest* ("Stipulation"). The Stipulation set forth the terms and conditions that would resolve the protests filed by the USFS and asked the hearing officer to issue an order approving the settlement and confirming that certain water right conditions would be included on any approvals issued by the Department. On April 17, 2023, the hearing officer issued an *Order Approving Settlement and Confirming Withdrawal of Protests*.

Pursuant to Rule 555 of the Department's Rules of Procedure (IDAPA 37.01.01), the Department consolidated Applications 77-14378, 85396, 85397, 85398, and 85538 with Applications for Permit 77-14377 and 77-14379 and Application for Transfer 85399 for hearing. The Department conducted an administrative hearing for these consolidated cases on December 11-15, 2023, in Boise. Perpetua was represented by attorneys Elijah Watkins and Wade Foster, NP Tribe was represented by attorneys Michael Lopez and Amanda Rogerson, and SSFS and ICL were represented by attorney Julia Thrower.

Exhibits 1a through 1h, 4, 5, 22, 23 (limited to pages 1-40 and 60-65), 25b, 26 (limited to pages 1-36 and 80-185), 27a, 29, 34, 46, 47, 58, 59, 60, 61, 63, 64, and 68 offered by Perpetua; Exhibits 201, 206, 238, 259, 260, 261, and 262 offered by NP Tribe; Exhibit 318 offered by

SSFS; and Exhibits 72 and 219A designated by the hearing officer through official notice were admitted into the record. Exhibits 18, 52, and 71 offered by Perpetua; and Exhibits 246, 277, 281, and 283 offered by NP Tribe were excluded from the record.

Perpetua called Alan Haslam, Terry Scanlan, Dan Stanaway, Gene Bosley, Doug Durbin, Paul Leonard, and Rob Richardson; ICL called John Robison; SSFS called Fred Coriell; and NP Tribe called Wes Keller, Betsy Semmens, Kendra Kaiser, and Ryan Kinzer as witnesses. Ted McManus, Kyle Smith, Rich Wensel, Dan Ostermiller, Zak Sears, Gary Brown, Michael Gibson, and Nick Kunath testified as public witnesses. Consistent with Rule 651 of the Department's Rules of Procedure (IDAPA 37.01.01), after the hearing the parties used a private company, K & K Reporting, to prepare a transcript of the hearing.

The hearing officer allowed the parties to file post-hearing briefs. On January 31, 2024, Perpetua filed *Perpetua Resources Idaho, Inc.'s Post Hearing Brief* ("Perpetua Brief") and NP Tribe, SSFS and ICL filed *Protestants' Joint Post-Hearing Brief* ("Protestants' Brief").

After carefully considering the evidence in the administrative record and the arguments made by the parties, the hearing officer finds, concludes, and orders as follows:

FINDINGS OF FACT

1.   Perpetua proposes to develop a mining project, known as the Stibnite Gold Project ("SGP"), in Valley County. Ex. 22 at 10.[1] Perpetua proposes to extract gold, silver, and antimony at the SGP. *Id.*

2.   The project site includes private land owned by Perpetua and land that is held by the USFS. Ex. 22 at 16. Perpetua is currently seeking an approved plan of operations from the USFS. Ex. 22.

3.   Perpetua projects that it will take approximately three years to construct the infrastructure and facilities needed to commence mining. Ex. 29 at 68; Ex. 22 at 36. Active mining will last approximately twelve years, followed by three years of additional ore processing. *Id.* The SGP will be comprised of three open pit mines, a mill site, various industrial buildings, a worker housing facility, and a tailings storage facility ("TSF"). Ex. 22.

4.   The open pit mining areas will include two existing pits, the Yellow Pine Pit and the West End Pit, which are remnants of previous mining activities at the site, and one new open pit, the Hangar Flats Pit. Ex. 22 at 36-37. Ore mined at the open pits will be hauled to the proposed on-site ore processing facility or stored at the SGP in stockpiles. *Id.* at 38-39. In addition to ore mined at the open pits, Perpetua will reprocess legacy tailings from past mining activities at the SGP site. *Id.* at 41-42. Tailings from the ore processing facility will be pumped in a slurry to the TSF for permanent storage. Ex. 27a at 31-32.

---

[1] All references to page numbers in this order indicate the page of the exhibit pdf not necessarily the page number shown on the document.

5.   In Application 77-14378, Perpetua proposes to divert up to 9.60 cubic feet per second ("cfs") from ground water wells or from the East Fork of the South Fork Salmon River ("EFSFSR"). Ex. 1g at 1.

6.   The proposed point of diversion from the EFSFSR is a pump station ("River Pump") to be constructed in the NESE of Section 3, T18N, R09E. Ex. 1g at 13-15.

7.   The proposed points of diversion from ground water include thirteen industrial supply wells, thirty-seven dewatering wells, three diversions of ground water from open pits, and two diversions of ground water through underground drains. Ex. 1g at 13-15. These ground water points of diversion are located within Sections 2, 3, 11, 14, 15, and 22, T18N, R09E. *Id.*

8.   The proposed industrial place of use in Application 77-14378 is the industrial and mining areas of the SGP ("industrial/mining POU") and encompasses portions of Sections 2, 3, 10, 11, 14, 15, 16, 17, 20, 21, 22, and 28, T18N, R09E, and Sections 34 and 35, T19N, R09E. Ex. 1g at 14.

9.   In Application 85396, Perpetua proposes to change the point of diversion and place of use for water right 77-7122. Ex. 1a at 7.

10.   Water right 77-7122 bears a priority date of April 16, 1981, and authorizes the diversion of 0.33 cfs and 7.1 acre-feet per year from the EFSFSR for mining storage. Ex. 1a at 10.

11.   The proposed point of diversion for Application 85396 is the River Pump. Ex. 1a at 2-6, 13. The proposed place of use for mining storage is the TSF. *Id.* The TSF will serve as a reservoir and a storage facility for processed mining tailings. Ex. 27a at 31-32. Water stored in the TSF will be used for industrial and mining purposes throughout the SGP area. *Id.* The proposed place of use for mining from storage is the industrial/mining POU. Ex. 1a.

12.   In Application 85397, Perpetua proposes to change the point of diversion and place of use for and add points of diversion to water right 77-7285. Ex. 1c at 2.

13.   Water right 77-7285 bears a priority date of November 7, 1988, and authorizes the diversion of 0.50 cfs and 30.2 acre-feet per year from ground water for mining. Ex. 1c at 11. 9.0 acre-feet of the 30.2 acre-feet authorized under the right may be diverted for mining storage. *Id.*

14.   The proposed points of diversion for Application 85397 are the thirteen industrial supply wells described in Application 77-14378. Ex. 1c at 8. These wells will be located in Section 15, T18N, R09E. *Id.* The proposed place of use for mining storage is two contact water detention ponds in Section 15, T18N, R09E. *Id.* at 14. The proposed place of use for mining and mining from storage is the industrial/mining POU. *Id.*

15.   In Application 85398, Perpetua proposes to change the place of use for water right 77-7293. Ex. 1e at 2.

16.   Water right 77-7293 bears a priority date of April 19, 1989, and authorizes the diversion of 0.25 cfs and 20 acre-feet per year from an Unnamed Stream (known locally as Hennessey Creek) for mining use. Ex. 1e at 10.

17.   The proposed place of use for Application 85398 is the industrial/mining POU. Ex. 1e at 13.

18.   In Application 85538, Perpetua proposes to change the point of diversion for water right 77-7293 from Hennessey Creek to the EFSFSR, at a location upstream of the confluence of Hennessey Creek and the EFSFSR. Ex. 1d at 4. Application 85538 is an application for exchange because the proposed point of diversion is upstream of the confluence.

19.   The proposed point of diversion for Application 85538 is the River Pump and is located approximately 2,000 feet upstream of the confluence of Hennessey Creek and the EFSFSR. Ex. 1d at 4.

20.   Currently, Hennessey Creek is diverted around the Yellow Pine Pit and injected into the EFSFSR near the confluence of EFSFSR and Sugar Creek. *See* Ex. 25b at 85 (map depicting current streamflow path of Hennessey Creek).

21.   During the period when the Yellow Pine Pit is actively mined, Perpetua will pipe Hennessey Creek around the mining area and will inject the water into the EFSFSR upstream of the River Pump. Ex. 22 at 63; Ex. 25b at 18-35. After the Yellow Pine Pit area is reclaimed, Hennessey Creek will flow into the EFSFSR near its historic confluence with the EFSFSR. *Id.*

22.   The following table summarizes Perpetua's industrial and mining applications:

Application	Water Right	Source	Diversion Rate (cfs)
77-14378	77-14378	Ground Water / EFSFSR	9.60
85396	77-7122	EFSFSR	0.33
85397	77-7285	Ground Water	0.50
85398 / 85538	77-7293	Unnamed Stream (Hennessey Cr.)	0.25
		Total:	**10.68**

23.   Although the water rights, in combination, could be used to divert up to 10.68 cfs, Perpetua seeks a maximum diversion rate of 9.60 cfs for industrial, diversion to storage, and mining use. Ex. 61 at 3. The 9.60 cfs could be diverted from the EFSFSR, ground water, or both sources at the same time.

24.   The peak water demand for industrial and mining use at the SGP will be 9.60 cfs. Ex. 1g at 48-58. This number represents the combined individual water demands associated with the SGP: 4.5 cfs for ore processing at the mill, 0.7 cfs for dust control, 0.1 cfs for drilling activities and 4.3 cfs for dewatering. *Id.* Even though these individual demands will likely not occur simultaneously, there are operational circumstances that may require Perpetua to divert the full 9.60 cfs. *Id.*; Scanlan Test., Tr. at 138-141.

25. Perpetua proposes to capture and store up to 600 acre-feet per year for industrial use under Application 77-14378. Ex. 1g at 55-57. This volume is comprised of the initial fill of the TSF and storage in the contact water detention ponds, with an approximate 35 percent contingency to account for variation in precipitation. *Id.*

26. The River Pump will have a capacity of approximately 4.5 cfs. Ex. 34 at 124, 139 (describing "maximum withdrawal rate" from the EFSFSR as 4.5 cfs); Ex. 47 at 2 ("Perpetua intends to supplement the site water balance with as much as 4.5 cfs of raw water from the EFSFSR.").

27. The EFSFSR will supply more of the annual water demand for the SGP in the early years of the project. Bosley Test., Tr. at 391-393. In later years, contact water, dewatered ground water, and effluent from the TSF will supply most of the annual water demands. *Id.*

28. "The most significant [SGP] water use will be for ore processing during operations, which accounts for 97 percent of the total water usage for the life of the project and includes tailings management." Ex. 26 at 84. "The primary source of water to be used in the ore processing circuit will be water recycled from the TSF." *Id.* "During normal operations, it is anticipated that, on average, approximately 80 percent . . . of the water used for ore processing will be reclaim[ed] water while the remaining 20 percent will [come from freshwater sources]." *Id.*

29. "The EFSFSR is designated critical habitat for Chinook salmon, steelhead, bull trout, and westslope cutthroat trout, all of which are listed as threatened, endangered, or sensitive." Ex. 259 at 9 (citations and scientific names of species omitted). The SGP site includes stream reaches that are designated as critical habitat for Chinook salmon, steelhead, and bull trout. Ex. 29 at 19-20.

30. The National Marine Fisheries Service ("NMFS") prioritizes actions for recovering ESA-listed species in the Salmon River drainage. These actions include removing fish passage barriers, eliminating impacts from legacy mining activities, and restoring degraded habitat. Leonard Test., Tr. at 655.

31. The Yellow Pine Pit was first mined and excavated in the 1930s. Ex. 29 at 38-39. As the Yellow Pine Pit was actively mined, the EFSFSR was routed around the pit. *Id.* When the site was abandoned in the late 1950s, the EFSFSR was allowed to flow over an unreclaimed high wall of the pit, forming a steep cascade, creating a complete barrier for upstream fish passage, and isolating the upstream populations of bull trout and westslope cutthroat trout. *Id.* The Yellow Pine Pit continues to be a complete barrier for upstream fish passage. *Id.*

32. The EFSFSR above the Yellow Pine Pit, including Meadow Creek up to an existing fish passage barrier (located upstream of the confluence with Blowout Creek) is adequate spawning habitat for Chinook salmon. Kinzer Test., Tr. at 1086, 1163.

33. Beginning in about 2000, the NP Tribe has operated a program to transplant Chinook salmon above the Yellow Pine Pit. Keller Test., Tr. at 921-22. Transplanted fish are released into Meadow Creek. *Id.* There are isolated populations of bull trout and westslope

cutthroat trout in the EFSFSR and its tributaries above the Yellow Pine Pit. Leonard Test., Tr. at 633.

34.   During the construction phase of the SGP, Perpetua proposes to route the EFSFSR around the Yellow Pine Pit through an engineered stream channel and fishway tunnel to provide volitional fish passage to the upper reaches of the EFSFSR and to allow additional mining at the Yellow Pine Pit. Ex. 22 at 61-62 (map of proposed tunnel); Ex. 46 at 4; Ex. 29 at 19. The stream channel and fishway tunnel will be approximately 0.9 miles long. Ex. 22 at 62.

35.   Volitional fish passage is the preferred means for ESA-listed species to access the available habitat in the upper reaches of the EFSFSR. Kinzer Test., Tr. at 1180-81.

36.   The administrative record includes a 2022 Design Manual from NMFS that "provides criteria and additional guidelines for the design and operation of facilities at barriers to fish migration and water intakes in California, Washington, Oregon, and Idaho." Ex. 246 at 17. These guidelines are intended to "create safe passage routes for adult and juvenile salmonids in rivers and streams and through reservoirs, restore habitat connectivity within watersheds, and enhance salmonid population productivity." *Id.*

37.   Although the NMFS design criteria "are not universally appliable and should not replace site specific recommendations," they are nevertheless "based on decades of experience developing, testing, operating fish passage systems and rel[y] on the best available scientific information." Ex. 246 at 17.

38.   According to the 2022 Design Manual from NMFS, "[t]he maximum hydraulic drop between fish ladder pools should be 1 foot or less" and "[f]ishway overflow weirs should be designed to provide at least 1 foot (+/- 0.1 foot) of flow depth over the weir crest." Ex. 246 at 68.

39.   The proposed fishway will be a fish ladder comprised of a series of pools and weirs. Ex. 34 at 35-36. The weirs are spaced to maintain no greater than a one-foot hydraulic drop between pools. *Id.*; Ex. 47 at 6.

40.   Perpetua hired an engineering firm, McMillan Jacobs Associates ("MJA") to design the stream channel and fishway tunnel and to prepare a hydraulic model to "investigate the lowest possible tunnel fishway flow that satisfies established fish passage design criteria." Ex. 47 at 3.

41.   Using design standards from NMFS, MJA evaluated flow rates that would avoid flow velocities greater than 6.6 feet per second (the burst speed of bull trout) and avoid water depths less than one foot (the minimum flow depth for adult Chinook salmon passage). Ex. 46 at 5-7; Ex. 47 at 3-4. Based on literature from NMFS, MJA also maintained a minimum weir length of 15 inches. Ex. 47 at 3. MJA reached the following conclusions:

[A flow rate of 7.25 cfs in the fishway] will meet the minimum flow depth of 1 ft as well as the other design criteria such as velocity and hydraulic drop. Lower flow

rates will meet velocity and hydraulic drop criteria, but will have less than 1 foot of depth over the weir.

Id. at 12.

> Results of the [computational fluid dynamics] simulations indicate that a flow rate of 7.25 [cfs] (6.89 to 7.61 [cfs], ±5% confidence level) is required to achieve a 1-foot weir flow depth over a 15-inch-wide weir; lower flows will result in flow depths not meeting the 1-foot criterion. Results also indicate that a flow rate of 18.97 [cfs] (18.02 to 19.92 [cfs], ±5% confidence level) is required to achieve a 2-foot weir flow depth. In both of these cases, the average velocity over the weir is expected to be less than 6.6 [feet per second], which satisfies fish passage criteria for maximum velocity.

Id. at 15.

42.   At a flow rate of 5.00 cfs, the fishway would provide a weir depth of 0.72 feet, an average velocity of 5.8 feet per second, and a hydraulic drop of 0.64 feet. Ex. 47 at 15. This would be sufficient for safe passage of bull trout, steelhead, and westslope cutthroat trout. *Id.*

43.   The spawning season for adult Chinook salmon in the EFSFSR is between June 30 and September 30. Ex. 219 at 3. If Perpetua maintains a flow rate of 7.25 cfs in the fishway between June 30 and September 30 and a flow rate of 5.00 cfs during the rest of the year, the fishway will provide safe, timely, and effective passage for Chinook salmon, steelhead, bull trout, and westslope cutthroat trout.

44.   The stream channel and fishway tunnel was also designed to pass the 500-year flood flow for the EFSFSR. Ex. 47 at 2.

45.   In approximately Year 10 of the mining activities, the stream channel and fishway tunnel will be replaced by a restored stream channel through the reclaimed Yellow Pine Pit area. Ex. 22 at 86-88; Ex. 29 at 19. The restored stream channel will preserve fish passage to the upper reaches of the EFSFSR. *Id.*

46.   In June 2022, Perpetua sent a written request to the Idaho Department of Fish & Game ("IDFG") and the Idaho Governor's Office of Species Conservation ("OSC"), seeking "a technical assistance review of Perpetua's water rights application [77-14378]." Ex. 206 at 3.

47.   Perpetua's request for a technical review by IDFG and OSC included a memo, dated June 27, 2022, which set forth a proposed water right condition intended to "minimize impacts to fish and aquatic habitat in the EFSFSR drainage." *Id.* at 9. The memo stated Perpetua's commitment to "operate in a manner that ensures sufficient fish passage between the EFSFSR POD [River Pump] and Sugar Creek." *Id.* The memo also noted that Perpetua and its consultant planned to update the design of the fishway and conduct additional analyses of the updated design but confirmed that any adjustments to the fishway would be constrained by the one-foot depth requirement to accommodate passage for adult Chinook salmon. *Id.* at 13.

48.   Perpetua proposes the following water right condition as a voluntary restriction on its diversions:

> Net diversions from EFSFSR and groundwater under water rights 77-7122, 77-7285, 77-7293, and 77-14378 shall not cause more than 20 percent depletion to the unimpaired streamflow in the EFSFSR below its confluence with Sugar Creek when unimpaired streamflow is less than 25 cfs. For purposes of this condition:
>
> a)   Percent depletion is equal to net diversion divided by unimpaired streamflow.
>
> b)   Net diversion is the sum of groundwater and EFSFSR diversions minus discharge of treated water to the EFSFSR and its tributaries.
>
> c)   Unimpaired streamflow is defined as the gaged flow at Sugar Creek (USGS 13311450), plus the gaged flow at EFSFSR above Sugar Creek (USGS 13311250), plus the net diversion from EFSFSR and groundwater under water rights 77-7122, 77-7285, 77-7293, and 77-14378.
>
> d)   Calculations shall be based on running 3-day averages of net diversion and gaged stream flows.

Ex. 206 at 9; *Perpetua Brief* at 31.

49.   "[IDFG's] mission is to preserve, protect, perpetuate, and manage Idaho's fish and wildlife resources for the public interest." Ex. 206 at 1 (citation omitted).

50.   "[OSC] is dedicated to planning, coordinating, and implementing the State's actions to preserve, protect, and restore species listed as candidate, threatened, or endangered under the Endangered Species Act of 1973, while considering Idaho's economic vitality and values." Ex. 206 at 1 (citation omitted).

51.   On August 2, 2022, IDFG and OSC sent a joint letter to Perpetua stating that the "fishery and aquatic habitat protection measures" proposed by Perpetua, including the proposed condition restricting diversions during low flow periods, "will likely protect fisheries and aquatic habitat in the EFSFSR." Ex. 206 at 1. The letter also recommended that IDWR adopt additional water right conditions for water right 77-14378 that "would ensure fish passage at the [SGP]." *Id.* IDFG and OSC proposed the following water right condition:

> Surface water diversions and infrastructure will not at any time impede the passage of any life stage of Chinook Salmon, Steelhead, Bull Trout, or Cutthroat Trout from the confluence of the EFSFSR and Sugar Creek upstream past the Point of Diversion [River Pump].

Id.

52.   The administrative record includes a summary of daily stream flow rates for the EFSFSR at USGS Gage No. 13311250 (EFSF Salmon River above Sugar Creek near Stibnite, ID) from January 2012 to October 2023. Ex. 261. Based on these flow records, the lowest flows in the EFSFSR occur from November to February. *Id.* The lowest average daily flow for that twelve-year period is approximately 10 cfs. *Id.*

53.   Perpetua hired Rio Applied Science and Engineering ("Rio ASE") to evaluate the effects of Perpetua's diversions on stream flow and fish passage in the EFSFSR from the proposed stream channel and fishway tunnel outlet to the confluence of the EFSFSR and Sugar Creek, a distance of approximately 1,700 feet. Ex. 219 at 33.

54.   Rio ASE developed a hydraulic model using 2009 Light Detection and Ranging (LiDAR) data and topographic and bathymetric data collected by Rio ASE in 2021 and 2022. Ex. 219 at 35.

55.   "Fish passage is typically evaluated at 5% (high flow) and 95% (low flow) exceedance flows." Ex. 219 at 35. "Passage is typically inhibited or prohibited at high flow because maximum swim velocity is exceeded and at low flow because flow depth is too low." *Id.*

56.   "At the reach-scale (evaluating all cross sections within the reach of interest) average conditions show that the flow depth is greater than minimum depth criteria at all species-specific 95% exceedance flows for existing and proposed conditions." Ex. 219 at 44. "Also, average reach conditions indicate the channel width meeting minimum depth criteria for existing and proposed conditions is greater than 32% and 26%, respectively, meeting requirements of a minimum 10% of the wetted width, as historically required by NMFS." *Id.*

57.   At the cross-section scale, Perpetua's proposed diversions would increase the number of cross sections that are out of compliance with minimum standards for fish passage. Ex 219 at 44-45.

58.   Under existing flow conditions, many of the cross sections evaluated by Rio ASE already do not meet the depth and velocity criteria for fish passage through man-made hydraulic structures. Ex. 219 at 44-48. Despite these existing stream channel conditions, Chinook salmon, steelhead, bull trout, and westslope cutthroat trout have successfully traversed the EFSFSR reach between the confluence with Sugar Creek and the Yellow Pine Pit. *Id.* at 47.

59.   Meadow Creek is a tributary to the EFSFSR. Ex. 63 at 11. The confluence of Meadow Creek and the EFSFSR is in the middle of the SGP. *Id.* Base flows in Meadow Creek range between 2.0 cfs and 3.0 cfs in low to average water years. Ex. 201 at 5.

60.   In its analysis of the effects of ground water diversions on surface water streams, Perpetua assumed that ground water diversions have a one-to-one impact on surface water streams within the boundaries of the SGP. Ex. 206 at 14.

61.   Additional mining at the Yellow Pine Pit and the West End Pit and new mining at the Hangar Flats Pit will require the excavated areas to be dewatered. Application 77-14378

proposes to divert ground water in and around the open pits, at dozens of well sites, to dewater the pits and facilitate mining activities. Ex. 1g.

62. When the Hangar Flats Pit area is dewatered, the ground water pumping would result in significant depletions to Meadow Creek. Stanaway Test.

63. To prevent Meadow Creek from being affected by the dewatering of the Hangar Flats Pit, Perpetua proposes to construct a new channel for Meadow Creek and to line the channel to prevent communication with the ground water table. Ex. 25b at 24 (map depicting the section of Meadow Creek to be reconstructed and lined). The reconstructed and lined section of Meadow Creek would be constructed in a way that maintains all the existing functions of the stream channel. Stanaway Test., Tr. at 259.

64. Even with a liner in Meadow Creek, Perpetua acknowledges that ground water pumping in the Meadow Creek drainage will reduce the streamflow in the creek. Ex. 63 at 20-21.

65. During operations, Perpetua proposes to divert ground water from thirteen supply wells in Section 15, T18N, R09E for industrial use. Ex. 25b at 44. These wells are in the Meadow Creek drainage. Ex. 63 at 11.

66. The cone of depression created by pumping ground water for industrial use or for dewatering could extend to areas of Meadow Creek upstream of the lined section. Stanaway Test., Tr. at 259-261. To attenuate the effects of ground water pumping on areas outside of the lined section, Perpetua proposes to limit its industrial production wells around Meadow Creek to an average monthly diversion rate of 0.5 cfs. *Id.*; Ex. 27a at 76. ("0.5 cfs was determined from the groundwater flow model . . . as an amount that could be withdrawn without adverse impacts on Meadow Creek."). An average monthly diversion rate of 0.5 cfs equates to a volume of approximately 31 acre-feet per month.

67. Depending on its industrial water demands, Perpetua may have to treat water pumped for dewatering purposes and release the treated water into existing stream channels. Perpetua proposes to inject the treated dewatering water into Meadow Creek above the confluence with Blowout Creek. Ex. 25b at 31 (map showing SGP at full build out) and 45.

68. The TSF will be constructed in the Meadow Creek drainage. Ex. 25b at 24. In addition to lining a lower section of Meadow Creek, Perpetua proposes to construct lined man-made stream channels to convey Meadow Creek and its tributaries around the TSF, during times when the TSF is actively used for tailings storage. *Id.* During the closure and reclamation phase of the SGP, Perpetua will line the top of the TSF and restore the Meadow Creek stream channel over the top of the TSF. Ex. 22 at 61, 89; Ex. 27a at 31-32; Ex. 29 at 69.

69. Although dewatering activities may have some effect on flows in Sugar Creek, Perpetua does not propose to divert any water directly from Sugar Creek. Ex. 25b at 54-55 (map of modeling results showing ground water pumping impacts propagating to Sugar Creek).

70.   The SGP site is currently a source of water contamination for the EFSFSR watershed. Ex. 259 at 9-11. Tailings and spent ore from previous mining activities on the site are uncontained. *Id.* As water flows through the project site, these legacy tailings release arsenic, antimony, and mercury into the water, contaminating the EFSFSR and its tributaries. *Id.* at 18; Ex. 23 at 28-29. Two of the primary sources of contamination are the Bradley Tailings Pile and the HECLA Heap. Haslam Test.; Ex. 259 at 9-11.

71.   Perpetua has been monitoring water quality at the SGP site since at least 2011. Ex. 259 at 9; Durbin Test. Current water quality conditions at the SGP site exceed the Idaho water quality limits for antimony, arsenic, mercury, and temperature. Ex. 259 at 9; Ex. 58 at 2; Durbin Test. Water samples confirm that the concentrations of dissolved antimony and dissolved arsenic exceed human-health based criterion. Ex. 259 at 9.

72.   "[D]ecades of mining activity that largely pre-dated state and federal regulatory guidelines, standards and oversight left the [SGP] area in need of repair and a legacy of millions of tons of unlined tailings, blocked fish passage and conditions degrading water quality." Ex. 72 (2018 Joint Resolution of the Idaho House of Representatives).

73.   "The [SGP] area, in the headwaters of the EFSFSR, was intermittently mined for most of the 20th century." Ex. 259 at 24. "[D]ecades after mining ceased, water quality in the area continues to be impaired." *Id.*

74.   Perpetua has already removed 300,000 tons of tailings and waste rock from the riparian areas of the SGP site to improve water quality. Haslam Test., Tr. at 76-77.

75.   Perpetua proposes to reprocess the Bradley Tailings Pile and the HECLA Heap to extract additional minerals. Ex. 22 at 41. The reprocessed material will be stored in the TSF, designed as a fully contained tailings storage facility, to prevent the tailings from contacting water in the hydrologic cycle. *Id.*

76.   In addition to surface water contamination at the SGP site, ground water at the SGP site is contaminated because of legacy mining impacts.

77.   During low flow periods, the base flow in the EFSFSR is primarily supported by ground water. Durbin Test. "The highest concentrations of both dissolved arsenic and dissolved antimony occur[ ] during low-flow periods (July -March), suggesting the constituents are present in groundwater." Ex. 259 at 9. Concentrations of contaminants during the low-flow period would be static. Durbin Test. Diversion of surface water during the low flow period would not change the contaminant concentration. *Id.*

78.   Any ground water pumped for dewatering purposes is considered contact water. Bosley Test, Tr. at 437-38. If Perpetua pumps ground water to dewater the land in and around the open pits and discharges the water into existing streams, Perpetua must first treat the water to remove the contaminants before injecting the water into streams. Diversion and treatment of excess dewatering will result in water quality improvements for the EFSFSR watershed.

79.   "Given the importance of the EFSFSR (and the [South Fork Salmon River] downstream) as critical habitat for Chinook salmon, steelhead, bull trout, and westslope cutthroat trout, the remediation of the Stibnite mining area is a priority for many government and non-government organizations." Ex. 259 at 25.

80.   Summer water temperatures "frequently exceed[ ] water temperature criteria related to salmonid spawning and (or) bull trout." Ex. 259 at 15 (citation omitted). "Exceedances occur[ ] June-September, but [are] most common in July and August." *Id.*

81.   Between 2011 and 2023, water temperatures in Meadow Creek and the EFSFSR above Meadow Creek remained below the "maximum optimum temperature among the species and life stages of interest." Ex. 201 at 16, Figure 4. Although temperatures were higher in the EFSFSR between the confluence with Meadow Creek and the confluence with Sugar Creek, the temperatures did not reach the threshold where physiological stress and eventual mortality occurs. *Id.*

82.   The SGP, if implemented as described in the proposed plan of operations, will improve stream temperatures for aquatic species relative to baseline conditions during and after operations. Ex. 58 at 5. The River Pump is located at the entrance to the stream channel and fishway tunnel to minimize the effect of diversions at the River Pump on water temperature.

83.   Perpetua proposes to convey streams around or pipe streams through all areas disturbed by mining activities to avoid contact with and contamination of the water. Ex. 26 at 98. Streams that are piped, including the 0.9-mile stream channel and fishway tunnel, will prevent some water temperature increases. Stream channel sections that are reconstructed or restored by Perpetua will also prevent temperature increases once the planted vegetation is tall enough to provide shade. Durbin Test.

84.   Blowout Creek, also known as East Fork Meadow Creek, is a tributary of Meadow Creek. Ex. 29 at 18. In 1965, a reservoir dam on Blowout Creek failed, introducing a large amount of sediment into the EFSFSR watershed. *Id.* at 69-70. Since that time, Blowout Creek has continued to erode the banks of the creek channel and is "one of the largest sources of fine sediment for the EFSFSR." Id. at 69; Richardson Test., Tr. at 729.

85.   As part of its operations, Perpetua will "stabilize and repair" Blowout Creek by constructing grade controls and a coarse rock drain system. Ex. 22 at 64-65. This will raise the ground water levels, significantly reduce current erosion, and prevent future erosion. *Id.*

86.   USFS holds water rights 75-13316 and 77-11941, which constitute the federal reserved water rights for the Salmon Wild and Scenic River between the mouth of the North Fork Salmon River and Long Tom Bar. Ex. 4 at 2.

87.   Water rights 75-13316 and 77-11941 bear a priority date of July 23, 1980, and entitle the USFS to all flows in the Salmon River, up to 28,400 cfs, when the stream flow in the river is greater than or equal to 13,600 cfs. Ex. 4 at 2. The rights also establish the wild and scenic flow rates (when the stream flow is less than 13,600 cfs) in two-week increments throughout the year. *Id.*

88.   Water rights 75-13316 and 77-11941 are subordinated to certain future water uses, including industrial uses, but are not subordinated to future water rights for storage use. Ex. 4 at 3. Perpetua's proposal to divert water to storage under Application 77-14378 would therefore be subject to water rights 75-13316 and 77-11941. *Id.* at 3-4.

89.   To mitigate the impacts of its industrial, mining and storage diversions on water rights 75-13316 and 77-11941, Perpetua prepared a Mitigation Plan, dated May 18, 2021, which proposes to hold water rights 72-149, 72-150, and 72-16273 from Morgan Creek and water rights 72-4031, 72-4032, 72-4033, and 72-4034 from the Salmon River unused for the duration of the project. Mitigation water will be available under the Mitigation Plan between April 1 and October 31.

90.   The Stipulation resolving the protests of the USFS set forth three conditions to be added to water right 77-14378, Transfers 85396, 85397, and 85398, and Exchange 85538, if they were approved:

> Condition 1: Perpetua will implement the mitigation plan attached to its application, with mitigation water available from April 1 to October 31.
>
> Condition 2: When the minimum instream flows of the W&SR [wild and scenic river] Water Right are not being met at the point of compliance between November 1 and March 31, Perpetua will curtail diversions to storage for Water Rights Nos. 77-14378, 77-07122, and 77-07285.
>
> Condition 3: Diversions to storage during the period from April 1 to October 31, at times when minimum instream flows of the W&SR Water Right are not being met at the Point of Compliance will not exceed the mitigation water-rights that are in priority pursuant to the mitigation plan as follows:
>
>> a. Diversions to storage under Water rights Nos. 77-14378, 77-07122, and 77-07285 will not exceed 10.75 cfs; and
>>
>> b. Perpetua will maintain an annual cumulative accounting of the volume of water diverted to storage under Water Rights Nos. 77-14378, 77-07122, and 77-07285 when flows at the point of compliance are at or below the minimum instream flows of the W&SR Water Right during the period from April 1 to October 31. If the cumulative accounting reaches 347-acre feet during the annual period, Perpetua will curtail diversions to storage for Water Rights Nos. 77-14378, 77-07122, and 77-07285 when W&SR flows are not being met at the Point of Compliance for the remainder of the period in that year.

Ex. 4 at 7.

91.   The "Point of Compliance" described in the Stipulation and its proposed conditions is "the Salmon River immediately below the mouth of the South Fork Salmon River." Ex. 4 at 5. Flow in the Salmon River at the Point of Compliance will be calculated using a formula described in the Stipulation. *Id.* at 5-6.

92.   The Idaho Water Resource Board holds water right 77-14190 which establishes a minimum stream flow on the EFSFSR. Water right 77-14190 bears a priority date of April 1, 2005, and would be senior to water right 77-14378. However, water right 77-14190 states that the right the right is subordinate to all future DCMI [domestic, commercial, municipal, and industrial] uses.

93.   Perpetua is actively pursuing other permits required by state and federal agencies. Bosley Test., Tr. at 389-390; *see also* Ex. 26 at 17-19 (summarizing the permits required to construct and operate the SGP).

94.   The initial cost of the SGP is $1.265 billion. Ex. 59 at 1. Perpetua is a publicly traded company with a strong shareholder base and will use a combination of financing options to fund the initial construction and operation of the SGP. *Id.* In addition to traditional funding sources, Perpetua has been awarded grants from the U.S. Department of Defense to offset some of the cost of environmental and engineering studies. Ex. 59 at 67.

95.   The public witnesses described the recreational activities occurring in the EFSFSR watershed. People who live in the area and people from outside of the watershed hike, fish, camp, kayak, and ski in the basin. EFSFSR is still a wild river with relatively few man-made alterations to streamflow. The public lands surrounding the river allow the public to access the river more easily.

96.   Public witnesses expressed concerns that the diversions at the SGP will reduce flows in the EFSFSR, negatively affecting water quality, fish habitat, and recreational opportunities within the basin.

RELEVANT STATUTES

Idaho Code § 42-203A(5) sets forth the criteria used to evaluate applications for permit and states, in pertinent part:

> In all applications whether protested or not protested, where the proposed use is such: (a) that it will reduce the quantity of water under existing water rights, or (b) that the water supply itself is insufficient for the purpose for which it is sought to be appropriated, or (c) where it appears to the satisfaction of the director that such application is not made in good faith, is made for delay or speculative purposes, or (d) that the applicant has not sufficient financial resources with which to complete the work involved therein, or (e) that it will conflict with the local public interest as defined in section 42-202B, Idaho Code, or (f) that it is contrary to conservation of water resources within the state of Idaho, or (g) that it will adversely affect the local economy of the watershed or local area within which the source of water for the proposed use originates, in the case where the place of use is outside of the

watershed or local area where the source of water originates; the director of the department of water resources may reject such application and refuse issuance of a permit therefor, or may partially approve and grant a permit for a smaller quantity of water than applied for, or may grant a permit upon conditions.

Idaho Code § 42-222(1) sets forth the criteria used to evaluate changes to water rights (applications for transfer) and states, in pertinent part:

The director of the department of water resources shall examine all the evidence and available information and shall approve the change in whole, or in part, or upon conditions, provided no other water rights are injured thereby, the change does not constitute an enlargement in use of the original right, the change is consistent with the conservation of water resources within the state of Idaho and is in the local public interest as defined in section 42-202B, Idaho Code, the change will not adversely affect the local economy of the watershed or local area within which the source of water for the proposed use originates, in the case where the place of use is outside of the watershed or local area where the source of water originates, and the new use is a beneficial use, which in the case of a municipal provider shall be satisfied if the water right is necessary to serve reasonably anticipated future needs as provided in this chapter.

Idaho Code § 42-202B sets forth the definition for "local public interest":

"Local public interest" is defined as the interests that the people in the area directly affected by a proposed water use have in the effects of such use on the public water resource.

Idaho Code § 42-240 sets forth the criteria used to evaluate applications to exchange water and states, in pertinent part:

The director shall examine all the evidence and available information and shall approve the exchange in whole, or in part, or upon conditions, provided no other water rights are injured thereby, the exchange does not constitute an enlargement in use of the original right or rights, the exchange is consistent with the conservation of water resources within the state of Idaho, the exchange is in the local public interest as defined in section 42-202B, Idaho Code, and the exchange will not adversely affect the local economy of the watershed or local area within which the source of water for the proposed use originates, in the case where the place of use is outside of the watershed or local area where the source of water originates.

ANALYSIS

The criteria used to evaluate applications for permit are somewhat different than those used to evaluate applications for transfer and applications for exchange. The criteria used to evaluate applications for permit are set forth in Idaho Code § 42-203A(5) and the Department's Water Appropriation Rules (IDAPA 37.03.08). The criteria used to evaluate applications for transfer are set forth in Idaho Code § 42-222(1). The criteria used to evaluate applications for

exchange arc set forth in Idaho Code § 42-240 and are nearly identical to the evaluation criteria for transfer applications. Therefore, this order contains one section evaluating Application 77-14378 and a separate section evaluating Applications 85396, 85397, 85398, and 85538.

I.   Evaluation of Application 77-14378

Reduction to Existing Water Rights

Rule 45.01.a of the Department's Water Appropriation Rules (IDAPA 37.03.08) sets forth the criteria used for determining whether a proposed use of water will reduce the quantity of water under an existing water right:

> A proposed use will be determined to reduce the quantity of water under an existing water right (i.e., injure another water right) if:
>
> i. The amount of water available under an existing water right will be reduced below the amount recorded by permit, license, decree or valid claim or the historical amount beneficially used by the water right holder under such recorded rights, whichever is less.
>
> ii. The holder of an existing water right will be forced to an unreasonable effort or expense to divert his existing water right. Protection of existing groundwater rights are subject to reasonable pumping level provisions of Section 42-226, Idaho Code; or
>
> iii. The quality of the water available to the holder of an existing water right is made unusable for the purposes of the existing user's right, and the water cannot be restored to usable quality without unreasonable effort or expense.
>
> iv. An application that would otherwise be denied because of injury to another water right may be approved upon conditions which will mitigate losses of water to the holder of an existing water right, as determined by the Director.

IDAPA 37.03.08.045.01.a.

Although the Idaho Water Resource Board holds water right 77-14190, which would be senior to water right 77-14378, the right is subordinate to future industrial uses. The wild and scenic water rights held by the USFS, 75-13316 and 77-11941, are also subordinate to future industrial uses but are not subordinate to future storage uses. Therefore, diversions to storage under water right 77-14378 could reduce the quantity of water available to satisfy water rights 75-13316 and 77-11941. Perpetua filed a mitigation plan with Application 77-14378 to mitigate any impact to water rights 75-13316 and 77-11941. The USFS withdrew its protest against Application 77-14378 based on the mitigation plan and other provisions of the Stipulation. USFS confirmed that these provisions, if followed, will adequately protect its senior rights. The hearing officer agrees with that assessment as reflected in the *Order Approving Settlement and Confirming Withdrawal of Protests*. The record does not contain reference to, and the hearing

officer is not aware of, any other water rights that could be affected by the diversion from the EFSFSR or ground water as proposed in Application 77-14378.

Sufficiency of Water Supply

Rule 45.01.b of the Department's Water Appropriation Rules sets forth the criteria for determining whether the water supply is sufficient for a proposed project: "The water supply will be determined to be insufficient for the proposed use if water is not available for an adequate time interval in quantities sufficient to make the project economically feasible . . . ." IDAPA 37.03.08.45.01.b.

Based on stream flow data in the record, the lowest average daily flow for the EFSFSR near the River Pump between 2012 and 2023 was approximately 10.0 cfs. The low flow period occurs in the winter months (Nov-Feb). Even if ground water diversions have an immediate and direct effect on flows in the EFSFSR, the average daily minimum flow still exceeds the total diversion rate sought by Perpetua. Perpetua has agreed to conditions that would limit its diversion rate during low flow periods. In its Stipulation with the USFS, Perpetua agreed to suspend its diversion to storage between November 1 and March 31 if the USFS wild and scenic water rights are not satisfied. Further, Perpetua proposes to limit its diversion from the EFSFSR at the River Pump to 4.5 cfs.

In addition to the diversion limits set forth in the Stipulation, Perpetua proposes to limit its depletion in the EFSFSR basin to no more than 20% of the total unimpaired stream flow in the basin just below the confluence of the EFSFSR and Sugar Creek during times when the unimpaired stream flow at that location is less than 25 cfs. Also, to preserve fish passage through the stream channel and fishway tunnel, Perpetua may not divert water under its industrial and mining water rights unless there is at least 7.25 cfs flowing through the fishway between June 30 and September 30 and at least 5.0 cfs flowing through the fishway between October 1 and June 29. These additional limitations are described in greater detail in the local public interest analysis below.

As a result of the low flow diversion limits, there may be times when Perpetua would have to scale back ore processing due to a lack of water. Bosley Test, Tr. at 542-48. The delayed production could be made up, however, when streamflow increases. *Id.* Perpetua will also be able to buffer water supply fluctuations with water from its storage facilities, including the TSF reservoir and contact storage ponds. Further, once the TSF is operational, much of the water used for ore processing will come from the TSF. Perpetua has demonstrated that water will be available for an adequate time interval and in sufficient quantities to make the project economically feasible.

Lack of Good Faith / Speculation

Rule 45.01.c of the Department's Water Appropriation Rules sets forth the criteria for determining whether an application is filed in good faith and not for delay or speculative purposes. "The applicant shall have legal access to the property necessary to construct and operate the proposed project, has the authority to exercise eminent domain authority to obtain such access, or in the instance of a project diverting water from or conveying water across land

in state or federal ownership, has filed all applications for a right-of-way." IDAPA 37.03.08.45.01.c.i. An applicant must also demonstrate that it is "in the process of obtaining other permits needed to construct and operate the project" and that there are no obvious legal impediments to prevent successful completion of the project. IDAPA 37.03.08.45.01.c.ii-iii.

The proposed points of diversion and place of use for Application 77-14378 include property that is held by the USFS. Perpetua is actively seeking an approved plan of operations from the USFS to construct and operate the SGP. The documents submitted by Perpetua to the USFS include detailed descriptions of the ground water wells, River Pump, and industrial facilities identified in Application 77-14378. Perpetua is actively pursuing the permits required from state and federal agencies to operate the SGP. Perpetua has demonstrated that the applications were filed in good faith and not for delay or speculative purposes.

Sufficient Financial Resources

Rule 45.01.d of the Department's Water Appropriation Rules sets forth the criteria for determining whether an applicant has sufficient financial resources to complete a project. "An applicant will be found to have sufficient financial resources upon a showing that it is reasonably probable that funding is or will be available for project construction or upon a financial commitment letter acceptable to the Director." IDAPA 37.03.08.45.01.d.ii. Perpetua has demonstrated that it is reasonably probable that funding is or will be available for project construction.

Local Public Interest

The local public interest analysis under Idaho Code § 42-203A(5)(e) is meant to be separate and distinct from the injury analysis under Idaho Code § 42-203A(5)(a). Local public interest is defined as "the interests that the people in the area directly affected by a proposed water use have in the effects of such use on the public water resource." Idaho Code § 42-202B(3).

Rule 45.01.e of the Department's Water Appropriation Rules (IDAPA 37.03.08) sets forth the criteria for determining whether a project conflicts with the local public interest. The current Water Appropriation Rules were adopted in the 1980s and have not been substantively changed since then. These rules were based on a now-obsolete, broader understanding of local public interest. Idaho Code § 42-202B(3) was adopted in 1996. The version of Rule 45.01.e in effect at the time of the administrative hearing (December 2023) is not consistent with Idaho Code § 42-202B(3) or judicial decisions interpreting that section.

In 2023, the Department initiated rulemaking to amend its Water Appropriation Rules. As part of the amendment process, Rule 45.01.e was updated to reflect the current definition of "local public interest" set forth in Idaho Code § 42-202B(3) and judicial decisions applying that section. The hearing officer finds that Proposed Rule 45.01.e from the revised Water Appropriation Rules provides an accurate summary of the current statutory definition and caselaw surrounding the local public interest review. Proposed Rule 45.01.e states:

18

Local public interest criteria. The Director will consider the following in determining whether the project will conflict with the local public interest:

> i. The direct effect the project will have on public water resources that are of interest to people in the local area directly affected by the proposed water use including, but not limited to, fish and wildlife habitat, aquatic life, recreation, aesthetic beauty, transportation, navigation, water quality, and the effect of such use on the availability of water for alternative water uses that might be made within a reasonable time; and

> ii. Whether the proposed water use is consistent with Idaho's policy of securing the maximum use and benefit from the public water resources.

> iii. Although the Director has independent responsibility for the overall assessment and balancing of factors weighing on the local public interest, the Director will give due regard to expertise of other state and federal regulatory agencies charged with assessing individual issues under Subparagraphs 045.01.e.i. and ii., recognizing that it is not the primary job of the Department to protect all aspects of the health and welfare of Idaho's citizens and visitors.

> iv. The Director may condition approval of an application on compliance with orders, rules, requirements, and authorizations issued or to be issued by state and federal regulatory agencies with jurisdiction over subject matter relevant to the local public interest.

> v. The Director will deny an application that conflicts with the local public interest unless the project can be approved with conditions to resolve the local public interest conflict.

Idaho Code § 42-203A "places upon the Director [of the Department] the affirmative duty to assess and protect the public interest." *Shokal v. Dunn*, 109 Idaho 330, 337, 707 P.2d 441, 448 (1985). "The relevant elements [of the local public interest] and their relative weights will vary with local needs, circumstances, and interests." *Id.* 109 Idaho at 339, 707 P.2d at 450. "The determination of what elements of the public interest are impacted, and what the public interest requires, is committed to [the Department's] sound discretion." *Id.* Permit conditions arising from the local public interest review should be based on specific information in the record, not on speculation or assertions of indeterminate impacts. *See Hardy v. Higginson*, 123 Idaho 485, 491, 849 P.2d 946, 952 (1993) (case remanded to Department because of insufficient evidence in the record to support permit conditions addressing local public interest issues).

The Protestants argue that the Department's local public interest review should be limited to evaluating the direct effects of the proposed diversions. *Protestants' Brief* at 16 ("Perpetua's claims of improving existing environmental conditions, especially with respect to water quality and fish and wildlife migrations, populations and habitat are not directly related to proposed water withdrawals and are not proposed as part of the water right applications to mitigate potential impacts to the public interest." (footnotes and quotations marks omitted)). The Protestants promote an interpretation of Idaho Code § 42-202B(3) that is too narrow. Section

42-202B(3) states that local public interest includes the "effects of [the proposed water use] on the public water resource." The proposed water use is broader than just the diversion of water. It includes the areas where water is used and the areas where a proposed project would interact with the public water resource. Proposed Rule 45.01.e, quoted above, establishes a project-wide application of the local public interest review. It requires the Department to evaluate the effect "the project" will have on public water resources, not just the diversion of water.

The Protestants correctly note that there are elements of the SGP that may fall outside of the jurisdiction of the Department. For example, the Department might not have the authority to require Perpetua to construct a stream channel and fishway tunnel around the Yellow Pine Pit. Nor can the Department require Perpetua to reclaim the Yellow Pine Pit and restore a stream channel for the EFSFSR over the Yellow Pine Pit once the area is reclaimed. A potential lack of jurisdiction, however, does not mean that the Department cannot consider these important effects on the public water resource in its review of the local public interest. The Department must consider the project as it is currently proposed and all interactions between the proposed project and the public water resource. If there are substantial differences between the project as it is currently proposed and the final plan of operations approved by USFS, the Department may have to re-evaluate the local public interest. This circumstance is adequately addressed by the following approval condition:

> The approval of this permit is in the local public interest based on the elements and actions described in the Modified Plan of Restoration and Operations, dated October 15, 2021. If the final plan of operations approved by the U.S. Forest Service differs substantially from the Modified Plan of Restoration and Operations, the permit holder shall file an application for amendment, updating the elements of the permit to reflect the final plan of operations and asking the Department to re-evaluate the local public interest of the project.

There are many local public interest factors to consider in the EFSFSR watershed. It is in the local public interest to protect the aquatic resources, habitat, recreational opportunities, and aesthetic values of the watershed. It is also in the local public interest to protect, preserve, and restore ESA-listed species in the watershed. It is also in the local public interest to protect and improve water quality in the watershed.

There are many local public interest factors directly related to the SGP. First, it is in the local public interest to improve water quality in the EFSFSR drainage through the clean-up and safe storage of legacy tailings at the SGP site. Perpetua proposes to re-process the Bradley Tailings Pile and HECLA Heap as part of its mining efforts. The reprocessing and safe storage of those legacy tailings would be accomplished with water diverted under water right 77-14378. The effects of such use on the public water resource would include not only the direct effects of diverting water, but also the indirect effects of removing a significant source of contamination from the EFSFSR watershed. After the tailings are reprocessed, the waste material will be stored in the TSF, which will be constructed in a way to prevent future contact with water in the hydrologic cycle.

Second, it is in the local public interest to improve water quality in the EFSFSR drainage by remediating the effects of the failed dam in the Blowout Creek drainage. Perpetua's remediation work on Blowout Creek will eliminate the greatest source of sediment in the EFSFSR drainage.

Third, it is in the local public interest to restore volitional fish passage to the upper reaches of the EFSFSR. The Yellow Pine Pit constitutes a complete barrier to upstream fish passage, impeding volitional fish passage to miles of suitable habitat for ESA-listed species. Removing fish passage barriers is one of the primary goals of NMFS in the Salmon River basin. To restore fish passage around the Yellow Pine Pit, Perpetua proposes to construct a 0.9-mile stream channel and fishway tunnel. The fishway is only effective at restoring fish passage if water flows through the fishway are sufficient to facilitate passage. IDFG and OSC requested that the Department condition its water right approvals to ensure that "[s]urface water diversions and infrastructure [at the SGP] will not at any time impede the passage of any life stage of Chinook Salmon, Steelhead, Bull Trout, or Cutthroat Trout from the confluence of the EFSFSR and Sugar Creek upstream past the Point of Diversion [River Pump]." Ex. 206 at 1. Infrastructure at the SGP would include the proposed fishway.

Fish Passage

To preserve flows in the fishway and in the EFSFSR between the fishway and the confluence of EFSFSR and Sugar Creek, Perpetua proposes the following condition, limiting its depletion effects on the EFSFSR below the confluence of EFSFSR and Sugar Creek:

Proposed 20% Condition: Net diversions from EFSFSR and groundwater under Water Rights 77-7122, 77-7285, 77-7293, and 77-14378 shall not cause more than 20 percent depletion to the unimpaired streamflow in the EFSFSR below its confluence with Sugar Creek when unimpaired streamflow is less than 25 cfs. For purposes of this condition:

a. Percent depletion is equal to net diversion divided by unimpaired streamflow.

b. Net diversion is the sum of groundwater and EFSFSR diversions minus discharge of treated water to the EFSFSR and its tributaries.

c. Unimpaired streamflow is defined as the gauged flow at Sugar Creek (USGS 13311450), plus the gauged flow at EFSFSR above Sugar Creek (USGS 13311250), plus the net diversion from EFSFSR and groundwater under Water Rights 77-7122, 77-7285, 77-7293, and 77-14378.

d. Calculations shall be based on running three-day averages of net diversion and gauged stream flows.

Ex. 206 at 9.

IDFG and OSC confirmed that the condition proposed by Perpetua "will likely protect fisheries and aquatic habitat in the EFSFSR." IDFG and OSC also recommended adopting

additional conditions to ensure fish passage at the SGP, particularly on the EFSFSR from the River Pump to the confluence with Sugar Creek. Consistent with Proposed Rule 45.01.e.iii, the hearing officer "will give due regard to expertise of other state and federal regulatory agencies charged with assessing individual [local public interest] issues." Part of the mission of IDFG and OSC is to protect, preserve, and restore ESA-listed species.

Evidence in the record confirms that Perpetua's proposed condition, alone, is not sufficient to preserve fish passage in the fishway under all flow scenarios. To adequately preserve fish passage through the fishway under all flow scenarios, two additional limits are required. To maintain sufficient flow in the fishway during the period of the year when adult Chinook salmon are migrating upstream (June 30 – September 30), Perpetua must pass a flow of at least 7.25 cfs. At other times of the year (October 1 – June 29), Perpetua must pass a flow of at least 5.00 cfs to facilitate unimpeded fish passage for other fish species.

In its initial evaluation of the proposed fishway, Perpetua determined that a flow rate of 7.25 cfs was needed to maintain a depth of one foot over the weirs. This water depth was identified in the NMFS fishway design manual as the depth needed for safe passage for adult Chinook salmon. At hearing and in its post-hearing brief, Perpetua argued that, rather than using the NMFS standards for man-made fish passage structures, flow depths in the fishway should be evaluated using a document produced by the California Department of Fish and Wildlife Instream Flow Program titled *Standard Operating Procedure for Critical Riffle Analysis for Fish Passage in California* ("CDFW Standards"). Ex. 238. The CDFW Standards recommend a flow depth of 0.9 feet for safe passage for adult Chinook salmon. This depth could be achieved with a flow rate of 6.60 cfs in the fishway.

Perpetua's arguments related to the CDFW Standards are not persuasive. The CDFW Standards state: "Fish passage criteria cited in this document are specific to California and should not be extrapolated beyond the state borders." Ex. 238 at 6. Further, the CDFW Standards state: "This [document] applies only to wadeable streams having low gradient riffles with less than 4% gradient and substrates dominated by gravel and cobble." *Id.* Most importantly, the CDFW Standards state: "[T]his procedure is not applicable to culverts, weirs, bedrock ledges, or anticlines with associated drops." *Id.* at 7.

Ultimately, whether Perpetua is required to maintain a bypass flow of 6.60 cfs or 7.25 cfs through the fishway between June 30 and September 30 is largely inconsequential. When the unimpaired streamflow in the EFSFSR below Sugar Creek drops below 25 cfs, Perpetua's 20% condition, in most years, would be the primary limiting factor in determining the amount Perpetua could deplete from the EFSFSR.

Exhibit 261 summarizes the daily stream flow for USGS Gage No. 13311250 (EFSFSR above Sugar Creek near Stibnite, ID) from 2012 to 2023. Exhibit 262 summarizes the daily stream flow for USGS Gage No. 13311450 (Sugar Creek near Stibnite, ID) from 2014 to 2023. Using the daily streamflow data from Exhibits 261 and 262, it is possible to evaluate how Perpetua's 20% condition and the 7.25 cfs bypass flow condition would be applied in an average year. According to one of Perpetua's technical reports, 2016 represents an average water year in the EFSFSR basin. Ex. 63 at 20. The following table sets forth the daily data for USGS Gages 13311250 and 13311450 for a select number of days between June 30, 2016, and September 30,

2016. The table shows the amount of water that Perpetua could deplete from the EFSFSR above the point of quantification under the 20% condition and under the 7.25 cfs bypass condition and shows which condition acts as the limiting factor for depletion.[2]

Date	USGS Gage #13311250 EFSFSR (cfs)	USGS Gage #13311450 Sugar Cr (cfs)	Total Flow (EFSFSR + Sugar Cr) (cfs)	Depletion Allowed under 20% Condition (cfs)	Depletion Allowed under 7.25 cfs Bypass Flow Condition (cfs)	Limiting Condition
6/30/2016	32.68	24.53	57.21	9.60	9.60	Neither
7/7/2016	24.13	21.31	45.44	9.60	9.60	Neither
7/14/2016	26.82	19.01	45.83	9.60	9.60	Neither
7/21/2016	20.53	15.21	35.74	9.60	9.60	Neither
7/28/2016	17.69	13.45	31.14	9.60	9.60	Neither
8/4/2016	15.74	11.88	27.62	9.60	8.49	Bypass
8/11/2016	14.94	10.96	25.90	9.60	7.69	Bypass
8/18/2016	13.54	9.82	23.36	4.67	6.29	20%
8/25/2016	12.85	9.12	21.97	4.39	5.60	20%
9/1/2016	12.01	8.38	20.39	4.08	4.76	20%
9/8/2016	12.32	8.38	20.70	4.14	5.07	20%
9/15/2016	13.17	8.58	21.75	4.35	5.92	20%
9/22/2016	13.94	8.96	22.90	4.58	6.69	20%
9/29/2016	11.40	7.76	19.16	3.83	4.15	20%

See Exs. 261 and 262.

As shown in the table, when the total unimpaired streamflow is high, Perpetua would be able to divert (and consume) the full 9.60 cfs proposed in its applications without any limitation. Once the total unimpaired streamflow drops below 25 cfs, however, the 20% condition becomes the greatest limiting factor for diversion rate. There is a transition period where the bypass flow condition would limit diversions more than the 20% condition. In 2016, this occurred when total unimpaired streamflow was between 25 and 30 cfs. This transition period came at the end of the high flow period, meaning Perpetua's storage facilities would be full, reducing Perpetua's demand for freshwater from EFSFSR or ground water and limiting the effect of the bypass flow condition on Perpetua's operations.

The hearing officer is not persuaded that the CDFW Standards for critical riffles in natural streams should be used to determine the proper bypass flow for the fishway. Evidence in the record supports maintaining a minimum depth of 1.0 feet over the fishway weirs between June 30 and September 30, the period when adult Chinook salmon would be passing upstream through the fishway. The record supports a minimum bypass flow of 7.25 cfs between June 30 and September 30 to maintain a one-foot depth over the fishway weirs. The record contains hundreds of pages of analysis and testimony arguing about whether 0.9 feet (6.6 cfs) or 1.0 feet

---

[2] The 20% condition proposed by Perpetua describes three-day averaging for stream flow and diversions. Even though the table does not apply three-day averaging, it is still effective in showing the relationship between the 20% condition and the 7.25 cfs bypass flow condition under various flow rates.

(7.25 cfs) is the appropriate bypass flow for preserving fish passage in the fishway. Ultimately, the arguments are of little consequence because Perpetua's 20% condition serves as the primary limiting factor for industrial diversions in an average water year, not the bypass flow conditions.

Ground Water Diversions near Meadow Creek

Idaho Code § 42-228 states: "The excavation and opening of wells and the withdrawal of water therefrom for the sole purpose of improving or preserving the utility of land by draining them shall not be forbidden or governed by this act . . . ." Therefore, Perpetua would not need a water right to pump ground water to dewater the Yellow Pine Pit, the West End Pit, or the Hangar Flats Pit, as long as Perpetua did not use the water for some other purpose. Perpetua proposes to use the ground water pumped for dewatering, at times, for industrial purposes.

The primary area of concern for ground water pumping affecting stream flow is in the Meadow Creek drainage. Meadow Creek provides habitat for ESA-listed species. Perpetua asserts that the reconstructed and lined Meadow Creek channel will be insulated from the effects of ground water pumping in the Meadow Creek and Hangar Flats area. The hearing officer declines to include a condition on the permit requiring Perpetua to construct a new Meadow Creek channel with a liner. Alterations of stream channels are governed by Chapter 38, Title 42, Idaho Code. Any proposal to change the location of or composition of the Meadow Creek channel must go through the application process described in Chapter 38. Rather than dictating how Meadow Creek channel should be reconstructed, the approval of Permit 77-14378 should instead restrict ground water pumping in the Meadow Creek drainage if the stream flow in Meadow Creek is not preserved. This is accomplished with the following condition:

> During all times when the right holder is diverting ground water under this right from any of the wells in Section 15, T18N, R09E, the right holder shall ensure a flow of at least 3.0 cfs in Meadow Creek from the existing fish passage barrier located above the confluence of Meadow Creek and Blowout Creek to the confluence of Meadow Creek and EFSFSR.

Summary

The Department has broad discretion to weigh and balance competing local public interest factors. In other words, the local public interest review is not a zero-impact setting. Some local public interest factors may be affected to allow other local public interest factors to be accomplished. A hearing officer for the Department must weigh all local public interest factors and the technical information in the record to determine whether the proposed permit can be approved with conditions to protect the local public interest.

In this case, the short-term and long-term benefits to water quality and fish passage resulting from the SGP outweigh any short-term impacts on fish habitat or fish passage resulting from mining activities at the SGP and the associated water diversions. Further, water right conditions, supported by technical information in the record, can be added to the permit to minimize project impacts on fish passage and fish habitat for ESA-listed species. The following conditions should be added to water right 77-14378:

24

1. The diversion of water directly from the East Fork of the South Fork Salmon River (EFSFSR), located in the NESE, Section 3, T18N, R09E, shall not exceed a maximum diversion rate of 4.50 cfs.

2. The thirteen industrial supply wells located in Section 15, T18N, R09E, shall not exceed a combined monthly diversion volume of 31 acre-feet.

3. The approval of this permit is in the local public interest based on the elements and actions described in the Modified Plan of Restoration and Operations, dated October 15, 2021. If the final plan of operations approved by the U.S. Forest Service differs substantially from the Modified Plan of Restoration and Operations, the permit holder shall file an application for amendment, updating the elements of the permit to reflect the final plan of operations and asking the Department to re-evaluate the local public interest of the project.

4. Net diversions from the EFSFSR and ground water under water rights 77-7122, 77-7285, 77-7293, and 77-14378 shall not cause more than twenty percent depletion to the unimpaired streamflow in the EFSFSR below its confluence with Sugar Creek when the unimpaired streamflow is less than 25 cfs. For purposes of this condition:

    a. Percent depletion is equal to net diversion divided by unimpaired streamflow.

    b. Net diversion is the sum of ground water and EFSFSR diversions minus the discharge of treated water to the EFSFSR and its tributaries.

    c. Unimpaired streamflow is defined as the gauged flow at Sugar Creek (USGS Gage #13311450) plus the gauged flow at EFSFSR above Sugar Creek (USGS Gage #13311250) plus the net diversion from EFSFSR and ground water under water rights 77-7122, 77-7285, 77-7293, and 77-14378.

    d. Calculations shall be based on three-day trailing averages of net diversions and gauged stream flows.

5. From June 30 to September 30, no water shall be diverted under this right unless there is at least 7.25 cfs passing the river pump point of diversion on the EFSFSR in the NESE, Section 3, T18N, R09E.

6. From October 1 to June 29, no water shall be diverted under this right unless there is at least 5.00 cfs passing the river pump point of diversion on the EFSFSR in the NESE, Section 3, T18N, R09E.

7. During all times when the right holder is diverting ground water under this right from any of the wells in Section 15, T18N, R09E, the right holder shall ensure a flow of at least 3.0 cfs in Meadow Creek from the existing fish passage barrier located above the confluence of Meadow Creek and Blowout Creek to the confluence of Meadow Creek and EFSFSR.

8. On or before March 1st each year, the right holder shall provide the Department with an annual report summarizing the diversion amounts and flow rates for the previous calendar year. The annual report shall include the following information: (1) the daily diversion rates for the river pump and ground water diversions (industrial supply, dewatering, open pit, underdrain); (2) daily streamflow rates for (a) Meadow Creek just above the confluence with Blowout Creek, (b) Meadow Creek just above the confluence with EFSFSR, and (c) EFSFSR at the entrance to the fishway tunnel downstream of the river pump on the EFSFSR; (3) an analysis of how the right holder complied with the USFS Stipulation and mitigation plan; and (4) an analysis of how the right holder satisfied the conditions of approval for this water right.

Conservation of Water Resources

Perpetua proposes to divert contact water and recycled water to satisfy most of its water demands for ore processing. Perpetua's water management plan relies heavily on contact water captured for water quality purposes and recycled water, minimizing the diversions from ground water and the EFSFSR. Perpetua has demonstrated that the water uses proposed in Application 77-14378 are consistent with the conservation of water resources within the state of Idaho.

II. Evaluation of Applications 85396, 85397, 85398, and 85538

Injury to Existing Water Rights

Water rights 77-7122, 77-7285, and 77-7293 are existing rights at the SGP and authorize mining and storage use at the site. Water right 77-14190 bears a priority date of April 1, 2005, and is junior to water rights 77-7122, 77-7285, and 77-7293. The changes proposed in Applications 85396, 85397, 85398, and 85538 will not significantly alter the effects of the diversion of water rights 77-7122, 77-7285, and 77-7293 on flows in the EFSFSR. Therefore, water right 77-14190 will not be affected by the proposed changes.

Water rights 77-7122, 77-7285, and 77-7293 are junior to water rights 75-13316 and 77-11941 held by the USFS for wild and scenic flows on the Salmon River. Water rights 77-7122, 77-7285, and 77-7293 are included in the mitigation plan set forth in the Stipulation between Perpetua and the USFS described above. Therefore, any impacts to water rights 75-13316 and 77-11941 are offset or prevented through the Stipulation and its associated mitigation plan. The record does not contain reference to, and the hearing officer is not aware of, any other water rights that could be affected by the changes proposed in Applications 85396, 85397, 85398, or 85538.

Enlargement in Use

The changes proposed in Applications 85396, 85397, 85398, and 85538 will not result in an enlargement in the use of water rights 77-7122, 77-7285, or 77-7293. Water right 77-7122 already authorizes the diversion of water from the EFSFSR for mining storage. Water right 77-7285 already authorizes the diversion of ground water for mining and mining storage. Water

right 77-7293 already authorizes the diversion of water from an Unnamed Stream (Hennessey Creek) for mining. These rights will continue to be used in the amounts and for the purposes stated in the water rights. The record does not contain clear and convincing evidence that any of the water rights, or portions thereof, have been lost and forfeited through non-use. All annual volume limits listed on the rights will be retained and carried forward in the transfer approvals.

Local Public Interest

The same local public interest factors evaluated under Application 77-14378 apply to the evaluation of Applications 85396, 85397, 85398, and 85538. If conditions are adopted addressing local public interest factors, Perpetua has demonstrated that the changes proposed in Applications 85396, 85397, 85398, and 85538 are in the local public interest.

Conservation of Water Resources

The evaluation of conservation of water resources for Applications 85396, 85397, 85398, and 85538 is identical to the evaluation for Application 77-14378. Perpetua has demonstrated that the changes described in Applications 85396, 85397, 85398, and 85538 are consistent with the conservation of water resources within the state of Idaho.

III.   Arguments from the Protestants

Climate Change

The NP Tribe, through its experts Kendra Kaiser and Ryan Kinzer, contends that "Perpetua's assessment of the effect of their proposed water rights on surface water and groundwater does not sufficiently evaluate or take into account future climate change conditions." Ex. 215 at 2. Kaiser argues that it is improper for Perpetua to use historical stream flow data to evaluate the effects of its diversions rather than using projected stream flow conditions based on climate change models. Ex. 215 at 5-7. According to Kinzer: "In the Pacific Northwest, summer months are anticipated to become progressively more stressful for salmonids as stream temperatures increase with warming air temperatures due to climate change, which is likely to shift and reduce suitable habitat for many species and increase the extinction risk for Snake River ESA-listed species." Ex. 201 at 15 (citations omitted).

Neither Idaho Code § 42-203A(5) nor Idaho Code § 42-222(1) nor the Department's Water Appropriation Rules (IDAPA 37.03.08) include climate change as a review criteria. Those provisions do not require applicants to perform studies or offer analyses of how the water supply may change in the future because of climate change. In the absence of clear statutory authority, the hearing officer declines to consider climate change in the evaluation of applications for permit or applications for transfer. Under the current statutes and rules, an applicant must only address the relevant evaluation criteria in terms of existing stream flows and existing diversions.

Quantity of Water

The Protestants argue that "Perpetua, through their expert reports and testimony, has not shown they need the full amount of water requested." *Protestants' Brief* at 17. The Protestants also argue that water right 77-14378 should be limited to an average monthly diversion rate or an average annual diversion rate, which would be significantly less than the 9.60 cfs proposed by Perpetua. *Id.* These arguments reflect a lack of understanding of water rights and water right elements.

Many water rights in Idaho list diversion rates that are only met during short periods of time, either because of limited water supply or because the peak water demand is of a short duration. Municipal rights, for example, often include diversion rates based on the peak summer demand. Similarly, an industrial right may include a diversion rate that reflects the amount of water needed to flush out a system a couple of times per year. The fact that a diversion rate may only be realized infrequently does not make the diversion rate unnecessary or illegitimate.

Through its exhibits, expert reports, and expert testimony, Perpetua established that the peak water demand for industrial use at the SGP would be 9.60 cfs. This number represents the combined individual demands associated with the SGP. Perpetua admits that diverting the full 9.60 cfs may be rare, depending on operational circumstances. This does not negate the fact that the proposed diversion rate is supported by evidence in the record.

Modeling

Throughout their post-hearing brief, the Protestants identify areas where, they argue, Perpetua should have conducted streamflow modeling or should have conducted additional modeling. The Department's processes for reviewing applications for permit or transfer are substantially different than the evaluation process used by the USFS under the National Environmental Protection Act. Idaho Code §§ 42-203A(5) and 42-222(1) do not require an applicant to create hydraulic or stream flow models. Further, the processes described in Idaho Code §§ 42-203A(5) and 42-222(1) are not iterative. An applicant must satisfy its burden of proof at hearing by providing sufficient evidence addressing the statutory review criteria. After an administrative hearing has concluded, applications are either approved, denied, or approved with limiting conditions. The Department does not request additional analysis, models, or reports from an applicant.

Perpetua's Proposed 20% Condition

As noted above, Perpetua proposes a condition that would limit the amount of water that could be consumed (depleted) at the SGP during low flow periods. Perpetua proposes to limit its diversions to deplete the EFSFSR (below the confluence with Sugar Creek) by no more than 20% of the total unimpaired flow in the stream during low flow periods. The point of quantification is a calculated value, representing the flow in the EFSFSR below the confluence with Sugar Creek. The Protestants argue that this point of quantification "obscures water withdrawal effects on the EFSFSR above its confluence with Sugar Creek." *Protestants' Brief* at 40. The hearing officer agrees. Perpetua contends that the dewatering activities around the Yellow Pine Pit mine will influence flows in Sugar Creek, so the point of quantification must be

below Sugar Creek. *Perpetua Brief* at 15. Perpetua's contention is not persuasive, however, because the depletion impacts to Sugar Creek are relatively small (when compared to the overall depletion impacts of the SGP) and do not occur until late in the project. Perpetua's proposed condition and the associated point of quantification mask the actual effects of Perpetua's diversions on the EFSFSR above Sugar Creek.

The Protestants contend that the proposed condition "does not ensure those upstream EFSFSR flows are adequately protected when flows downstream at the point of quantification drop below 25 cfs." *Protestants' Brief* at 41. The hearing officer agrees. Consistent with the comments from IDFG and OSC, and to avoid impacts to local public interest factors, this order adopts additional diversion limits as described above. First, the River Pump is limited to a maximum diversion rate of 4.50 cfs. Second, Perpetua must maintain a minimum bypass flow of 7.25 cfs downstream of its River Pump from June 30 to September 30 and a minimum bypass flow of 5.00 cfs at all other times of the year. These additional diversion limits adequately protect fish passage through the tunnel fishway and support fish passage in the reach between the fishway outlet and the confluence of EFSFSR and Sugar Creek.

Other Local Public Interest Arguments

As described in the local public interest review for Application 77-14378, the hearing officer has weighed and balanced the local public interest factors in this case and has determined that conditions should be included on the permit and transfer approvals to protect local public interest values in aquatic habitat and fish passage for ESA-listed species in the EFSFSR watershed. These local public interest conditions render many of the arguments advanced by the Protestants moot. For example, the Protestants argue that Perpetua's diversions from the EFSFSR basin will cause the fishway to drop below safe fish passage levels during low flows in August and September. The condition to require a minimum bypass flow that will preserve fish passage during critical times for adult Chinook salmon addresses this concern. If streamflow drops below the minimum flow needed for safe fish passage, Perpetua's must curtail its diversions. Protestants also raise a concern that ground water pumping in the Meadow Creek drainage would dewater Meadow Creek entirely. The condition requiring Perpetua to maintain a flow of 3.0 cfs in Meadow Creek at all times when the Perpetua wells are in operation addresses this concern.

The application review processes described in Idaho Code §§ 42-203A and 42-222(1) can sometimes create a unique challenge for protestants. A hearing officer does not weigh and balance the local public interest factors until after the hearing. Therefore, protestants do not know at hearing whether the hearing officer will adopt conditions to reduce impacts to local public interest factors. Without this knowledge, protestants must make arguments based on the authority sought on the face of an application. In this case, much of the evidence provided by the Protestants was based on the full diversion rate sought by Perpetua and does not account for the diversion limits adopted through this order.

CONCLUSIONS OF LAW
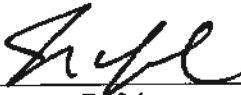
Perpetua has demonstrated that Application 77-14378 will not reduce the quantity of water under existing water rights, that the water supply is sufficient to satisfy the proposed uses,

that the application was made in good faith and not for speculative purposes, that it has sufficient financial resources to complete the proposed project, and that the proposed uses are consistent with the conservation of water resources within the state of Idaho and are in the local public interest. Perpetua has also demonstrated that the changes proposed in Applications 85396, 85397, 85398, and 85538 will not injure other water rights, will not enlarge the use of water rights 77-7122, 77-7285, or 77-7293, that the changes are consistent with the conservation of water resources within the state of Idaho and are in the local public interest. Therefore, Applications 77-14378, 85396, 85397, 85398, and 85538 should be approved.

ORDER

IT IS HEREBY ORDERED that Applications 77-14378, 85396, 85397, 85398, and 85538 filed in the name of Perpetua are APPROVED subject to the conditions set forth in the approval documents issued in conjunction with this order.

Dated this **10**ᵗʰ day of April 2024.

James Cefalo
Hearing Officer

CERTIFICATE OF SERVICE

I HEREBY CERTIFY that on this __10ᵗʰ__ day of April 2024, true and correct copies of the documents described below were served by placing a copy of the same with the United States Postal Service, certified mail with return receipt requested, postage prepaid and properly addressed to the following:

Documents: Preliminary Order Approving Applications
Permit 77-14378
Transfer Approvals 85396, 85397, 85398
Exchange Approval 85538

PERPETUA RESOURCES IDAHO, INC
PO BOX 429
DONNELLY, ID 83615
ahaslam@midasgoldinc.com

ELIJAH WATKINS
STOEL RIVES LLP
101 S CAPITOL BOULEVARD, STE 1900
BOISE, ID 38702
kevin.beaton@stoel.com
elijah.watkins@stoel.com
wade.foster@stoel.com

MICHAEL LOPEZ
OFFICE OF LEGAL COUNSEL
PO BOX 305
LAPWAI, ID 83540
mlopez@nezperce.org

AMANDA W ROGERSON
WRIGHT ROGERSON PLLC
PO BOX 2321
BOISE, ID 83701
amanda@wrightrogerson.com

SAVE THE SOUTH FORK SALMON, INC.
and IDAHO CONSERVATION LEAGUE
JULIA S THROWER
MOUNTAIN TOP LAW PLLC
614 THOMPSON AVE
MCCALL, ID 83638
jthrower@mtntoplaw.com

Courtesy copy sent only by email to:
kathryn.conant@usda.gov
mleah.woodard1@usda.gov
nicholas.pino@usda.gov
mark.rosebrough@usda.gov

Christina Henman
Administrative Assistant

31

EXPLANATORY INFORMATION TO ACCOMPANY A PRELIMINARY ORDER

(To be used in connection with actions when a hearing was held)

The accompanying order is a **Preliminary Order** issued by the Idaho Department of Water Resources (Department) pursuant to section 67-5243, Idaho Code. **It can and will become a final order without further action of the Department unless a party petitions for reconsideration or files an exception and brief as further described below:**

PETITION FOR RECONSIDERATION

Any party may file a petition for reconsideration of a preliminary order with the hearing officer within fourteen (14) days of the service date of the order as shown on the certificate of service. **Note: the petition must be <u>received</u> by the Department within this fourteen (14) day period.** The hearing officer will act on a petition for reconsideration within twenty-one (21) days of its receipt, or the petition will be considered denied by operation of law. See section 67-5243(3) Idaho Code.

EXCEPTIONS AND BRIEFS

Within fourteen (14) days after: (a) the service date of a preliminary order, (b) the service date of a denial of a petition for reconsideration from this preliminary order, or (c) the failure within twenty-one (21) days to grant or deny a petition for reconsideration from this preliminary order, any party may in writing support or take exceptions to any part of a preliminary order and may file briefs in support of the party's position on any issue in the proceeding to the Director. Otherwise, this preliminary order will become a final order of the agency.

If any party appeals or takes exceptions to this preliminary order, opposing parties shall have fourteen (14) days to respond to any party's appeal. Written briefs in support of or taking exceptions to the preliminary order shall be filed with the Director. The Director retains the right to review the preliminary order on his own motion.

ORAL ARGUMENT

If the Director grants a petition to review the preliminary order, the Director shall allow all parties an opportunity to file briefs in support of or taking exceptions to the preliminary order and may schedule oral argument in the matter before issuing a final order. If oral arguments are to be heard, the Director will within a reasonable time period notify each party of the place, date and hour for the argument of the case. Unless the Director orders otherwise, all oral arguments will be heard in Boise, Idaho.

CERTIFICATE OF SERVICE

All exceptions, briefs, request for oral argument and any other matters filed with the Director in connection with the preliminary order shall be served on all other parties to the proceedings in accordance with Rules of Procedure 302 and 303.

FINAL ORDER

The Department will issue a final order within fifty-six (56) days of receipt of the written briefs, oral argument or response to briefs, whichever is later, unless waived by the parties or for good cause shown. The Director may remand the matter for further evidentiary hearings if further factual development of the record is necessary before issuing a final order. The Department will serve a copy of the final order on all parties of record.

Section 67-5246(5), Idaho Code, provides as follows:

Unless a different date is stated in a final order, the order is effective fourteen (14) days after its service date if a party has not filed a petition for reconsideration. If a party has filed a petition for reconsideration with the agency head, the final order becomes effective when:

(a)   The petition for reconsideration is disposed of; or

(b)   The petition is deemed denied because the agency head did not dispose of the petition within twenty-one (21) days.

APPEAL OF FINAL ORDER TO DISTRICT COURT

Pursuant to sections 67-5270 and 67-5272, Idaho Code, if this preliminary order becomes final, any party aggrieved by the final order or orders previously issued in this case may appeal the final order and all previously issued orders in this case to district court by filing a petition in the district court of the county in which:

i.   A hearing was held,

ii.   The final agency action was taken,

iii.   The party seeking review of the order resides, or

iv.   The real property or personal property that was the subject of the agency action is located.

The appeal must be filed within twenty-eight (28) days of this preliminary order becoming final. See section 67-5273, Idaho Code. The filing of an appeal to district court does not itself stay the effectiveness or enforcement of the order under appeal.

Environmental Toxicology

Increased Mercury and Reduced Insect Diversity in Linked Stream–Riparian Food Webs Downstream of a Historical Mercury Mine

Johanna M. Kraus,[a,]* JoAnn M. Holloway,[b] Michael J. Pribil,[b] Ben N. McGee,[b] Craig A. Stricker,[c] Danny L. Rutherford,[b] and Andrew S. Todd[d]

[a]Columbia Environmental Research Center, US Geological Survey, Columbia, Missouri, USA
[b]Geology, Geophysics, and Geochemistry Science Center, US Geological Survey, Denver, Colorado, USA
[c]Fort Collins Science Center, Denver Field Station, US Geological Survey, Denver, Colorado, USA
[d]US Environmental Protection Agency, Denver, Colorado, USA

Abstract: Historical mining left a legacy of abandoned mines and waste rock in remote headwaters of major river systems in the western United States. Understanding the influence of these legacy mines on culturally and ecologically important downstream ecosystems is not always straightforward because of elevated natural levels of mineralization in mining-impacted watersheds. To test the ecological effects of historic mining in the headwaters of the upper Salmon River watershed in Idaho (USA), we measured multiple community and chemical endpoints in downstream linked aquatic–terrestrial food webs. Mining inputs impacted downstream food webs through increased mercury accumulation and decreased insect biodiversity. Total mercury (THg) in seston, aquatic insect larvae, adult aquatic insects, riparian spiders, and fish at sites up to 7.6 km downstream of mining was found at much higher concentrations (1.3–11.3-fold) and was isotopically distinct compared with sites immediately upstream of mining inputs. Methylmercury concentrations in bull trout and riparian spiders were sufficiently high (732–918 and 347–1140 ng MeHg g^{-1} dry wt, respectively) to affect humans, birds, and piscivorous fish. Furthermore, the alpha-diversity of benthic insects was locally depressed by 12%–20% within 4.3–5.7 km downstream from the mine. However, because total insect biomass was not affected by mine inputs, the mass of mercury in benthic insects at a site (i.e., ng Hg m^{-2}) was extremely elevated downstream (10–1778-fold) compared with directly upstream of mining inputs. Downstream adult aquatic insect–mediated fluxes of THg were also high (~16 ng THg m^{-2} day^{-1}). Abandoned mines can have ecologically important effects on downstream communities, including reduced biodiversity and increased mercury flux to higher order consumers, including fish, birds, and humans. *Environ Toxicol Chem* 2022;00:1–15. Published 2022. This article is a U.S. Government work and is in the public domain in the USA.

Keywords: Mercury; Aquatic–terrestrial linkages; Food web; Bull trout; Nez Perce Tribe; Hard-rock mining; Headwater streams

INTRODUCTION

Headwater streams play ecologically important roles in retaining nutrients, processing terrestrial organic matter, maintaining biodiversity, and supporting animals of cultural importance such as anadromous fish (Lowe & Likens, 2005). Because of the high length-to-width ratios of headwater streams, ecological processes in these streams are strongly influenced by their connections with adjacent terrestrial ecosystems. For example, inputs of nutrients, organic matter, and contaminants from land play a central role in determining stream chemistry and food web dynamics (Clements et al., 2000; Lowe & Likens, 2005; Wipfli & Baxter, 2010). Furthermore, these streams can recirculate resources and contaminants back to the terrestrial environment in the bodies of animals with complex life histories like aquatic insects and amphibians that have aquatic juvenile and terrestrial adult stages or in fish that are carried to land by consumers (Baxter et al., 2005; Naiman et al., 2002; Walters et al., 2008).

Historical hard rock mining activity in the western United States has left a legacy of abandoned mine works and

concentrated waste rock in remote headwaters of major river systems (DeGraff, 2007). Runoff, weathering products, and local atmospheric deposition from abandoned mines contain metals and other elements that can alter stream chemistry and increase exposure of stream organisms to toxicants, with negative consequences for connected terrestrial and downstream food webs. In areas of mercury (Hg) mining where Hg was mined or used in processing ore (e.g., gold and silver mining), headwater streams can receive runoff containing Hg from mine tailing piles and soil porewater, as well as local atmospheric deposition (Wiener & Suchanek, 2008). The more abundant inorganic Hg (e.g., cinnabar or mercury sulfide [Hg^{2+}]) contained in these inputs can be ingested and adsorb to the outside of organisms, but it is the more bioavailable organic methylmercury (MeHg), a potent neurotoxin, that biomagnifies in the food chain and is usually a concern for biota (Lepak et al., 2016; Wiener & Suchanek, 2008). Depending on its characteristics and concentrations, Hg can reduce reproductive success, resulting in population declines for fish and birds; they can also accumulate, and biomagnify through the food web, and flux from aquatic to terrestrial ecosystems during metamorphosis of aquatic insects and amphibians (Chasar et al., 2009; Chaves-Ulloa et al., 2016; Chumchal & Drenner, 2015; Tsui et al., 2012; D. M. Ward et al., 2010; Wiener & Suchanek, 2008).

Despite the strong effects of Hg mining on stream chemistry and potential biological exposure, understanding its negative impacts of Hg mining on stream and terrestrial food webs is not straightforward. Mined watersheds are often in areas with elevated background levels of economically important and ore-associated metals and, in the case of Hg, they may receive atmospheric inputs from nonpoint sources as well (Donovan et al., 2016). Mining activities that enhance environmental concentrations of Hg can have additional effects on water quality including toxic concentrations of other ore-related trace metals, changes in pH, and increased fine sediment that can affect multiple components of aquatic food webs including macro-invertebrate abundance and diversity (Beltman et al., 1999; Hepp et al., 2017; Holloway et al., 2017; Lewis & Burraychak, 1979). Finally, although Hg at sufficiently high concentrations can have toxic effects at the base of the food web (Boening, 2000), the societal impacts of environmental Hg exposures usually occur at higher trophic levels, such as commercial and sport fishes, due to trophic biomagnification of MeHg. Mercury speciation (organic vs. inorganic), which can be influenced by pH, oxidation-reduction potential, and dissolved organic carbon (DOC), and food web structure are usually identified as the main mechanisms driving Hg biomagnification and the effects of Hg on higher order consumers (Chasar et al., 2009; Jardine et al., 2012; Mason et al., 2000). However, direct effects of Hg on the base of the food web could include reducing the insect prey biomass necessary to support productive fisheries.

We investigated the ecological effects of a historical Hg mine site on stream insects and food web accumulation of Hg in a linked headwater stream–riparian ecosystem. The abandoned Cinnabar mine site is in the Salmon River Mountains of central Idaho near the town of Yellow Pine, nestled in the headwaters of the Salmon River, a major tributary of the

Columbia River. To test for community and food web effects of Hg mining in this system, we characterized patterns up- and downstream of mining inputs of (1) Hg concentrations and flux through the aquatic food web (sediment, seston, biofilm, larval aquatic insects, adult aquatic insects, fish) and effects on riparian consumers (spiders) via adult aquatic insect emergence; and (2) aquatic insect species' diversity, abundance, and biomass. We also measured isotopic compositions to assess Hg source ($\delta^{203}Hg$) and trophic position ($\delta^{15}N$) of the organisms included in our study (Tsui et al., 2012; Vander Zanden & Fetzer, 2007; but see Jardine et al., 2006, 2014 for limitations to tracer approaches). We hypothesized that inputs from the mine would result in elevated Hg in the downstream and riparian food webs but were unlikely to occur at concentrations that would influence the diversity and abundance of aquatic insects. However, we suspected that additional effects of mining on downstream ecosystems, such as elevated concentrations of co-occurring metals (like arsenic) and physical habitat alteration, could alter aquatic insect communities (Griffith et al., 2001; Holloway et al., 2017; Lewis & Burraychak, 1979; Maret et al., 2003). We also expected higher trophic organisms to contain higher concentrations of MeHg, but not total Hg (THg), compared with basal resources due to biomagnification of MeHg as it moves through the food web.

MATERIALS AND METHODS

Study area

Our study took place near the Cinnabar mine site in the East Fork South Fork Salmon River watershed, an area of 528 km^2 in the Salmon River Mountains in central Idaho, USA. Streams within the watershed provide critical habitat for threatened anadromous fish including Chinook salmon (*Oncorhynchus tshawytscha*), steelhead trout (*Oncorhynchus mykiss*), and bull trout (*Salvelinus confluentus*). The watershed is within the 7.5-million-acre area established by the 1855 Treaty for Nez Perce Tribe (Nimpipuu) rights to religious practices and subsistence activities, including fishing and hunting (Oklahoma State University Library, 2022). Tribe members continue to harvest Chinook salmon on the East Fork South Fork Salmon River, and the Nez Perce Tribe Department of Fisheries Resources collects data on fishery and harvest and conducts fisheries restoration projects on the South Fork Salmon River (Nez Perce Tribe Fisheries Resource Program, 2019).

The Cinnabar mine site operated in the early to mid-20th century and processed cinnabar ore on site to produce Hg (Eckley et al., 2021). Historical mining for gold, antimony, tungsten, and Hg in the East Fork South Fork Salmon River watershed at the Cinnabar mine site resulted in elevated Hg and arsenic (As) concentrations in sediments and water in Cinnabar Creek and in Sugar Creek below the confluence with Cinnabar Creek relative to unmined background concentrations (Eckley et al., 2021; Holloway et al., 2017). The Cinnabar mine is the primary mine input to the tributaries included in our study. Background stream reach sites in the present study include Cane Creek above the confluence with Sugar Creek (site ID021) and Sugar Creek directly upstream of

the confluence with Cane Creek and above the confluence with Cinnabar Creek (ID020, Sugar Creek Up, also referred to as "upstream comparison site"). Mining-impacted sites include Cinnabar Creek upstream of the confluence with Sugar Creek (ID019, ~4.3 km downstream of the mine site), Sugar Creek approximately1.4 km downstream of Cinnabar Creek (~5.7 km downstream of mining; ID018, Sugar Creek Mid), and Sugar Creek approximately 3.3 km downstream of Cinnabar Creek (~7.6 km downstream of mining; ID010, Sugar Creek Down; Supporting Information, Table S1 and Figure 1). These five sites were selected to examine background and mining-influenced Hg effects on linked stream-riparian food webs as well as extent (i.e., distance) of downstream patterns of biotic impairment.

Field sampling

Field sampling focused on characterizing spatial effects of mine drainage on (1) benthic and adult aquatic insect density,

biomass, and species diversity (see Samples for Ecological Analysis section); and (2) Hg accumulation and flux through the aquatic-riparian food web. Mercury metrics included total Hg (THg) and MeHg concentrations in sediment, organic matter, and biota and the total mass of Hg m^{-2} (or m^{-2} day^{-1}) in the aquatic insect community (see also Hg flux, Samples for Chemical Analysis section). Sampling was conducted within two 50-m reaches at each stream site during summer base flow on July 23–28, 2015, and August 3, 2016. Seston, biofilm, benthic aquatic insects, and spiders were collected from the downstream reach, and emerging adult aquatic insects were collected from the undisturbed upstream reach in 2015. Additional riparian spiders were collected from the same sites in 2016 to augment biomass for chemistry. Water, sediment, and fish, mainly native resident bull trout, were also collected as part of an extended study of the area in 2015–2016 (Holloway et al., 2016, 2017, 2018; McGee & Todd, 2016; Rutherford et al., 2020). All fish chemistry data were collected in 2016. Field water chemistry parameters, including pH, dissolved oxygen, and specific conductance, were measured at
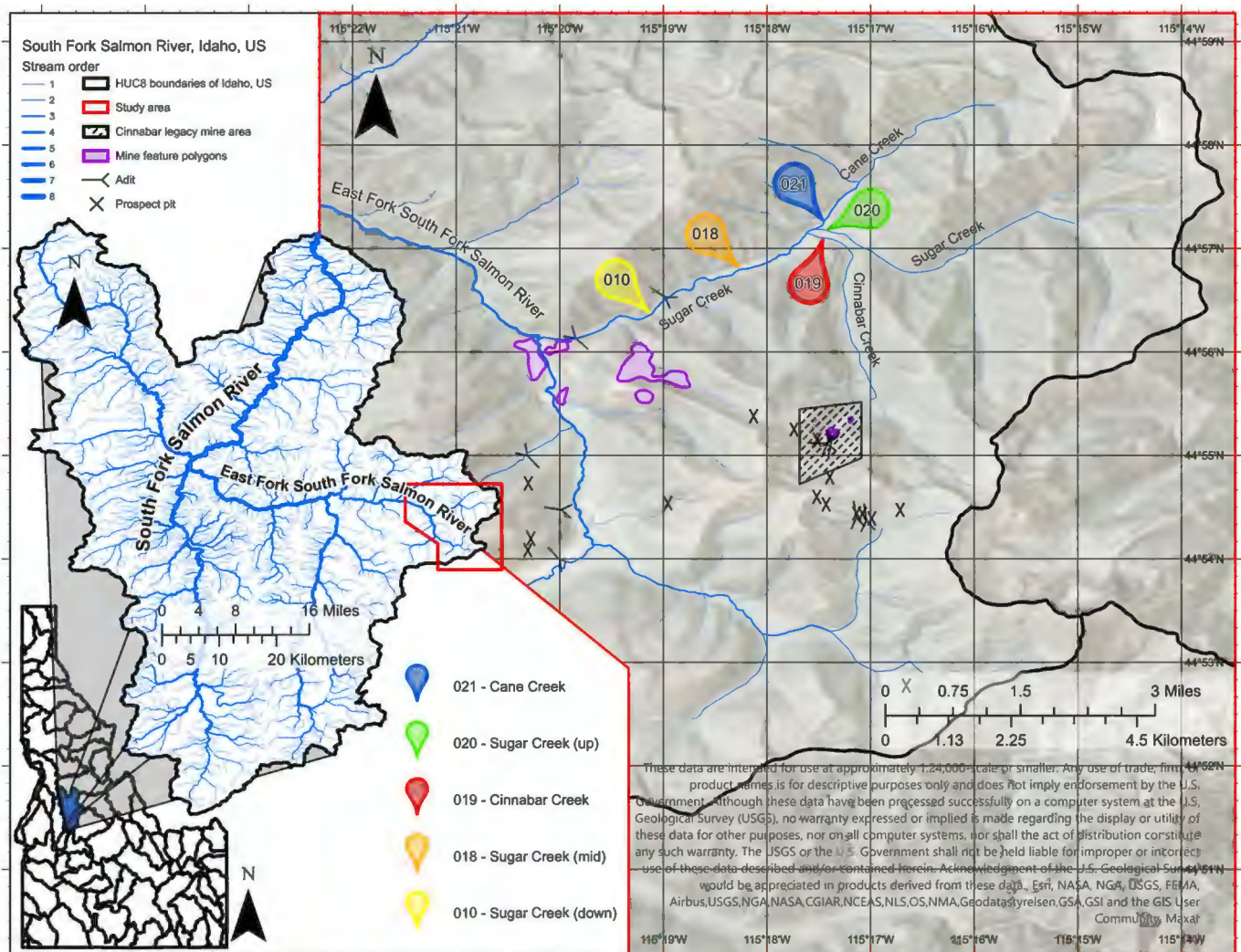
FIGURE 1: Location map for sites up and downstream of inputs from a historical mercury mine in the headwaters of the East Fork South Fork Salmon River, Idaho, USA.

each site during 2015 stream ecology sampling (Supporting Information, Table S1). Stream geomorphology and riparian vegetation metrics were also measured within each reach at that time (Supporting Information, Tables S1 and S2).

Samples for ecological analysis. Benthic aquatic insects (larvae, pupae, and adults) were sampled for biomass, density, and diversity from the stream bottom using a Hess sampler (Wildco® Hess Stream Bottom Sampler; 243 µm net, bottom open area: 0.086 m^2). The sampler was placed opportunistically in areas where an effective seal against invertebrate escape could be obtained along the stream bottom. All hand-sized and larger cobbles were scrubbed and checked for invertebrates before they were removed from the sampler. Finer substrate was thoroughly disturbed with a gardening claw, and buried cobbles were dislodged. Samples were not elutriated in the field but transferred directly to a 532-ml polyethylene plastic bag (Whirl-Pak® sample bags) and preserved in 80% ethanol. Three Hess samples were collected from each stream site within a 50-m reach. Habitats targeted for sampling were characterized by coarse, stable substrate, intermediate depths, and a moderate current (i.e., low-gradient riffles or runs). Water depth at the sample location was recorded.

Emerging adult aquatic insects (also termed emergence) were collected for biomass, density, and diversity using floating emergence traps (bottom open area, 0.36 m^2; Cadmus et al., 2016; Kraus et al., 2014). Briefly, mesh traps were built on a polyvinyl chloride pyramid-shaped frame floating on polyethylene foam and anchored by a nylon cord tied to rebar. High-density polyethylene collection bottles were attached to the side of the trap near the top. Collection bottles were preservative-free to allow for chemical analysis of samples; thus, loose mesh was placed in the bottles to provide substrate for the captured insects. Traps were deployed over pools or areas of slow-moving water (Iwata, 2007). After 4 days, bottles were capped, and trap contents were hand aspirated. Samples were placed on ice in the field and then frozen in a conventional freezer. Five traps total were deployed per stream site, with one trap placed within each of the 10-m stretches available in the 50-m reach. Location and water depth under the traps were recorded.

Samples for chemical analysis. Collection of sediment samples (includes organic and inorganic fractions) is described in Holloway et al. (2017). Briefly, stream sediment was collected into precleaned glass jars and frozen on dry ice for transport to the US Geological Survey (USGS) Mercury Laboratories in Middleton, Wisconsin (USA). An additional split of sediment was shipped frozen to USGS laboratories in Denver, Colorado (USA), where the material was air-dried and sieved to less than 2 mm for full chemical analyses (Holloway et al., 2016). Seston, that is, particulate matter in the water column, was collected using a plankton net fitted with a dolphin bucket (Wildco® Dolphin Plankton Bucket; 1000 ml, 241 µm mesh) and set in the water column for 1.5–4 h as a modified drift net. Material collected in the dolphin bucket was filtered through a plastic 250-µm sieve

to remove large coarse particulate organic matter, and then through a 30-µm sieve to remove excess water. Insects were not knowingly included in seston samples. Periphyton and associated biofilm (hereforth referred to as biofilm) were collected by scrubbing four to five cobble-sized rocks from three locations within each stream site. Rocks were chosen that had abundant biofilm and no filamentous algae. Macroinvertebrates and *Nostoc* cyanobacterial mats were removed from the rocks before scrubbing. Biofilm and attached particulates were scrubbed from the rocks using a coarse brush and Teflon scraper, excess water was decanted, and biofilms were transferred to a polyethylene tube.

Larval benthic aquatic insects (also termed larvae) were collected for chemical analysis by kicking the substrate and capturing drifting insects in a net downstream (i.e., kick-netting). Kick-net samples were sorted in the field. Abundant large taxa and common taxa found at multiple sites were targeted. Emerging adult aquatic insects (also termed adults) were collected for chemical analysis using emergence traps floating on the surface of pools over a 4-day period (same samples as for density, biomass, and diversity). To avoid sample contamination for chemical analysis, no preservatives were used in the collection bottles associated with the kick samples or emergence traps (see the *Samples for ecological analysis* section for details).

Fish were collected by a two-person quantitative sampling crew using a Smith-Root LR24 backpack electrofishing unit. One reach at each site was surveyed using two-pass removal (quantitative depletion) methods (Saunders et al., 2011). All salmonids were measured for length (mm) and salmonids greater than 75 mm were weighed (g) using spring drop scales. Up to 10 bull trout collected at each site were harvested for Hg tissue analysis and the remaining fish were released. Fish tissue sampling efforts were conducted in accordance with US Fish and Wildlife Service Endangered Species Permit Office, Native Threatened Species Recovery Permit TE-89855B-0 and the US Department of Commerce, National Oceanic and Atmospheric Administration, National Marine Fisheries Service Guidelines for Electrofishing Waters Containing Salmonids Listed Under the Endangered Species Act, June 2000. Further details are provided in McGee and Todd (2016).

Riparian web-building spiders were collected off terrestrial vegetation, mainly *Alnus* and *Salix* shrubs, within 1 m of the stream channel using beat sheets or hand collection methods. Spiders in the family Tetragnathidae (Araneae) were targeted because their diets have been previously found to consist largely of adult aquatic insects (Iwata, 2007; Kraus et al., 2014; Sanzone et al., 2003). Leaves from shrubs from which spiders were sampled were also hand-collected to rule out a terrestrial source of Hg for riparian spiders (mediated by terrestrial insect herbivores).

All samples destined for chemical analysis were collected using clean techniques for metals (i.e., nitrile gloves rinsed with deionized water, fiber forceps, polyethylene vials), stored on ice in the field, and frozen in a conventional freezer until sorting and analysis (Kraus et al., 2014). In addition, all fish processing

equipment was sterilized with 20% bleach solution and triple rinsed with deionized water between each monitoring location.

Taxonomy

Benthic aquatic insect samples were sorted and identified to the lowest practical taxonomic level (mainly genus) by Timberline Aquatics (Fort Collins, CO, USA). Almost all organisms in these samples were larval insects (98%), with 2% pupae and 0.2% adults. Thus, benthic insect or larvae is used to refer to all insects captured in these samples. Body length was measured for each specimen to the nearest millimeter. Biomass for insect taxa was estimated using length–mass regressions (Benke et al., 1999). Emerged adult aquatic insects were sorted and identified to taxonomic family using McAlpine et al. (1981), J. V. Ward et al. (2002), and Merritt et al. (2008). After sorting, samples were freeze-dried and weighed separately by family and trap using a six-point microbalance (Sartorius MSE6.6S). Riparian spiders were identified to taxonomic family or genus using Dondale et al. (2003), freeze-dried, and weighed separately by individual using a six-point microbalance.

Chemical analyses

Sample preparation. After sorting and identification, seston, biofilm, benthic aquatic insects, adult aquatic insects, and spiders were freeze-dried and prepared for chemical analysis. Fish samples were stored at approximately −60 °C until they were moved to a −16 °C freezer during sample preparation events. Fish were laterally filleted to remove muscle tissue along the anterior dorsal fin using a presterilized stainless steel surgical blade. Skin was removed, and muscle tissue was placed into a labeled metal-free polycarbonate tube. Once processed, tissue sample tubes were again stored at approximately −60 °C until analysis.

For analysis of THg and MeHg concentrations and THg stable isotopic composition ($\delta^{202}Hg_{total}$ only reported in the present study), sorted samples were composited by family and trap (insects) or family, size class, and trap (spiders). Only benthic larvae were collected and analyzed for chemistry due to their relative abundance compared with pupae and adults. Thus, when referring to the chemistry of benthic insects, the term "larvae" is used. After compositing, a split of each analytical sample was removed for carbon and nitrogen isotope analysis ($\delta^{13}C$, $\delta^{15}N$). Samples were prepared for carbon and nitrogen stable isotope analysis by using stainless steel instruments to fill a tin capsule with approximately 1 mg of dried, homogenized material. Composited samples and their splits were then shipped to the laboratories for chemical analysis (see the *Data analysis* section). Samples were prioritized for analysis based on study questions and sample mass.

Hg analysis. Samples were analyzed for Hg in two different laboratories. Samples were analyzed for THg concentration and isotopic composition in the High-Resolution Laboratory at the USGS (Denver, CO, USA) using a Nu Instruments HR®

multicollector inductively coupled plasma mass spectrometer (MC–ICP–MS). Detailed sample preparation and instrument procedures were described previously (Gray et al., 2013; Pribil et al., 2020). Briefly, all samples were digested in concentrated HNO_3 and HCl (9:1; Foucher & Hintelmann, 2006). In addition, 1 ml of concentrated H_2O_2 was added to aid in the digestion of organic matter. Samples were heated on a hot plate at 80 °C for 4–6 h and diluted with 18 MΩ water. For isotopic analyses, Hg was introduced into the MC–ICP–MS using a CETAC HGX-200 cold vapor generation system. Argon carrier gas was introduced into the cold vapor system at a flow rate of 55–65 ml/min, and a 3% w/v solution of $SnCl_2$ was used as the reductant. Thallium (National Institute of Standards and Technology [NIST] standard reference material [SRM] 997) was introduced to the cold vapor system sample flow via a desolvating nebulizer to correct for mass bias. All isotope samples are reported in ‰ (delta notation [δ]) relative to NIST SRM 3131. The UM-Almadén secondary isotopic reference standard (NIST SRM 8610) resulted in an average $\delta^{202}Hg$ of $−0.56 \pm 0.08$‰ (mean ± 2 SD) and $\Delta^{199}Hg$ of $−0.02 \pm 0.08$‰ ($n = 50$). In addition, a sediment reference material (NIST SRM 1944) was prepared multiple times and resulted in an average $\delta^{202}Hg$ of $−0.53$‰ ± 0.04‰ and $\Delta^{199}Hg$ of $−0.00$‰ ± 0.08‰ ($n = 5$) within the error of previously reported values (Georg & Newman, 2015). Calibration curves were created by using varying concentrations of NIST SRM 3133 (ranging from 0 to 4 ng g^{-1}; using THg response in volts) and checked throughout the sampling period using a 2.5 ng g^{-1} SRM 3133 bracketing standard. The 2.5 ng g^{-1} SRM 3133 solution resulted in an average concentration of 2.47 ± 0.12 ng g^{-1} (2 SD) over a 4-month period. All samples were dried before analysis except for fish tissue. Total Hg concentrations in fish tissue were converted from wet weight to dry weight concentrations by dividing by 0.25. (The THg concentration in wet fish tissue was empirically determined to be 24% ± 2% [mean ± SD] of dry wt concentrations for $n = 4$ fish).

A subset of biota and seston samples, some splits and some previously unanalyzed, were analyzed for THg and MeHg concentrations in the USGS Mercury Laboratory in Wisconsin. See Ogorek et al. (2021) for details. Briefly, samples were analyzed for THg and MeHg by atomic florescence using a Brooks Rand MERX-T Automated Total Mercury System. Data review suggested that two samples for fish (ID018 and ID020) had been mislabeled, so values were switched. One spider sample (for spider greater than 11 mg) was removed as an outlier due to the unusually low MeHg% (6.5%) that was 1 order of magnitude lower than all other spider samples, suggesting contamination issues.

Light stable isotope analysis. Sample splits (~1 mg dry mass) for stable isotope analyses were transferred to 4- × 6-mm tin capsules (Costech Analytical) using an analytical balance, sealed, and stored in 96-well titer plates for analysis by continuous flow isotope ratio analysis using a Micromass Optima mass spectrometer at the USGS Stable Isotope Laboratory in Denver. Isotopic data expressed in per mil notation (‰) were normalized to the respective scales using USGS 40 (−4.52‰ for

δ^{15}N, −26.24‰ for δ^{13}C), USGS 41 (47.57‰ for δ^{15}N, 37.76‰ for δ^{13}C), and USGS 41a (47.55‰ for δ^{15}N, 36.55‰ for δ^{13}C). Analytical precision and replicate sample analyses were generally ±0.2‰ for both isotopes with some exceptions.

Data analysis

To test the hypotheses that (1) sites downstream of mining inputs would show higher concentrations of bioaccumulated Hg; and (2) organisms occupying higher trophic positions would show higher concentrations of MeHg, but not THg, compared with basal resources, analysis of covariance tests (ANCOVA) were used to test the effects of stream site and δ^{15}N (covariate) on MeHg and THg concentrations in biota and seston. Only samples that were analyzed for THg, MeHg, and δ^{15}N were used in the ANCOVA ($n = 26$). Concentrations for THg and MeHg in all analytical samples analyzed in both laboratories and summarized by sample type were also plotted for visual comparison ($n = 117$ for THg; $n = 29$ for MeHg).

To confirm that the mine was the source of THg downstream of mining inputs, an analysis of variance test was used to test effects of mining inputs on THg concentrations in biota, seston, and sediment grouped a posteriori into one upstream and two downstream categories (upstream group = mean sediment, seston, larval insect, adult aquatic insect, fish, and riparian spider isotopic composition from sites ID021 and ID020; downstream group 1 = mean adult aquatic insects, fish, and riparian spider isotopic composition from sites ID019, ID018, and ID010; downstream group 2 = sediment, seston, and larval insect isotopic composition from sites ID019, ID018, and ID010). General linear models (GLMs) were used to make pairwise comparisons between the upstream comparison site (ID020) and sites downstream of mining (i.e., ID019, ID018, and ID010). Comparisons between the upstream comparison site and another upstream tributary (Cane Creek, ID021) were used to assess variability in responses not attributable to mine drainage. Only samples analyzed for δ^{202}Hg were used in this comparison ($n = 86$).

To test the hypothesis that effects of mining could impact downstream aquatic insect communities, GLMs were used to test for differences among sites in benthic and emerging aquatic insect biomass, density, and species richness. Biomass and density are presented as m^{-2} or m^{-2} day^{-1}, but species richness is presented as number of taxa/trap because the value cannot be accurately scaled to larger areas without more information. For species richness, rarefaction curves were generated to test for differences in Shannon diversity among sites controlling for differences in insect density. To test the hypothesis that Hg inputs from the mine would elevate Hg mass and fluxes through downstream food webs, GLMs were used to test for differences among sites in total THg and MeHg present in benthic and emerging aquatic insect communities. One-way analysis of variance tests were used to test for differences in stream geomorphology and riparian vegetation metrics among sites.

Measured δ^{15}N were used to estimate relative trophic position of biota at a site. Site-adjusted δ^{15}N isotopic

compositions of biota and seston to biofilm δ^{15}N (i.e., δ^{15}N$_{adjusted} = \delta^{15}N_{biota} - \delta^{15}N_{biofilm}$) were not used in our study (Post, 2002; Vander Zanden & Rasmussen, 1999) because of the contiguous nature of the sites. Light stable isotopes and Hg concentrations were analyzed for split analytical samples. Source of THg was estimated using δ^{202}THg isotopic composition of sediment and biota (Tsui et al., 2012). Biomass was calculated as the dry mass of insects collected in each sample at a site. Density was calculated for benthic aquatic insects (count m^{-2}) and emerging adult aquatic insects (count m^{-2} day^{-1}) based on abundance of insects captured in samplers/traps and the surface area of substrate (benthic) and water sampled. Density was also analyzed separately by taxonomic order for benthic insects. Sample size was not sufficient to analyze density separately by order for emerging adult aquatic insects. Diversity was calculated as number of insect taxa at the lowest taxonomic resolution present in each sample at a site (genus and species for benthic insects, family for emerging aquatic insects). Mercury mass or flux was defined as the total Hg accumulated and adsorbed in the insect community as a whole (Hg mass m^{-2} for larvae and Hg mass m^{-2} day^{-1} for emerging adults) and represents an estimate of the Hg available to move through the stream–riparian food web. Mercury mass and flux were estimated as the product of insect biomass and mean concentration of THg and/or MeHg in analytical samples of insects from each stream site. Replication for insect biomass, density, and Hg mass (or flux) was $n = 3$ for benthic aquatic insects and $n = 5$ emerging aquatic insects/stream site.

All analyses were conducted in R (R Core Team, 2020) with glm (Venables & Ripley, 2002), anova_test (Kassambara, 2021), and iNext (Hsieh et al., 2020). Figures were produced in R using the package ggplot2 (Wickham, 2016). In several cases, variables were log-transformed to meet model assumptions.

RESULTS

The geometric means of THg in biota (i.e., mean of means for biofilm, insect larvae, insect adults, spiders, and fish) varied by 1 order of magnitude among sites (ID021 = 410.6 ng g^{-1}; ID020 = 265.7 ng g^{-1}; ID019 = 4462.0 ng g^{-1}; ID018 = 2391.9 ng g^{-1}; ID010 = 2889.0 ng g^{-1}; Kraus et al., 2022). Measured THg concentrations in biota at ID019, ID018, and ID010 also appeared to be elevated compared with ID020 for all sample types separately (sediment, seston, biofilm, benthic insects, and fish; Figure 2). When trophic position was included in the model, the THg concentration in biota was related to both stream site and trophic position (i.e., δ^{15}N), although the effects of trophic position on THg concentration differed by site (Figure 3 and Table 1). The differences in THg concentrations among sites were largest at the base of the food web. Near the base of the food web (δ^{15}N = 0), THg concentration in biota and seston was highest in the Cinnabar Creek tributary (ID019) below the mine and remained elevated downstream of mining inputs: THg concentrations in ID019, ID018, and ID010 were 1000, 178, and 53 times the concentrations in the upstream comparison site, ID020, respectively (Figure 3 and Table 2). Among higher
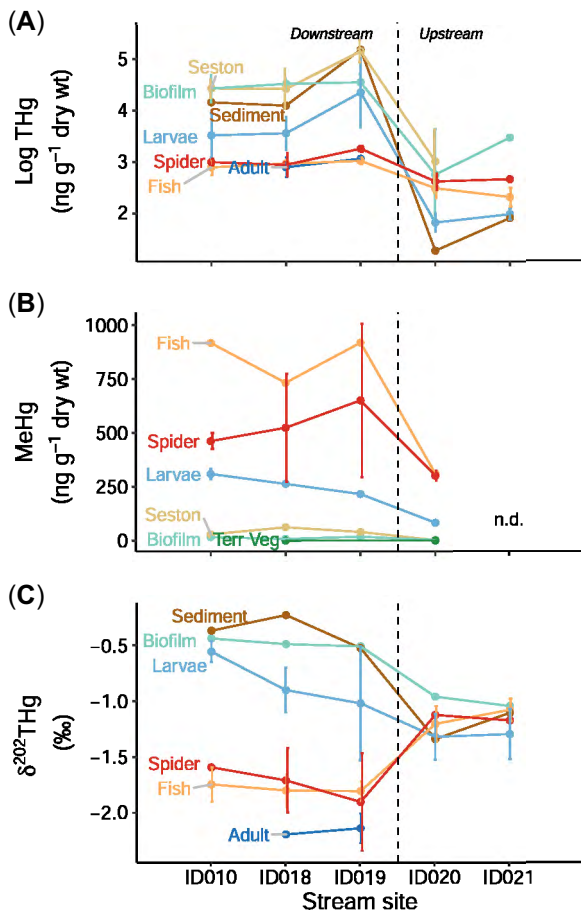
FIGURE 2: Mercury concentrations (dry mass) for total mercury (THg) (**A**), methylmercury (MeHg) (**B**), and THg stable isotope composition (δ^{202}THg; **C**) expressed in nanograms/gram dry weight in food webs up- and downstream of inputs from a historical mercury mine in the headwaters of the East Fork South Fork Salmon River, Idaho, USA. Mean (±SD) of analytical samples for each sample type are shown. Samples include all seston, biofilm, larval aquatic insects (larvae; i.e., benthic), adult aquatic insects (adult; i.e., emergence), spiders, and fish samples collected for chemistry. Solid lines connecting points within a sample type are shown for illustration. Dashed line delineates sites upstream and downstream of mining inputs. No data (n.d.) were generated for MeHg at site ID021. The MeHg concentrations in terrestrial vegetation (terr veg) are shown for reference.

FIGURE 3: Relation of stream site and nitrogen stable isotope composition (δ^{15}N) with (**A**) total mercury (THg) and (**B**) methyl mercury concentrations expressed in nanograms/gram dry weight up- and downstream of inputs from a historical mercury mine in the headwaters of the East Fork South Fork Salmon River, Idaho, USA. Samples include seston, biofilm, larval insects, fish, and spiders for which there were both mercury concentration and nitrogen isotope data. Least squares regression lines for each site are shown for visual comparison. For statistical model results, see Tables 1 and 2.

order consumers (δ^{15}N = 8), patterns of THg concentration in biota and seston among sites were similar, and differences were much smaller: THg concentrations in ID019, ID018, and ID010 were 1.9, 1.0, and 1.4 times the concentrations in the upstream comparison site, ID020, respectively (Figure 3 and Table 2). There was no effect of trophic position on THg concentration in biota at the upstream site (Table 2). However, there was a negative effect of trophic position on THg concentration in biota for ID019, ID018, and ID010 sites (Table 2). Total mercury concentrations in biota decreased by 49%, 41%, and 29% with every 1‰ increase in δ^{15}N at ID019, ID018, and ID010, respectively (Figure 3 and Table 2).

The geometric means of MeHg in biota (i.e., biofilm, insect larvae, spiders, and fish) varied by a factor of three among sites (ID020 = 69.3 ng g^{-1}; ID019 = 214.1 ng g^{-1}; ID018 = 164.8 ng g^{-1}; ID010 = 214.4 ng g^{-1}; Kraus et al., 2022).

Measured MeHg concentrations appeared to show similar patterns to THg (elevated in ID019, ID018, and ID010) for benthic insects, fish, and riparian spiders (Figure 2). When trophic position was included in the model, MeHg concentration in biota was related to trophic position but only marginally related to stream site (Figure 1 and Tables 1 and 2). In our model, MeHg concentrations were highest furthest downstream of mining inputs in Sugar Creek and tended to be elevated at the other sites downstream of those inputs: the mean MeHg concentration in biota was 2.8, 2.7, and 3.2 times higher in ID019, ID018, and ID010 at all trophic positions, respectively, compared with the upstream comparison site, ID020 (Figure 3 and Table 2). Furthermore, MeHg concentrations in biota increased by 69% with every 1‰ increase in δ^{15}N (Figure 3 and Table 2). No significant interactions between stream site and δ^{15}N on MeHg concentration (i.e., differences in slope among sites) were detected, and the interaction term was not included in the final model.

Mercury isotopic composition was different upstream than it was downstream of mining inputs (Figure 2). Upstream of mining inputs, sediment, biofilm, larval aquatic insects, adult aquatic insects, fish, and spider δ^{202}THg was −1.2‰ ± 0.1‰ (mean ± SD, n = 10), whereas downstream of mining inputs, δ^{202}THg composition bifurcated (Figure 2). Downstream of mining inputs, Hg isotopic composition of sediment, biofilm, and larval insect analytical samples were similar to each other

TABLE 1: Analysis of covariance and general linear models testing effects of stream site location on benthic aquatic insects, emergence, and food web chemistry in headwaters of the East Fork South Fork Salmon River (Idaho, USA) up- and downstream of surface water and sediment inputs from a historical mercury mine[a]

Model	df_n	df_d	F	p	η^2
Food web					
Log_{10} (THg concentration) ~ stream site +	3	18	25.3	**<0.001**	0.66
$\delta^{15}N^+$	1	18	34.5	**<0.001**	0.81
Stream site × $\delta^{15}N$	3	18	8.5	**<0.001**	0.59
Log_{10} (MeHg concentration) ~ stream site +	3	21	1.9	0.16	0.21
$\delta^{15}N$	1	21	58.3	**<0.001**	0.74
Benthic insects	df_{diff}	LL_{diff}	χ^2	p	$R^2_{Cox-Snell}$
Log_{10}(density) ~ stream site	−4	−3.75	7.5	0.11	0.39
Log_{10} (Diptera density) ~ stream site	−4	−6.86	13.7	**0.008**	0.60
Log_{10} (Ephemeroptera density) ~ stream site	−4	−6.49	13.0	**0.011**	0.58
Log_{10} (Plecoptera density) ~ stream site	−4	−13.0	26.0	**<0.001**	0.82
Log_{10} (Trichoptera density) ~ stream site	−4	3.42	6.8	0.14	0.37
Taxa count ~ stream site	−4	−7.97	15.9	**0.003**	0.65
Log_{10} (biomass) ~ stream site	−4	−4.64	9.3	*0.054*	0.46
Log_{10} (THg flux) ~ stream site	−4	−40.6	81.2	**<0.001**	1.00
MeHg flux ~ stream site	−3	−8.47	16.9	**<0.001**	0.76
Emergence					
Log_{10} (density) ~ stream site	−4	−2.89	5.8	0.21	0.21
Taxa count ~ stream site	−4	−1.86	3.7	0.45	0.14
Log_{10} (biomass) ~ stream site	−4	−4.23	8.5	*0.076*	0.29
Log_{10} (THg mass) ~ stream site	−1	0.10	0.2	0.66	0.02

[a]Model significance was assessed using a log-likelihood test. Significant models ($p < 0.05$) are indicated in bold. Marginally significant models ($p < 0.1$) are italicized. For analysis of covariances, numerator (df_n) and denominator (df_d) degrees of freedom are used to calculate test statistic (F). Partial eta squared (η^2) is the proportion of variance that can be explained by a variable in the model after accounting for variance explained by other variables in the model. For general linear models, degrees of freedom (df_{diff}) and difference in log-likelihood (LL_{diff}) are used to calculate test statistic (χ^2). Cox and Snell psuedo-R^2 values ($R^2_{Cox-Snell}$) show the percentage of variance in the data explained by the model penalized for number of terms.
THg = total mercury; MeHg = methylmercury; $\delta^{15}N$ = nitrogen stable isotope.

($−0.6 \pm 0.3$, $n = 9$), but differed from emerging adult aquatic insects, fish, and riparian spider samples ($−1.9 \pm 0.2$, $n = 8$; Figure 2). Overall, Hg isotopic composition differed significantly among the upstream and two downstream groups ($F_{2,24} = 91.1$, $p < 0.001$, $\eta^2 = 0.88$; Tukey, $p < 0.001$ for all pairwise comparisons).

Biomass of benthic and emerging adult aquatic insects differed marginally among sites, with benthic insect biomass declining downstream of mine drainage compared with the upstream comparison site ($p = 0.054$; ID021; Figure 4 and Table 1). However, benthic insect biomass differed between the two sites upstream of mining inputs: biomass was lower in Cane Creek (ID021) than it was in the upstream comparison site in Sugar Creek (ID020). Density of total benthic and emerged adult insects did not vary among stream sites (Figure 4 and Table 1). However, density of three of the four main taxonomic orders of benthic insects did vary among sites: Diptera, Ephemeroptera, and Plecoptera were marginally or significantly lower in at least one site downstream of mine drainage compared with the upstream comparison site (ID020; Table 2). Similar to biomass, plecopteran density was also marginally lower in Cane Creek upstream of mining inputs (ID021) compared with the upstream comparison site (Table 2).

Taxa count (i.e., richness) for benthic aquatic insects, but not emerging adult aquatic insects, differed among sites, and was lower downstream of mining (Figure 4 and Table 1). The number of benthic insect taxa was 20% lower in ID019 and 12% lower in ID018 than in the upstream comparison site (ID020; Figure 4 and Tables 1 and 2). Rarefaction curves for Shannon

diversity index confirmed that benthic insect diversity in ID019 was lower than in the upstream comparison site, even when controlling for insect density (Supporting Information, Figure S1). However, benthic insect diversity was also higher in ID021 and ID010 than in the upstream comparison site (Supporting Information, Figure S1).

Masses of THg and MeHg in benthic aquatic insects (i.e., the product of insect biomass and measured Hg concentrations) varied among sites and were higher downstream from mine drainage (Figure 5 and Tables 1 and 2). For THg, mass m^{-2} in benthic insects at ID019 was 1778 times the mass in benthic insects in the upstream comparison site. At ID018 and ID010, respectively, THg mass was 186 and 151 times the mass in the upstream comparison site. For MeHg, mass m^{-2} in benthic insects at ID019 was 10 times the mass of the upstream comparison site. At ID018, and ID010, however, MeHg mass in benthic insects increased to 126 and 48 times the mass in the upstream comparison site, respectively. For emerging adult aquatic insects, fluxes of THg were only estimated downstream of mining inputs at ID019 and ID018 because biomasses of adults collected from other sites were unlikely to be sufficient for Hg detection. Mercury fluxes from those sites were not significantly different from one another but were high compared with the literature (Figure 5; *Discussion* section). The MeHg fluxes in emerging adult aquatic insects were not estimated due to small sample mass.

Riparian vegetation metrics and stream width varied among stream sites (Supporting Information, Tables S1 and S2 and Figure S2). Streams had higher canopy cover at upstream sites,

TABLE 2: Parameter estimates (β) and their standard errors (SE) for significant models explaining variation in benthic insects and food web chemistry in stream sites up- and downstream of inputs from a historical mercury mine[a]

Dependent variable	Parameter	β	SE	t	p
Food web					
Log$_{10}$ (THg concentration)	ID020 (intercept)	2.28	0.22	10.3	**<0.001**
	δ^{15}N	0.05	0.05	1.0	0.35
	ID019 (vs. ID020)	3.00	0.35	8.5	**<0.001**
	ID018 (vs. ID020)	2.25	0.37	6.1	**<0.001**
	ID010 (vs. ID020)	1.74	0.31	5.7	**<0.001**
	δ^{15}N × ID019 (vs. δ^{15}N × ID020)	−0.34	0.07	−4.7	**<0.001**
	δ^{15}N × ID018 (vs. δ^{15}N × ID020)	−0.28	0.08	−3.7	**0.002**
	δ^{15}N × ID010 (vs. δ^{15}N v ID020)	−0.20	0.07	−3.1	**0.007**
Log$_{10}$ (MeHg concentration)	ID020 (intercept)	0.91	0.20	4.6	**<0.001**
	δ^{15}N	0.23	0.03	7.6	**<0.001**
	ID019 (vs. ID020)	0.44	0.23	1.9	*0.067*
	ID018 (vs. ID020)	0.43	0.25	1.7	0.10
	ID010 (vs. ID020)	0.50	0.23	2.2	**0.043**
Benthic insects					
Log$_{10}$ (Diptera density)	ID020 (intercept)	2.83	0.13	21.8	**<0.001**
	ID021 (vs. ID020)	0.11	0.18	0.6	0.55
	ID019 (vs. ID020)	−0.35	0.18	−1.9	*0.084*
	ID018 (vs. ID020)	0.11	0.18	0.6	0.57
	ID010 (vs. ID020)	0.33	0.18	1.8	0.10
Log$_{10}$ (Ephemeroptera density)	ID020 (intercept)	3.46	0.09	48.0	**<0.001**
	ID021 (vs. ID020)	−0.22	0.13	−1.7	0.11
	ID019 (vs. ID020)	−0.30	0.13	−2.4	**0.04**
	ID018 (vs. ID020)	−0.09	0.13	−0.2	0.89
	ID010 (vs. ID020)	−0.37	0.13	−2.9	**0.016**
Log$_{10}$ (Plecoptera density)	ID020 (intercept)	2.99	0.09	33.4	**<0.001**
	ID021 (vs. ID020)	−0.27	0.13	−2.1	*0.06*
	ID019 (vs. ID020)	0.15	0.13	1.2	0.26
	ID018 (vs. ID020)	−0.38	0.13	−3.0	**0.01**
	ID010 (vs. ID020)	−0.62	0.13	−4.8	**<0.001**
Taxa count	ID020 (intercept)	33.3	1.26	26.5	**<0.001**
	ID021 (vs. ID020)	−0.67	1.76	−0.4	0.72
	ID019 (vs. ID020)	−6.67	1.76	−3.7	**0.004**
	ID018 (vs. ID020)	−4.00	1.76	−2.2	**0.048**
	ID010 (vs. ID020)	−1.67	1.76	−0.9	0.37
Log$_{10}$ (THg flux)	ID020 (intercept)	−0.53	0.05	−10.5	**<0.001**
	ID021 (vs. ID020)	0.02	0.07	0.2	0.84
	ID019 (vs. ID020)	2.72	0.07	38.2	**<0.001**
	ID018 (vs. ID020)	1.74	0.07	24.4	**<0.001**
	ID010 (vs. ID020)	1.65	0.07	23.1	**<0.001**
MeHg flux	ID020 (intercept)	4.10	1.00	4.1	**0.004**
	ID019 (vs. ID020)	5.09	1.42	3.6	**0.007**
	ID018 (vs. ID020)	6.20	1.42	4.4	**0.002**
	ID010 (vs. ID020)	5.78	1.42	4.1	**0.004**

[a]Units for density and taxa count are number/sample. Stream site ID020, with which the other sites are compared, is directly upstream of inputs from the mine. Significant terms from the general linear model generating the comparisons ($p < 0.05$) are indicated in bold for the test statistic (t). Total mercury (THg) and methylmercury (MeHg) results are listed.
δ^{15}N = nitrogen stable isotope.

but density of riparian shrubs and riparian spider web-building substrate over streams varied among sites (Supporting Information, Figure S2). Canopy cover was highest in ID019, with ID020 and ID021 also showing higher coverage than ID018 and ID010 (Supporting Information, Figure S2). Number of shrubs and trees along the banks was higher at ID020 than ID010 but was similar among the other sites (Supporting Information, Figure S2). Volume of riparian substrate (branches and logs) within a 2-m height above the stream was highest in ID021, but was similar among the other sites (Supporting Information, Figure S2). Streams were also narrower at upstream sites: ID018 and ID010 had significantly wider active channels than ID021, ID020, and ID019 (Supporting Information, Figure S2).

Measured aspects of stream chemistry were similar among sites, with the exception of concentrations of dissolved As, which were highest at ID019 and elevated downstream of mining inputs compared with upstream sites (Supporting Information, Table S1; Holloway et al., 2018).

DISCUSSION

Abandoned mines in the western United States have left a legacy of altered water chemistry and physical alterations to the landscape resulting in ecological consequences for downstream food webs (Clements et al., 2000; DeGraff, 2007;
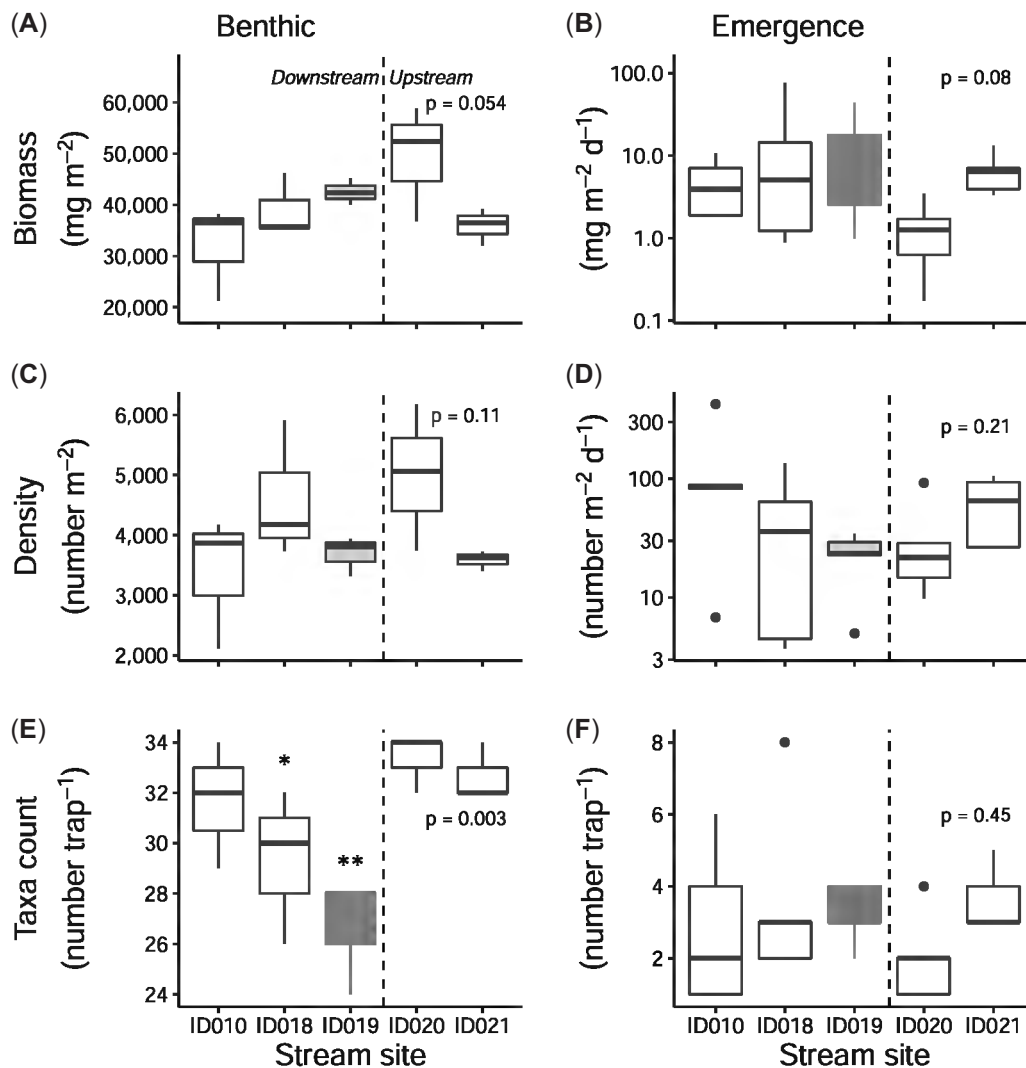
FIGURE 4: Box plots of insect biomass (**A** and **B**), density (**C** and **D**), and taxa count (**E** and **F**) for benthic and emerging aquatic insects in the headwaters of the East Fork South Fork Salmon River up- and downstream of inputs from a historical mercury mine. Whiskers are ranges from the 5th to 95th percentiles of the data, boxes are from the 25th to 75th percentiles, and dark horizontal line is the median. Samples are traps ($n = 3$ and 5 samples for benthic and emergence, respectively). Circles are outliers. Gray filling highlights a mining-impacted tributary. Dashed line delineates sites upstream and downstream of mining inputs. Note that (**B**) and (**D**) are plotted on the log-scale for ease of visualization. The p values are reported for the general linear models testing effects of site on a response variable (Table 1). Asterisks indicate site is significantly different from site ID020 (*$p < 0.05$, **$p < 0.01$). Benthic insects include mostly larval insects. Emergence includes newly emerged adult aquatic insects.

Kraus et al., 2014). However, distinguishing the effects of mining from other influences within a watershed can be challenging. We found evidence that Hg concentrations increased in aquatic–riparian food webs in the East Fork South Fork Salmon River watershed due to inputs from an abandoned Hg mine site. Specifically, Hg concentrations in sediment, seston, aquatic insect larvae, adult aquatic insects, fish, and riparian spiders downstream of mining were generally much higher and isotopically distinct compared with upstream of mining inputs. Increases in modeled THg concentrations in biota and seston downstream of mine inputs were largest at low trophic positions (53–1000 times upstream concentrations), likely because of the presence of large quantities of inorganic Hg adsorbed or accumulated in those samples. Modeled MeHg concentrations, on the other hand, increased with trophic positions and downstream of mining inputs, where concentrations were 2.8–3.2 times those upstream

regardless of trophic position. Mercury stable isotope (δ^{202}THg) compositions of sediment and biota upstream were intermediate between the δ^{202}THg of endpoints with lower (seston, biofilm, and larvae) and higher (spider, fish, and adult aquatic insects) trophic positions downstream of mining. The bifurcating δ^{202}THg downstream of mining is likely due to changes in THg source (up- vs. downstream of mining) and differences in proportion of MeHg among samples. These differences in Hg concentrations and stable isotope composition up- and downstream of mining indicate that the Hg accumulated in downstream food webs likely originated from the mine site. The limited distance between sample sites in our study area adds confidence to this conclusion.

The increase in Hg concentrations due to mining inputs propagated through the downstream food webs, with MeHg concentrations increasing by 69% for every 1‰ δ^{15}N increase in
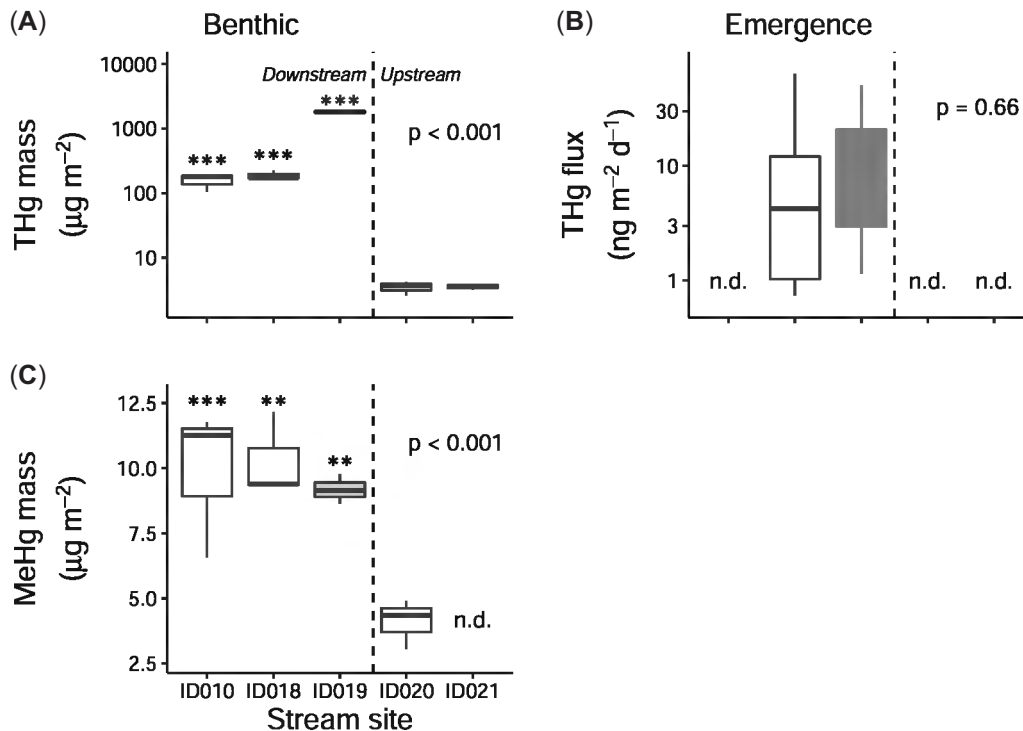
FIGURE 5: Box plots of total mercury (THg) mass and flux in benthic (**A**) and emerging aquatic insects (**B**), and methylmercury (MeHg) mass in benthic aquatic insects (**C**) up- and downstream of inputs from a historical mercury mine in the headwaters of the East Fork South Fork Salmon River, Idaho, USA. Gray filling highlights a mining-impacted tributary. Dashed line delineates sites upstream and downstream of mining inputs. The *p* values are reported for the general linear models testing effects of site on response variable (Table 1). For significant models, asterisks indicate site is significantly different from site ID020 (**$p < 0.01$, ***$p < 0.001$). n.d. = no data.

trophic position. As a result, MeHg and THg concentrations in predatory fish downstream of mining (732–918 ng MeHg g^{-1} dry wt; 404–1212 ng THg g^{-1} dry wt; 0.10–0.30 µg THg g^{-1} wet wt) reached levels known to have effects on fish gene expression, reproduction, and behavior (Lepak et al., 2016). Notably, THg concentrations in bull trout observed in our study were also within the range of human consumption advisories (1 and 2 fish meals/week; 0.05–0.22 µg THg g^{-1} wet wt axial muscle, Lepak et al., 2016) and of having reproductive effects on piscivorous fish and birds (Ackerman et al., 2016; A. Jackson et al., 2016). Similarly, MeHg and THg concentrations in spiders collected downstream of mining (347–1140 ng MeHg g^{-1} dry wt; 453–2060 ng THg g^{-1} dry wt) were at the upper end of concentrations previously observed in riparian spiders and of potential risk to arachnivorous birds (Chaves-Ulloa et al., 2016; Gann et al., 2015; Hannappel et al., 2021; Ortega-Rodriguez et al., 2019; Otter et al., 2013; Pennuto & Smith, 2015; Twining et al., 2021). Similar concentrations in arachnids near Caddo Lake (a wetland–lake complex) in Texas and Louisiana (USA; 19.4–256 ng MeHg g^{-1} wet wt; 90–1182 ng THg g^{-1} dry wt) were reported to have posed a risk of physiological impairment for young black-capped chickadees (*Poecile atricapillus*) ranging from 122% to 434% of wildlife values (Gann et al., 2015).

In addition to mining-elevated concentrations of Hg in biota being high enough to cause reproductive problems in fish and higher order consumers (Gann et al., 2015; A. Jackson et al., 2016; Lepak et al., 2016), concentrations in sediment and biota also appear to have been high enough to account for a localized reduction in benthic insect diversity downstream of mining (Gimbert et al., 2016; Xie et al., 2009). The number of benthic insect taxa at sites within approximately 6 km downstream of mining inputs were 20% and 12% fewer, and rarefied Shannon diversity was similarly lower, than in the site directly upstream of mining inputs. The concentrations of Hg in sediment (12.5–151.9 µg THg g^{-1}) and benthic insect tissue (216–326 ng MeHg g^{-1} dry wt; 1100–81 518 ng THg g^{-1} dry wt) downstream of mining in our study were high enough to cause this reduction in taxonomic diversity by increasing oxidative stress and potentially limiting growth and survival for some taxa (Azevedo-Pereira & Soares, 2010; Chibunda, 2009; Gimbert et al., 2016; Xie et al., 2009). For example, accumulated concentrations of Hg in caddisfly (Trichoptera) and mayfly (Ephemeroptera) larvae ranging from 107 to 270 ng g^{-1} wet weight were associated with 35%–48% reduction in the activity of an antioxidant enzyme (superoxide dismutase; Xie et al., 2009). Furthermore, sediment concentrations of 1.3–3.2 µg THg g^{-1} have been associated with an approximately 20% reduction in growth and 20% effect concentration for growth in *Chironomus riparius* larvae (Gimbert et al., 2016). These types of lethal and sublethal effects of elevated environmental and whole-body Hg concentrations on aquatic insect larvae could have led to local extirpation of the most sensitive taxa and thus reduced diversity at sites downstream of mining. Other explanations of the decline, including geomorphological and physicochemical mechanisms (Flanders

et al., 2019), although possible, were not detected in our study. No other metrics, including water quality variables (As concentrations, DOC, % oxygen, pH, temperature, total dissolved solids), riparian metrics, and stream width varied in a way that could explain the reduced diversity downstream of mining (Holloway et al., 2018; Mogren et al., 2012; US Environmental Protection Agency, 2018).

Despite the apparent effect of mining on benthic insect diversity, there were only marginally significant changes in biomass and no large consistent changes in total density of insects downstream of mining. As a result, greatly elevated Hg concentrations in insects downstream of mining led to a very high mass of Hg m^{-2} in the benthic insect community and Hg fluxed by emerging adult aquatic insects. The mass of THg in the benthic aquatic insect community downstream of mining inputs was 151–1778 times, and MeHg was 10–126 times, greater than those directly upstream, again indicating increased Hg exposure potential for aquatic insectivores downstream of mining. Elevated THg concentrations in emerging aquatic insects (581–1175 ng THg g^{-1} dry wt) only measured downstream of mining also led to high adult aquatic insect-mediated fluxes of THg (16.3 ng m^{-2} day^{-1} on average). The concentrations found in adult aquatic insects downstream of mining fell within the range of those reported for adult aquatic insects emerging from hydroelectric reservoirs (140–1500 ng THg g^{-1} dry wt; Tremblay et al., 1998), but were higher than those reported from streams in New Hampshire (USA; Chaves-Ulloa et al., 2016), streams in the southern Finger Lakes region (NY, USA; Twining et al., 2021), the Willamette River (OR, USA; A. K. Jackson et al., 2021), the Upper Mississippi River (USA; Dukerschein et al., 1992), and the Buffalo Area of Concern in the contaminated Buffalo River (NY, USA; Pennuto & Smith, 2015). As a result, the adult aquatic insect-mediated flux of THg downstream of mining was almost double that reported from seminatural fishless experimental ponds (less than 7 ng MeHg m^{-2} day, converted to less than 8.8 ng THg m^{-2} day following Chaves-Ulloa et al., 2016; also see Tweedy et al., 2013). Combined with elevated MeHg concentrations in riparian spiders and the finding that riparian consumer Hg concentrations increase with their dependence on aquatic insects (A. K. Jackson et al., 2021), these results indicate that locally foraging riparian insectivores could be exposed to high and potentially harmful doses of Hg downstream of mining. This phenomenon may be compounded as stream width increases downstream, because stream surface area contributes to the realized insect-mediated flux of contaminants from a stream reach (Otter et al., 2020).

Headwater streams comprise more than 70% of stream channel length in the United States. However, due to their small size, their impact on downstream water quality, biodiversity, and ecological health of freshwater ecosystems can be overlooked (Lowe & Likens, 2005). In the present study we found that a historic Hg mine site led to increased Hg concentrations, Hg flux, and decreased diversity in downstream and linked riparian food webs. The Hg concentrations in fish, riparian spiders, and emerging aquatic insects were elevated enough to be of concern to higher order predators, including

humans. Management of historical mines and ecological risk assessment needs to consider both the local and downstream consequences for linked stream–riparian food webs, particularly in terms of the bioaccumulation and Hg flux within and from freshwaters.

REFERENCES

Ackerman, J. T., Eagles-Smith, C. A., Herzog, M. P., Hartman, C. A., Peterson, S. H., Evers, D. C., Jackson, A. K., Elliott, J. E., Vander Pol, S. S., & Bryan, C. E. (2016). Avian mercury exposure and toxicological risk across western North America: A synthesis. *Science of the Total Environment*, 568, 749–769. https://doi.org/10.1016/j.scitotenv.2016.03.071

Azevedo-Pereira, H. M., & Soares, A. M. (2010). Effects of mercury on growth, emergence, and behavior of *Chironomus riparius* Meigen (Diptera: Chironomidae). *Archives of Environmental Contamination and Toxicology*, 59(2), 216–224. https://doi.org/10.1007/s00244-010-9482-9

Baxter, C. V., Fausch, K. D., & Carl Saunders, W. (2005). Tangled webs: Reciprocal flows of invertebrate prey link streams and riparian zones. *Freshwater Biology*, *50*(2), 201–220. https://doi.org/10.1111/j.1365-2427.2004.01328.x

Beltman, D. J., Clements, W. H., Lipton, J., & Cacela, D. (1999). Benthic invertebrate metals exposure, accumulation, and community-level effects downstream from a hard-rock mine site. *Environmental Toxicology and Chemistry*, *18*(2), 299–307. https://doi.org/10.1002/etc.5620180229

Benke, A. C., Huryn, A. D., Smock, L. A., & Wallace, J. B. (1999). Length-mass relationships for freshwater macroinvertebrates in North America with particular reference to the Southeastern United States. *Journal of the North American Benthological Society*, *18*(3), 308–343. https://doi.org/10.2307/1468447

Boening, D. W. (2000). Ecological effects, transport, and fate of mercury: A general review. *Chemosphere*, *40*(12), 1335–1351. https://doi.org/10.1016/s0045-6535(99)00283-0

Cadmus, P., Pomeranz, J. P. F., & Kraus, J. M. (2016). Low-cost floating emergence net and bottle trap: Comparison of two designs. *Journal of Freshwater Ecology*, *31*(4), 653–658. https://doi.org/10.1080/02705060.2016.1217944

Chasar, L. C., Scudder, B. C., Stewart, A. R., Bell, A. H., & Aiken, G. R. (2009). Mercury cycling in stream ecosystems. 3. Trophic dynamics and methylmercury bioaccumulation. *Environmental Science & Technology*, *43*(8), 2733–2739. https://doi.org/10.1021/es8027567

Chaves-Ulloa, R., Taylor, B. W., Broadley, H. J., Cottingham, K. L., Baer, N. A., Weathers, K. C., Ewing, H. A., & Chen, C. Y. (2016). Dissolved organic carbon modulates mercury concentrations in insect subsidies from streams to terrestrial consumers. *Ecological Applications*, *26*(6), 1771–1784. https://doi.org/10.1890/15-0025.1

Chibunda, R. T. (2009). Chronic toxicity of mercury ($HgCl_2$) to the benthic midge *Chironomus riparius*. *International Journal of Environmental Research*, *3*(3), 455–462.

Chumchal, M. M., & Drenner, R. W. (2015). An environmental problem hidden in plain sight? Small human-made ponds, emergent insects, and mercury contamination of biota in the Great Plains. *Environmental Toxicology and Chemistry*, *34*(6), 1197–1205. https://doi.org/10.1002/etc.2954

Clements, W. H., Carlisle, D. M., Lazorchak, J. M., & Johnson, P. C. (2000). Heavy metals structure benthic communities in Colorado mountain streams. *Ecological Applications*, *10*(2), 626–638. https://doi.org/10.1890/1051-0761(2000)010[0626:Hmsbci]2.0.Co;2

DeGraff, J. V. (Ed.). (2007). *Understanding and responding to hazardous substances at mine sites in the Western United States*. The Geological Society of America.

Dondale, C. D., Redner, J. H., Paquin, P., & Levi, H. W. (2003). *The insects and arachnids of Canada series, part 23: Orb-weaving spiders of Canada and Alaska–Araneae: Uloboridae, Tetragnathidae, Araneidae, Theridiosomatidae*. NRC Research Press.

Donovan, P. M., Blum, J. D., Singer, M. B., Marvin-DiPasquale, M., & Tsui, M. T. K. (2016). Isotopic composition of inorganic mercury and methylmercury downstream of a historical gold mining region. *Environmental Science & Technology*, *50*(4), 1691–1702. https://doi.org/10.1021/acs.est.5b04413

Dukerschein, J. T., Wiener, J. G., Rada, R. G., & Steingraeber, M. T. (1992). Cadmium and mercury in emergent mayflies (*Hexagenia bilineata*) from the upper Mississippi River. *Archives of Environmental Contamination and Toxicology*, *23*(1), 109–116.

Eckley, C. S., Luxton, T. P., Stanfield, B., Baldwin, A., Holloway, J., McKernan, J., & Johnson, M. G. (2021). Effect of organic matter concentration and characteristics on mercury mobilization and methylmercury production at an abandoned mine site. *Environmental Pollution*, *271*, 116369. https://doi.org/10.1016/j.envpol.2020.116369

Flanders, J. R., Long, G., Reese, B., Grosso, N. R., Clements, W., & Stahl, R. G., Jr. (2019). Assessment of potential mercury toxicity to native invertebrates in a high-gradient stream. *Integrated Environmental Assessment and Management*, *15*(3), 374–384. https://doi.org/10.1002/ieam.4133

Foucher, D., & Hintelmann, H. (2006). High-precision measurement of mercury isotope ratios in sediments using cold-vapor generation multi-collector inductively coupled plasma mass spectrometry. *Analytical and Bioanalytical Chemistry*, *384*(7), 1470-1478. https://doi.org/10.1007/s00216-006-0373-x

Gann, G. L., Powell, C. H., Chumchal, M. M., & Drenner, R. W. (2015). Hg-contaminated terrestrial spiders pose a potential risk to songbirds at Caddo Lake (Texas/Louisiana, USA). *Environmental Toxicology and Chemistry*, *34*(2), 303–306. https://doi.org/10.1002/etc.2796

Georg, R. B., & Newman, K. (2015). The effect of hydride formation on instrumental mass discrimination in MC-ICP-MS: A case study of mercury (Hg) and thallium (Tl) isotopes. *Journal of Analytical Atomic Spectrometry*, *30*(9), 1935–1944. https://doi.org/10.1039/c5ja00238a

Gimbert, F., Geffard, A., Guedron, S., Dominik, J., & Ferrari, B. J. (2016). Mercury tissue residue approach in *Chironomus riparius*: Involvement of toxicokinetics and comparison of subcellular fractionation methods. *Aquatic Toxicology*, *171*, 1–8. https://doi.org/10.1016/j.aquatox.2015.11.027

Gray, J. E., Pribil, J., & Higueras, P. L. (2013). Mercury isotope fractionation during ore retorting in the Almaden mining district, Spain. *Chemical Geology*, *357*, 150-157. https://doi.org/10.1016/j.chemgeo.2013.08.036

Griffith, M. B., Kaufmann, P. R., Herlihy, A. T., & Hill, B. H. (2001). Analysis of macroinvertebrate assemblages in relation to environmental gradients in Rocky Mountain streams. *Ecological Applications*, *11*(2), 489–505. https://doi.org/10.1890/1051-0761(2001)011[0489:Aomair]2.0.Co;2

Hannappel, M. P., Chumchal, M. M., Drenner, R. W., Kennedy, J. H., Barst, B. D., Castellini, J. M., Nolan, A. R., Willoughby, F. M., & Trauffler, L. P. (2021). Effect of body size on methylmercury concentrations in shoreline spiders: Implications for their use as sentinels. *Environmental Toxicology and Chemistry*, *40*(4), 1149–1154. https://doi.org/10.1002/etc.4964

Hepp, L. U., Pratas, J. A., & Graca, M. A. (2017). Arsenic in stream waters is bioaccumulated but neither biomagnified through food webs nor biodispersed to land. *Ecotoxicology and Environmental Safety*, *139*, 132–138. https://doi.org/10.1016/j.ecoenv.2017.01.035

Holloway, J. M., Pribil, M. J., McCleskey, R. B., Etheridge, A. B., Krabbenhoft, D. P., & Aiken, G. R. (2017). Mobilization of mercury and arsenic from a carbonate-hosted ore deposit, central Idaho, U.S.A. *Procedia Earth and Planetary Science*, *17*, 610–613. https://doi.org/10.1016/j.proeps.2016.12.163

Holloway, J. M., Pribil, M. J., McCleskey, R. B., Rutherford, D., Repert, D. A., DeWild, J., Breitmeyer, S., Berry, C., & Adams, M. (2016). *Water and sediment geochemistry data from the vicinity of Yellow Pine, Idaho, 2014–2015*. U.S. Geological Survey Data Release. https://doi.org/10.5066/F7TB150Z

Holloway, J. M., Pribil, M. J., McCleskey, R. B., Rutherford, D. L., Baldwin, A. K., DeWild, J. F., et al. (2018). *Water, soil, rock, and sediment geochemistry data from the vicinity of Yellow Pine, Idaho, 2015–2017*. U.S. Geological Survey Data Release. https://doi.org/10.5066/P9WC9J0M

Hsieh, T., Ma, K., & Chao, A. (2020). *iNEXT: Interpolation and extrapolation for species diversity*. R package version 2.0.20. http://chao.stat.nthu.edu.tw/wordpress/software_download/

Iwata, T. (2007). Linking stream habitats and spider distribution: Spatial variations in trophic transfer across a forest–stream boundary. *Ecological Research*, *22*(4), 619–628. https://doi.org/10.1007/s11284-006-0060-6

Jackson, A., Evers, D. C., Eagles-Smith, C. A., Ackerman, J. T., Willacker, J. J., Elliott, J. E., Lepak, J. M., Vander Pol, S. S., & Bryan, C. E. (2016). Mercury risk to avian piscivores across western United States and Canada. *Science of the Total Environment*, *568*, 685–696. https://doi.org/10.1016/j.scitotenv.2016.02.197

Jackson, A. K., Eagles-Smith, C. A., & Robinson, W. D. (2021). Differential reliance on aquatic prey subsidies influences mercury exposure in riparian arachnids and songbirds. *Ecology and Evolution*, *11*(11), 7003–7017. https://doi.org/10.1002/ece3.7549

Jardine, T. D., Hadwen, W. L., Hamilton, S. K., Hladyz, S., Mitrovic, S. M., Kidd, K. A., Tsoi, W. Y., Spears, M., Westhorpe, D. P., Fry, V. M., Sheldon, F., & Bunn, S. E. (2014). Understanding and overcoming baseline isotopic variability in running waters. *River Research and Applications*, *30*(2), 155–165. https://doi.org/10.1002/rra.2630

Jardine, T. D., Kidd, K. A., & Fisk, A. T. (2006). Applications, considerations, and sources of uncertainty when using stable isotope analysis in ecotoxicology. *Environmental Science & Technology*, *40*(24), 7501–7511. https://doi.org/10.1021/es061263h

Jardine, T. D., Kidd, K. A., & Rasmussen, J. B. (2012). Aquatic and terrestrial organic matter in the diet of stream consumers: Implications for mercury bioaccumulation. *Ecological Applications*, *22*(3), 843–855. https://doi.org/10.1890/11-0874.1

Kassambara, A. (2021). *rstatix: Pipe-friendly framework for basic statistical tests R package version 0.7.0*. https://CRAN.R-project.org/package=rstatix

Kraus, J. M., Pribil, M. J., Rutherford, D. L., Stricker, C. A., McGee, B. N., & Todd, A. S. (2022). Mercury concentrations, isotopic composition, biomass, and taxonomy of stream and riparian organisms in the vicinity of Yellow Pine, Idaho, 2015–2016. U.S. Geological Survey Data Release. 10.5066/P9P43XBX

Kraus, J. M., Schmidt, T. S., Walters, D. M., Wanty, R. B., Zuellig, R. E., & Wolf, R. E. (2014). Cross-ecosystem impacts of stream pollution reduce resource and contaminant flux to riparian food webs. Ecological Applications, 24(2), 235–243. https://doi.org/10.1890/13-0252.1

Lepak, J. M., Hooten, M. B., Eagles-Smith, C. A., Tate, M. T., Lutz, M. A., Ackerman, J. T., Willacker, J. J., Jr., Jackson, A. K., Evers, D. C., Wiener, J. G., Pritz, C. F., & Davis, J. (2016). Assessing potential health risks to fish and humans using mercury concentrations in inland fish from across western Canada and the United States. Science of the Total Environment, 571, 342–354. https://doi.org/10.1016/j.scitotenv.2016.03.031

Lewis, M. A., & Burraychak, R. (1979). Impact of copper mining on a desert intermittent stream in central Arizona: A summary. Journal of the Arizona-Nevada Academy of Science, 14(1), 22–29.

Lowe, W. H., & Likens, G. E. (2005). Moving headwater streams to the head of the class. BioScience, 55(3), 196–197. https://doi.org/10.1641/0006-3568(2005)055[0196:MHSTTH]2.0.CO;2

Maret, T. R., Cain, D. J., MacCoy, D. E., & Short, T. M. (2003). Response of benthic invertebrate assemblages to metal exposure and bioaccumulation associated with hard-rock mining in northwestern streams, USA. Journal of the North American Benthological Society, 22(4), 598–620. https://doi.org/10.2307/1468356

Mason, R. P., Laporte, J., & Andres, S. (2000). Factors controlling the bioaccumulation of mercury, methylmercury, arsenic, selenium, and cadmium by freshwater invertebrates and fish. Archives of Environmental Contamination and Toxicology, 38(3), 283–297. https://doi.org/10.1007/s002449910038

McAlpine, J. F., Peterson, B. V., Shewell, G. E., Teskey, H. J., Vockeroth, J. R., & Wood, D. M. (1981). Manual of Nearctic Diptera. Volume 1. Agriculture Canada.

McGee, B. N., & Todd, A. (2016). Electrofishing results and sampling of bull trout and other aquatic vertebrates in the vicinity of Yellow Pine. U.S. Geological Survey Data Release, Idaho. https://doi.org/10.5066/F7M61JGJ

Merritt, R. W., Cummins, K. W., & Berg, M. B. (2008). An introduction to the aquatic insects of North America (4th ed.). Kendall/Hunt Publishing.

Mogren, C. L., von Kiparski, G. R., Parker, D. R., & Trumble, J. T. (2012). Survival, reproduction, and arsenic body burdens in Chironomus riparius exposed to arsenate and phosphate. Science of the Total Environment, 425, 60–65. https://doi.org/10.1016/j.scitotenv.2012.03.009

Naiman, R. J., Bilby, R. E., Schindler, D. E., & Helfield, J. M. (2002). Pacific salmon, nutrients, and the dynamics of freshwater and riparian ecosystems. Ecosystems, 5(4), 399–417. https://doi.org/10.1007/s10021-001-0083-3

Nez Perce Tribe Fisheries Resource Program. (2019). Nez Perce Tribe interests and activities in and around the Stibnite Gold Project Area. https://www.nezperce.org/wp-content/uploads/2019/06/Whitepaper_NPT-interests-and-activities-in-and-around-the-Stibnite-gold-project-area_Final.pdf

Ogorek, J. M., Lepak, R. F., Hoffman, J. C., DeWild, J. F., Rosera, T. J., Tate, M. T., Hurley, J. P., & Krabbenhoft, D. P. (2021). Enhanced susceptibility of methylmercury bioaccumulation into seston of the Laurentian great lakes. Environmental Science & Technology, 55(18), 12714–12723. https://doi.org/10.1021/acs.est.1c02319

Ortega-Rodriguez, C. L., Chumchal, M. M., Drenner, R. W., Kennedy, J. H., Nowlin, W. H., Barst, B. D., Polk, D. K., Hall, M. N., Williams, E. B., Lauck, K. C., Santa-Rios, A., & Basu, N. (2019). Relationship between methylmercury contamination and proportion of aquatic and terrestrial prey in diets of shoreline spiders. Environmental Toxicology and Chemistry, 38(11), 2503–2508. https://doi.org/10.1002/etc.4579

Otter, R. R., Beaubien, G. B., Olson, C. I., Walters, D. M., & Mills, M. A. (2020). Practical considerations for the incorporation of insect-mediated contaminant flux into ecological risk assessments. In Contaminants and ecological subsidies, pp. 179–195. Springer.

Otter, R. R., Hayden, M., Mathews, T., Fortner, A., & Bailey, F. C. (2013). The use of tetragnathid spiders as bioindicators of metal exposure at a coal ash spill site. Environmental Toxicology and Chemistry, 32(9), 2065–2068. https://doi.org/10.1002/etc.2277

Oklahoma State University Library. (2022). Tribal Treaties Database: Treaty with the Nez Perces, 1855. June 11, 1855, 12 Stat. 957. https://treaties.okstate.edu/treaties/treaty-with-the-nez-perces-1855.-(0702)

Pennuto, C. M., & Smith, M. (2015). From midges to spiders: Mercury biotransport in riparian zones near the Buffalo River Area of Concern (AOC), USA. Bulletin of Environmental Contamination and Toxicology, 95(6), 701–706. https://doi.org/10.1007/s00128-015-1658-6

Post, D. M. (2002). Using stable isotopes to estimate trophic position: Models, methods, and assumptions. Ecology, 83(3), 703–718. https://doi.org/10.1890/0012-9658(2002)083[0703:Usitet]2.0.Co;2

Pribil, M. J., Rimondi, V., Costagliola, P., Lattanzi, P., & Rutherford, D. L. (2020). Assessing mercury distribution using isotopic fractionation of mercury processes and sources adjacent and downstream of a legacy mine district in Tuscany, Italy. Applied Geochemistry, 117, 104600. https://doi.org/10.1016/j.apgeochem.2020.104600

R Core Team. (2020). R: A language and environment for statistical computing. R Foundation for Statistical Computing. https://www.R-project.org/

Rutherford, D. L., McGee, B. N., & Pribil, M. (2020). Hg concentrations of fish tissue samples in the vicinity of Yellow Pine. U.S. Geological Survey Data Release. 10.5066/P9G2B6HF

Sanzone, D. M., Meyer, J. L., Marti, E., Gardiner, E. P., Tank, J. L., & Grimm, N. B. (2003). Carbon and nitrogen transfer from a desert stream to riparian predators. Oecologia, 134(2), 238–250. https://doi.org/10.1007/s00442-002-1113-3

Saunders, W. C., Fausch, K. D., & White, G. C. (2011). Accurate estimation of salmonid abundance in small streams using nighttime removal electrofishing: An evaluation using marked fish. North American Journal of Fisheries Management, 31(2), 403–415. https://doi.org/10.1080/02755947.2011.578526

Tremblay, A., Cloutier, L., & Lucotte, M. (1998). Total mercury and methylmercury fluxes via emerging insects in recently flooded hydroelectric reservoirs and a natural lake. Science of the Total Environment, 219(2–3), 209–221. https://doi.org/10.1016/s0048-9697(98)00227-7

Tsui, M. T., Blum, J. D., Kwon, S. Y., Finlay, J. C., Balogh, S. J., & Nollet, Y. H. (2012). Sources and transfers of methylmercury in adjacent river and forest food webs. Environmental Science & Technology, 46(20), 10957–10964. https://doi.org/10.1021/es3019836

Tweedy, B. N., Drenner, R. W., Chumchal, M. M., & Kennedy, J. H. (2013). Effects of fish on emergent insect-mediated flux of methyl mercury across a gradient of contamination. Environmental Science & Technology, 47(3), 1614–1619. https://doi.org/10.1021/es303330m

Twining, C. W., Razavi, N. R., Brenna, J. T., Dzielski, S. A., Gonzalez, S. T., Lawrence, P., Cleckner, L. B., & Flecker, A. S. (2021). Emergent freshwater insects serve as subsidies of methylmercury and beneficial fatty acids for riparian predators across an agricultural gradient. Environmental Science & Technology, 55(9), 5868–5877. https://doi.org/10.1021/acs.est.0c07683

U.S. Environmental Protection Agency. (2018). Cinnabar Mine Site 2018 removal site evaluation summary report, Yellow Pine, Idaho (Contract Number EP-S7-13-07; Task Order, 0030).

Vander Zanden, M. J., & Fetzer, W. W. (2007). Global patterns of aquatic food chain length. Oikos, 116(8), 1378–1388. https://doi.org/10.1111/j.2007.0030-1299.16036.x

Vander Zanden, M. J., & Rasmussen, J. B. (1999). Primary consumer $\delta^{13}C$ and $\delta^{15}N$ and the trophic position of aquatic consumers. Ecology, 80(4), 1395–1404. https://doi.org/10.1890/0012-9658(1999)080[1395:Pccana]2.0.Co;2

Venables, W. N., & Ripley, B. D. (2002). Modern applied statistics with S. (4th ed.). Springer.

Walters, D. M., Fritz, K. M., & Otter, R. R. (2008). The dark side of subsidies: Adult stream insects export organic contaminants to riparian predators. Ecological Applications, 18(8), 1835–1841. https://doi.org/10.1890/08-0354.1

Ward, D. M., Nislow, K. H., & Folt, C. L. (2010). Bioaccumulation syndrome: Identifying factors that make some stream food webs prone to elevated mercury bioaccumulation. Annals of the New York Academy of Sciences, 1195(1), 62–83. https://doi.org/10.1111/j.1749-6632.2010.05456.x

Ward, J. V., Kondratieff, B. C., & Zuellig, R. E. (2002). *An illustrated guide to the mountain stream insects of Colorado*. University Press of Colorado.

Wickham, H. (2016). *ggplot2: Elegant graphics for data analysis*. Springer-Verlag.

Wiener, J. G., & Suchanek, T. H. (2008). The basis for ecotoxicological concern in aquatic ecosystems contaminated by historical mercury mining. *Ecological Applications*, *18*(8 Suppl), A3–A11. https://doi.org/10.1890/06-1939.1

Wipfli, M. S., & Baxter, C. V. (2010). Linking ecosystems, food webs, and fish production: Subsidies in salmonid watersheds. *Fisheries*, *35*(8), 373–387. https://doi.org/10.1577/1548-8446-35.8.373

Xie, L., Flippin, J. L., Deighton, N., Funk, D. H., Dickey, D. A., & Buchwalter, D. B. (2009). Mercury(II) bioaccumulation and antioxidant physiology in four aquatic insects. *Environmental Science & Technology*, *43*(3), 934–940. https://doi.org/10.1021/es802323r

Can stream and riparian restoration offset climate change impacts to salmon populations?

5 authors, including:

Casey Justice
Columbia River Inter-Tribal Fish Commission
13 PUBLICATIONS 128 CITATIONS

SEE PROFILE

Seth M. White
Columbia River Inter-Tribal Fish Commission
27 PUBLICATIONS 265 CITATIONS

SEE PROFILE

Dale Mccullough
Columbia River Inter-Tribal Fish Commission
23 PUBLICATIONS 1,099 CITATIONS

SEE PROFILE

Monica R Blanchard
1 PUBLICATION 61 CITATIONS

SEE PROFILE

Some of the authors of this publication are also working on these related projects:

Riverscape studies of salmonids in the American West View project

Communicating sustainable forestry issues in the American West View project

Research article

Can stream and riparian restoration offset climate change impacts to salmon populations?

Casey Justice[*], Seth M. White, Dale A. McCullough, David S. Graves, Monica R. Blanchard

Columbia River Inter-Tribal Fish Commission, 700 NE Multnomah St., Portland, OR 97232, USA

ABSTRACT

Understanding how stream temperature responds to restoration of riparian vegetation and channel morphology in context of future climate change is critical for prioritizing restoration actions and recovering imperiled salmon populations. We used a deterministic water temperature model to investigate potential thermal benefits of riparian reforestation and channel narrowing to Chinook Salmon populations in the Upper Grande Ronde River and Catherine Creek basins in Northeast Oregon, USA. A legacy of intensive land use practices in these basins has significantly reduced streamside vegetation and increased channel width across most of the stream network, resulting in water temperatures that far exceed the optimal range for salmon growth and survival. By combining restoration scenarios with climate change projections, we were able to evaluate whether future climate impacts could be offset by restoration actions. A combination of riparian restoration and channel narrowing was predicted to reduce peak summer water temperatures by 6.5 °C on average in the Upper Grande Ronde River and 3.0 °C in Catherine Creek in the absence of other perturbations. These results translated to increases in Chinook Salmon parr abundance of 590% and 67% respectively. Although projected climate change impacts on water temperature for the 2080s time period were substantial (i.e., median increase of 2.7 °C in the Upper Grande Ronde and 1.5 °C in Catherine Creek), we predicted that basin-wide restoration of riparian vegetation and channel width could offset these impacts, reducing peak summer water temperatures by about 3.5 °C in the Upper Grande Ronde and 1.8 °C in Catherine Creek. These results underscore the potential for riparian and stream channel restoration to mitigate climate change impacts to threatened salmon populations in the Pacific Northwest.

1. Introduction

The warming effects of climate change and land use on streams threaten to drastically reduce fish distribution and viability throughout the Pacific Northwest (Beechie et al., 2013) and across the globe (Ficke et al., 2007). Human alterations to the atmosphere and landscape and can influence water temperature by changing one or more of the primary factors that regulate stream temperature, including climatic drivers (e.g., air temperature and precipitation), discharge, stream morphology, groundwater interactions, and riparian canopy condition (Poole and Berman, 2001). Human-caused CO_2 emissions have contributed to a significant warming trend in Pacific Northwest streams during summer of approximately 0.22 °C/decade between 1980 and 2009 (Isaak et al., 2012),

and August stream temperatures are projected to increase on average, +2.83 °C by the 2080s (Isaak et al., 2015). In addition to climate impacts, increases in water temperature can result from decreased streamflow, simplification of stream channels (e.g., increased width-to-depth ratio and reduced hyporheic exchange), and reduction of riparian vegetation cover (i.e., increased solar radiation reaching the stream) (Poole and Berman, 2001). These modifications are often the consequence of land use activities such as water diversions for irrigation or urban use, tree harvest in riparian zones (Beschta et al., 1987; Moore et al., 2005), poorly managed livestock grazing (Kauffman and Krueger, 1984; Belsky et al., 1999), and stream channelization associated with construction of roads, levees, and other impediments (e.g., mine tailings) (Simon and Rinaldi, 2006).

Water temperature is widely recognized as one of the most important environmental factors influencing the geographic distribution, growth, and survival of fish and other aquatic organisms (Regier et al., 1990; Armour, 1991; McCullough, 1999). Temperature

---

can directly affect physiological processes such as cardiorespiratory performance, food consumption, and osmoregulation (Whitney et al., 2016), as well as migratory behavior, resistance to disease and parasites, and inter- and intra-specific competitive interactions (Armour, 1991; Lynch et al., 2016). In addition, fish will often exhibit thermoregulatory behavior to optimize physiological performance, such as seeking out cold water refuges when ambient temperatures approach stressful levels (Breau et al., 2011; Myrick and Cech, 2004). As stream temperature regimes change in response to land management and climate change, cold-water fishes such as Chinook Salmon (*Oncorhynchus tshawytscha*) and steelhead (*O. mykiss*) may be exposed to temperatures that are outside of their physiologic optimum, resulting in changes to fish communities and potential increased risk of extinction (Poole et al., 2001; Urban, 2015).

Salmon populations are an important cultural, economic and food resource for indigenous tribes and others in the Columbia River basin and throughout the Pacific Northwest. Tributary and estuarine habitat degradation, combined with other factors such as hydroelectric operations in the mainstem Snake and Columbia rivers, predation, and commercial and sport fishing contributed to the decline and subsequent listing of numerous Columbia River basin salmon populations under the Endangered Species Act (ESA) (NOAA, 2008). Recovery of these salmon populations will require a comprehensive management approach that addresses all limiting factors to salmon viability including tributary and estuarine habitat, hydropower impacts, and predation. However, recent emphasis and considerable expense has been directed at restoration of tributary habitat conditions as a means to mitigate for hydropower impacts to threatened salmon populations (BPA, 2008; NOAA, 2008). The extent to which habitat restoration can achieve this goal, particularly in the context of warming stream temperatures due to climate change, has been identified as a critical uncertainty in the Columbia River basin (ISAB/ISRP, 2016).

Given the threat that high water temperature poses on fish populations throughout the Pacific Northwest (Beechie et al., 2013) and across North America (Lynch et al., 2016), it is important to understand the extent to which stream and riparian restoration activities can mitigate future water temperature increases due to climate change (Bernhardt et al., 2005; Ficklin et al., 2014). While similar studies in the Pacific Northwest have examined the potential influence of riparian and channel restoration on water temperature (Chen et al., 1998; Sullivan and Rounds, 2004; Watanabe et al., 2005; Butcher et al., 2010), few have integrated riparian restoration with climate change projections to evaluate whether restoration actions would be sufficient to offset climate change impacts (Battin et al., 2007; Bond et al., 2015). Our research additionally draws on fish-habitat relationships developed from empirical fish and habitat data to evaluate how fish populations would respond to simulated changes in water temperature. Integrating predicted changes in habitat conditions with fish population response provides a critical link needed by natural resource managers to evaluate the potential benefits of restoration actions and to plan and adjust management decisions accordingly.

We used a water temperature simulation model to investigate potential thermal benefits of riparian reforestation and channel narrowing in context of future climate change to Chinook Salmon populations in the Upper Grande Ronde River and Catherine Creek in Northeast Oregon. Our specific objectives were 1) to simulate water temperature changes that may result from restoration actions, 2) to evaluate whether future climate change impacts could be offset by riparian and channel restoration actions, 3) to predict how simulated temperature changes would influence the abundance of Chinook Salmon summer parr, and 4) to develop a tool that can be used by restoration planners and practitioners to investigate alternative land-management strategies and prioritize restoration actions.

2. Methods

2.1. Study area

The Grande Ronde River is a major tributary of the Snake River, originating in the Blue Mountains of NE Oregon and flowing approximately 340 km north/northwest before joining the Snake River in SE Washington. The study area included select reaches of the Upper Grande Ronde Basin (UGRB), which is located upstream of the Catherine Creek confluence near the city of La Grande, and the Catherine Creek Basin (CCB), a large tributary of the Grande Ronde River (Fig. 1). The UGRB and CCB drain areas of approximately 1896 and 1051 km^2, respectively. This area is typified by cold winters with ample snow in its headwaters areas, and hot, dry summers. Basin tributaries are primarily fed by snowmelt, with peak flows occurring during the spring, and base flows occurring during the late summer. Due to the relatively lower elevation of headwater peaks in the UGRB compared with CCB, snowmelt generally occurs earlier in the UGRB, often resulting in very low summer base flows and warmer water temperatures.

Habitat for fish and other aquatic life in the Grande Ronde basin has been steadily degraded since the mid-1800s due to land use, with water temperature being arguably one of the most impaired and influential factors for ESA-listed Chinook Salmon, steelhead, and bull trout in the basin. The Environmental Protection Agency (EPA) established a set of temperature water quality standards for the Pacific Northwest region to protect threatened salmonids which include a maximum weekly maximum temperature of 16 °C for juvenile salmon/trout rearing, 18 °C for salmon/trout migration plus non-core rearing, and 20 °C for salmon/trout migration (EPA, 2003). As of 1999, approximately 92% of the Grande Ronde River upstream of the Wallowa River confluence exceeded the 18 °C temperature standard (ODEQ, 2000).

This study focused on two threatened salmon populations within the Snake River spring/summer Chinook Evolutionary Significant Unit (ESU), the Upper Grande Ronde River Spring Chinook and Catherine Creek Spring Chinook. These focal populations were chosen because of the perceived large juvenile life-stage survival gaps due to habitat impairments and because of the existence of high quality fish and habitat monitoring data.

2.2. Temperature model

We used a deterministic water temperature model, Heat Source (Boyd and Kasper, 2003), to simulate water temperature and flow dynamics in major salmon-bearing streams of the UGRB and CCB (Fig. 1). Heat Source uses stream channel geometry, hydrology, climatic conditions, and riparian vegetation cover and height to simulate stream temperature and effective shade at 100 m intervals (termed model nodes) throughout the stream network. The Heat Source model was selected because it has been applied extensively throughout Oregon (ODEQ, 2000; Crown et al., 2008; Watershed Sciences, 2008; Butcher et al., 2010) and elsewhere in the Pacific Northwest to evaluate compliance with water temperature standards, and because it's well suited to simulating the effects of riparian vegetation on stream temperature at a fine spatial resolution—a feature that is useful for restoration prioritization.

Model inputs including channel topography (i.e., stream width and gradient) and riparian vegetation (canopy height and density) were measured using light detection and ranging (LiDAR) data collected in 2009. Climatic data, including air temperature, cloud cover, relative humidity, and wind speed, were recorded by the National Weather Service at the La Grande airport and by the US
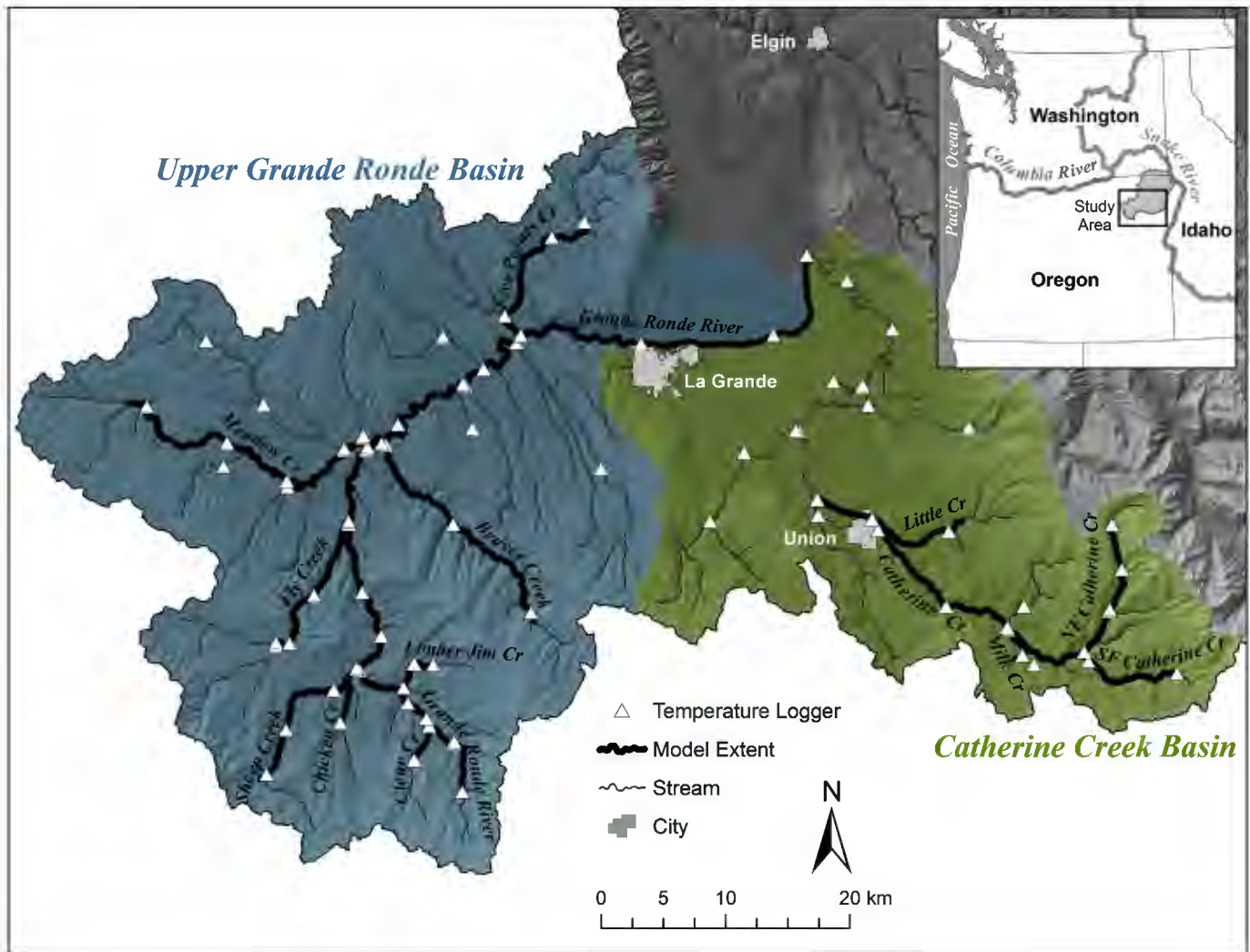
Fig. 1. Map of the study area in the Upper Grande Ronde River and Catherine Creek basins in NE Oregon showing the stream segments that were modeled using Heat Source.

Forest Service at the J Ridge weather station in the UGRB. Streamflow inputs were obtained from nearby gaging stations and manual streamflow measurements collected at discrete locations throughout the stream network. Water temperature was measured using HOBO temperature loggers placed at model boundaries and tributary junctions (Fig. 1). In addition, remotely-sensed forward looking infrared (FLIR) surveys were conducted during summer of 2010 to capture a snapshot of peak daily water temperatures throughout the stream network (Watershed Sciences, 2010). The model was calibrated to conditions observed during 2010 by adjusting model parameters such as channel roughness and hyporheic exchange to minimize the deviation between observed and predicted water temperatures.

The model extent was intended to represent all stream reaches within current and historic Chinook Salmon spawning and rearing areas in the UGRB and CCB. However, some portions of the stream network were excluded from the temperature model because low stream flows precluded accurate temperature modeling with Heat Source (e.g., lower Catherine Creek). Modeling of water temperatures downstream of the Catherine Creek confluence (i.e., migration corridor to the Pacific Ocean) was beyond the scope of this study. A complete description of model development procedures is provided in Watershed Sciences (2012).

Model parameters from the calibrated 2010 model (hereby referred to as current conditions) were used as a baseline for evaluating a suite of model scenarios representing different assumptions about potential riparian restoration, channel morphology restoration, and climate change (Table 1). The model provides hourly temperature predictions for a 10-week period between July 10 and September 20, 2010, a time frame chosen to represent summer base flow conditions when water temperatures are typically highest and salmonids are consequently at risk. For consistency with EPA water quality standards (EPA, 2003), we calculating the maximum 7-day running average of the daily maximum temperature in degrees Celsius, hereby referred to as maximum weekly maximum temperature (MWMT) for each model node. Water temperature predictions were summarized by basin (i.e., UGRB and CCB) to simplify model outputs and aid in interpretation of the results.

Examination of historical air temperature and streamflow data indicated that 2010 was a fairly average year and was therefore a reasonable baseline for comparison with model scenarios investigating future restoration benefits. For example, average summer air temperature (July–September) measured in the city of La Grande between 1965 and 2010 ranged from 13.9 to 21.4 °C (mean = 18.2 °C), compared with an average summer temperature

Table 1
Description of ten model scenarios used to evaluate the influence of riparian restoration, channel narrowing, and climate change on water temperature.

Model number	Model name	Model description
1	Current	Baseline model calibrated using 2010 temperature, climate, vegetation, and hydrologic conditions
2	PNV	Vegetation across the entire model extent set to potential natural vegetation (PNV) cover and height.
3	High Priority	Vegetation in high priority areas set to PNV and other areas set to current conditions.
4	High/Med Priority	Vegetation in high and medium priority areas set to PNV and all other areas set to current conditions.
5	High/Med/Low Priority	Vegetation in high, medium, and low priority areas set to PNV and very low priority areas set to current conditions.
6	Width	Channel width set to historic conditions and vegetation set to current conditions.
7	Width/PNV	Channel width set to historic conditions and vegetation set to PNV.
8	Climate 2080s	Air temperature and streamflow set to 2080s climate projections.
9	Climate 2080s/Veg	2080s climate projections and vegetation set to potential cover and height at 75 years.
10	Climate 2080s/Veg/ Width	2080s climate projections, vegetation set to potential cover and height at 75 years, and channel width set to historic conditions.

of 17.4 °C in 2010 (2010 percentile = 27%). Similarly, average summer streamflow (July–September) in the Grande Ronde River near Perry between 1993 and 2014 ranged from 0.6 to 6.8 m^3/s (mean = 1.9 m^3/s), while summer streamflow in 2010 averaged 1.6 m^3/s (2010 percentile = 57%).

2.3. Riparian restoration

To simulate restoration of riparian vegetation, we first needed to estimate the potential height and canopy cover of trees and shrubs in the riparian zone under natural historic conditions (i.e., prior to intensive anthropogenic disturbance). To do this, we assembled a team of riparian ecologists with extensive experience in the Blue Mountains region to develop a detailed map of current vegetation and potential natural vegetation (PNV) for a 100-m wide stream buffer (each side of stream centerline) throughout the Chinook-bearing portions of the Upper Grande Ronde and Catherine Creek watersheds that incorporates physiography, geomorphology, soils, vegetation, and disturbance (Wells et al., 2015).

Potential tree and shrub canopy cover was estimated from extensive field measurements of canopy cover collected within each plant association group (PAG) as documented in local vegetation classifications (Kauffman et al., 1985; Johnson and Simon, 1987; Johnson and Clausnitzer, 1992; Crowe and Clausnitzer, 1997; Crowe et al., 2004; Wells, 2006). Specifically, potential tree and shrub cover were estimated independently by summing the product of constancy (proportion of total vegetation plots in which a species occurred) and average cover (percent canopy cover for a species averaged over all vegetation plots where the species occurred) across all species within each PAG.

Potential tree height was estimated from species-specific dominant tree height growth curves from regional forestry literature (Dahms, 1975; Clendenen, 1977; Barrett, 1978; Herman et al., 1978; Cochran, 1979, 1985; Monserud, 1985; Nussbaum, 1996). Within each PAG, we calculated a weighted-average growth curve by averaging all species-specific growth curves weighted by the average canopy cover value for each species. We used these growth curves to estimate the average tree height under fully restored PNV conditions (model scenario 2). Height at 300 years was assumed to represent the maximum potential tree height due to limitations with extrapolating the growth curves too far beyond the range of the data and because tree growth beyond 300 years is minimal. For scenarios that combined climate change impacts with riparian restoration (i.e., scenarios 9 and 10), we estimated tree height at 75 years from current to correspond approximately with the time frame for which climate projections were available. Tree height and cover for these scenarios represents a snapshot at 75 years along the trajectory toward the PNV condition.

Potential shrub heights were obtained from Steele and Geier-

Hayes (1987, 1989, 1992, 1993, 1994) and from species descriptions in the Fire Effects Information System (USFS, 2015). Shrub heights were weighted by average cover of each species within each PAG to produce an average potential shrub canopy height.

To determine how quickly water temperatures could be reduced by riparian restoration, we ran a series of model scenarios (results not shown) representing maximum vegetation growth at 25, 50, 75, and 100 years from current, assuming that trees were planted at maximum density in year 1. For each of these scenarios, we calculated the percentage of maximum temperature change, assuming that the maximum temperature change was represented by the difference between the current and PNV (i.e., tree height and density at 300 years) scenarios.

2.3.1. Restoration prioritization

We developed four riparian restoration scenarios (model scenarios 2–5) by dividing the stream network into priority areas (high, medium, low, and very low priority). We started by weighting each model node by its distance from current spawning areas. For each model node i, the distance weight (DW_i) was given by the formula:

$$DW_i = e^{-0.075 \times d_i}, \tag{1}$$

where d_i is the distance in kilometers from the model node to the boundary of the nearest spawning area. This weighting scheme was based on a "restore from the core" perspective in which the most productive areas are restored first, and additional areas are subsequently restored moving in a downstream (i.e., less productive) direction. Sites within the current spawning area received a weight of 1, and the weight declined exponentially to near-zero as the distance from spawning increased to about 60 km. This formula was developed subjectively to conform to our general assumption that the value of riparian restoration to salmon population viability would decline steeply as the distance from productive spawning and rearing habitats increased, with most of the benefit occurring within a distance of 10–20 km from the current spawning extent and very limited benefit (i.e., $DW_i < 0.05$ wt) beyond a distance of 40 km.

Next we assigned each model node a weight based on the shade deficit (i.e., the difference between current and potential effective shade). Effective shade is a simulated output from the Heat Source model and is defined as the fraction of the total solar radiation that is blocked by streamside vegetation. Sites with the greatest difference between current and potential shade received a weight of 1, and the weight declined to zero as the shade deficit decreased. This approach essentially assigns the greatest weight to areas with the largest shade deficit, and thus the greatest potential to benefit from

riparian restoration. The shade weight (SW_i) at each model node i was given by the formula:

$$SW_i = (SP_i - SC_i)/SDMax, \qquad (2)$$

where SP_i is the effective shade under fully restored PNV conditions, SC_i is the effective shade under current conditions, and $SDMax$ is the maximum difference in effective shade between PNV and current conditions across all model nodes. Shade differences were divided by SDMax to ensure that the shade weights ranged from 0 to 1, consistent with the distance weights.

A final integrated weight for each model node was then calculated as the product of the distance and shade weights. Final weights were then averaged over 1 km stream segments and simplified into categories of high, med, low, and very low priority (Fig. 2). Model nodes with final weights that were at or above the 75th percentile of all final weight values were assigned to the high priority category. Model nodes between the 50th and 75th percentile were assigned to the medium category. Model nodes with weights between the 25th and 50th percentile were assigned as low priority, and nodes with weights below the 25th percentile were assigned as very low priority. The resulting four riparian restoration scenarios were implemented in Heat Source by setting the tree and shrub cover and height values to their maximum

potential within selected priority areas including: 1) high priority, 2) high and medium priority, 3) high, medium and low priority, and 4) high, medium, low, and very low priority (i.e., PNV).

2.4. Channel width

We simulated the influence of channel narrowing and deepening—a common restoration goal—on water temperature by adjusting channel width inputs in Heat Source to correspond with observed historical changes in stream width (model scenarios 6, 7 and 10). To define a historical baseline for channel width, we described changes to river channel widths since the late 1800s, with expectations that the magnitude of change would be greater in areas with more intense ranching, logging, agriculture, and other forms of land use. Historical estimates of river width were based on General Land Office (GLO) surveys (Principle Clerk of Surveys, General Land Office, 1855) conducted in the mid to late 1800s. Contemporary estimates of river width (1990s and 2000s) were based on Oregon Department of Fish and Wildlife's (ODFW) Aquatic Inventories Project (AIP) (Moore et al., 2008), a spatially continuous survey of common fish habitat characteristics across the river network.

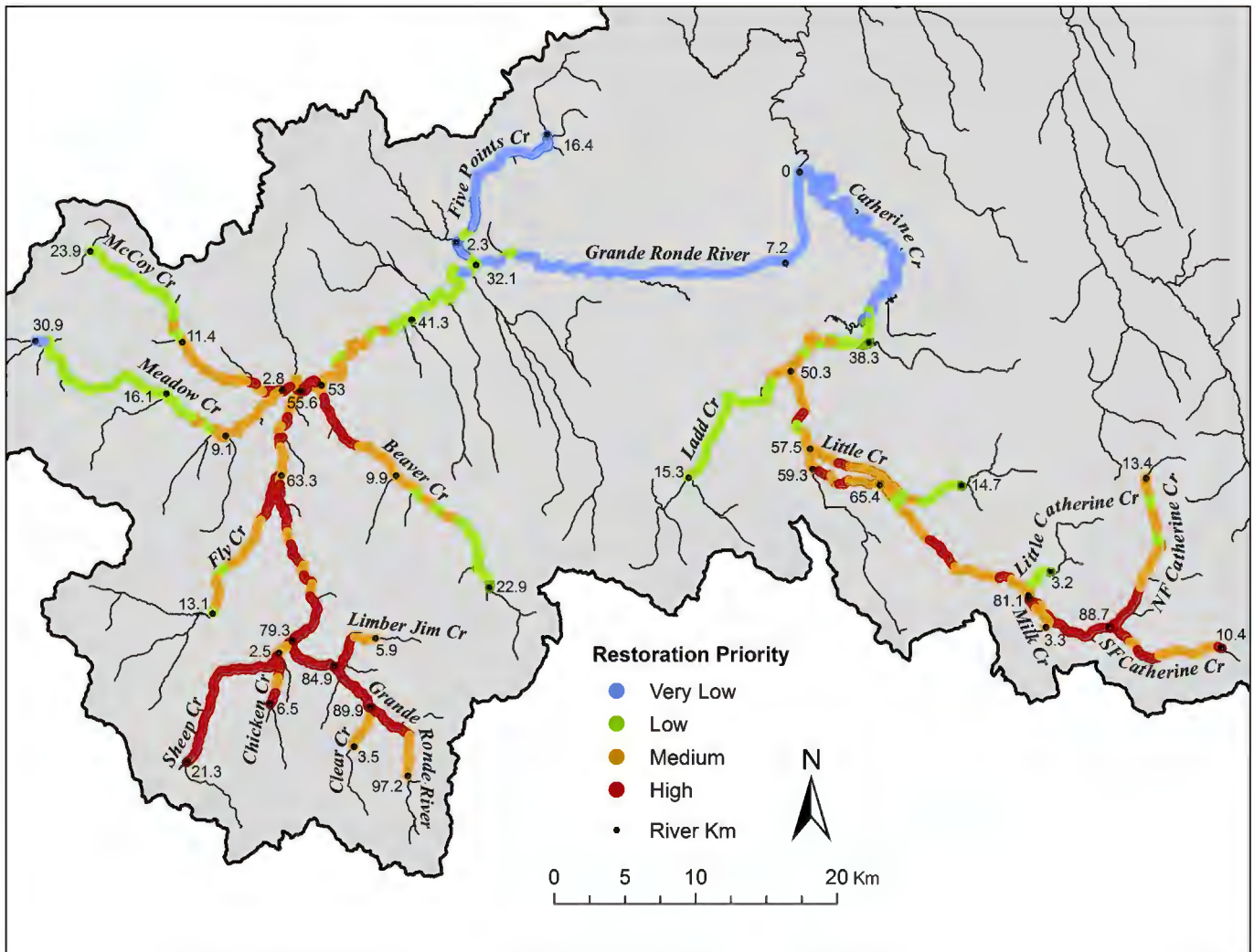Observed changes in channel width since the historical period

Fig. 2. Map of restoration priority areas in the Upper Grande Ronde and Catherine Creek basins.

were summarized using a geomorphic valley setting classification. The classification system consisted of dividing the stream network into small and large streams using an 8-m bankfull width criterion (Beechie and Imaki, 2014). Next, we divided the stream network into three valley types based on valley confinement (laterally unconfined, partly confined, and confined) following the methodology described in the River Styles Framework (Brierley and Fryirs, 2005). We simplified the classification into three classes for this analysis: (1) large streams, (2) small/partly confined and confined streams, and (3) small/laterally unconfined streams. For each class, we calculated the average percentage change in channel width from historic to current (i.e., large streams = 45.9%, small/partly confined and confined streams = 31.2%, small unconfined streams = 115.8%), and used these average values to simulate restoration of channel width across the stream network. Due to model constraints limiting the amount of channel narrowing possible for a given discharge, we fixed the % increase from historic to current for mainstem Catherine Creek to 25%. A detailed description of the channel width analysis used to support this modeling work is provided in McCullough et al. (2016).

2.5. Climate change

Air temperature and streamflow inputs to the temperature model were modified to predict how future climate change would influence water temperature (model scenarios 8–10). Projected changes to monthly air temperature and stream discharge for the 2080s future time period (2070–2099) were obtained from University of Washington Climate Impacts Group (UWCIG) (Littell et al., 2011). For this assessment, we used a composite of modeled changes to local climate, which includes an average of the ten global climate models with the best performance at simulating observed historical summer temperature and precipitation trends across the U.S. Pacific Northwest region. We used the A1B scenario family, which lies between the middle and high end of the spectrum of projected anthropogenic greenhouse gas emissions (UWCIG, 2010) and was previously chosen for region-wide stream temperature modeling efforts (Isaak et al., 2011). Projected changes to stream discharge for this scenario were produced with the VIC hydrology model by the UWCIG using the same set of global climate models.

In order to use these data in our assessment, we first needed to adjust for the differences between the baseline period in our study (2010) and the baseline period used by the UWCIG (i.e., 1916–2006). To do this, we used the Pacific Northwest Index (Ebbesmeyer and Strickland, 1995) summarized online by the UWCIG (2012) that includes measurements of air temperature, precipitation, and snowpack at three stations in the Pacific Northwest from 1891 to 2011. Using this index, we calculated the difference between the 2010 and 1916–2006 periods to be as follows: air temperature +0.8 °C; precipitation +1.6%. These differences were then used to modify the future climate change scenario adjustments so that they appropriately pertained to the 2010 baseline period. The final set of monthly projected changes in air temperature and streamflow used in the Heat Source model are provided in Table 2.

2.6. Fish abundance

We developed a statistical model using empirical fish abundance and remotely-sensed habitat data from the Upper Grande Ronde and Catherine Creek basins to predict how simulated water temperatures for each model scenario would influence juvenile Chinook Salmon abundance. Specifically, we used a linear mixed-effects model with Chinook summer parr density (fish/m stream length) as the dependent variable (*Density*), survey location (*Site*) as a random effect, and cumulative watershed area (km^2) upstream of the site (*Area*), site gradient (%) (*Gradient*), site *MWMT* (°C), and average redd density (redds/100 m stream length) within 2 km upstream of the site (*Redds*) as fixed-effect explanatory variables.

Snorkel counts of juvenile salmonids were conducted by field crews from the Columbia River Inter-Tribal Fish Commission (CRITFC) and ODFW at 77 sites in the Grande Ronde basin between 2011 and 2014 using a spatially balanced random survey design (Stevens and Olsen, 2004). A portion of sites were surveyed every year while others were surveyed every 3 years, resulting in a total sample size of 129. We used a mixed-model approach in order to utilize all of the data (i.e., increase statistical power) without violating the assumption of independence (i.e., samples within a site are not statistically independent). Snorkel counts at each site were expanded using a correction factor developed from paired mark-recapture and snorkel survey data to account for fish that were not observed by snorkelers (Jonasson et al., 2015).

Watershed area and gradient estimates were obtained from NetMap (http://www.terrainworks.com). Water temperature data were measured at each site using HOBO water temperature loggers as part of the Columbia Habitat Monitoring Program (CHaMP; https://www.champmonitoring.org/). Redd densities were calculated from GPS coordinates of all Chinook Salmon redds surveyed by ODFW and the Confederated Tribes of the Umatilla Indian Reservation (CTUIR) between 2010 and 2013 (McCullough et al., 2015). Redd locations were joined to the NetMap stream layer using ArcGIS and redd densities were calculated for each 100 m stream reach. For predictions of fish abundance by model scenario, we used the average redd density for all years combined (2010–2013). Redd densities during this time period were generally representative of typical redd abundance in the basin. For example, the number of redds observed in the Upper Grande Ronde River between 2010 and 2013 averaged 184 compared with a 10-year mean (2005–2014) of 122 (range 1–360). For portions of the river network that were not surveyed, we assumed redd densities were equivalent to the average value by river class (see classification system description in Channel Width). In addition, we applied a temperature screen of 22 °C *MWMT* (i.e., redd densities in unsurveyed reaches with *MWMT* > 22 °C were set to 0) to ensure that redds were not extrapolated into areas with temperatures exceeding the upper tolerance limits for Chinook spawning (Cooney et al., 2007).

Fish density, watershed area, and redd density were log transformed (natural logarithm) prior to analysis to ensure normality and homogeneity of variance. We added a small constant k to parr density ($k = 0.005$) and redd density ($k = 0.02$) values prior to transforming to avoid problems with log transformation of zero values. The relationship between temperature and fish density conformed to a piecewise functional relationship with a threshold temperature of 18 °C based on visual inspection of the raw data and documentation in the literature of 18 °C as a common upper threshold for rearing preference of juvenile salmonids (Welsh et al., 2001; EPA, 2003). Model assumptions were tested using standard diagnostic plots as well as formal tests of normality (Shapiro-Wilks Test). Potential collinearity among predictor variables was assessed by evaluating the variance inflation factors (VIF), where a VIF of <3 was interpreted as low evidence for collinearity (Zuur et al., 2010).

We used the linear mixed-effects model to predict fish density at each NetMap reach for each of the 10 model scenarios. Model predictions were based on fixed-effects only (i.e., random effects for *Site* were set to 0) to allow for predictions at out-of-sample locations. We assumed that fish could distribute into any stream reach within the model extent, which included both current and historic use areas for Chinook Salmon, at densities determined by the

Table 2
Projected changes in monthly air temperature and streamflow resulting from climate change for the 2080s time period.

Climate projections	Month			Average
	July	August	September	
Air temperature increase (°C) from 2010	4.7	5.0	4.3	4.7
Change in streamflow (%) from 2010	−21.2	−20.7	−18.3	−20.1

predictive model. Thus, as temperatures in currently warm areas are improved due to restoration, the predicted distribution and abundance of salmon expands accordingly. Density estimates were converted to abundance for each reach by multiplying the predicted fish density by reach length. Reach-scale abundance predictions were then summed for each basin (UGRB and CCB) to calculate total population abundance.

3. Results

3.1. Water temperature

Simulated water temperatures from the calibrated 2010 model tracked very closely with measured FLIR data. Root mean square error (RMSE) for all mainstem and tributary models ranged from 0.26 °C to 1.16 °C (mean = 0.62 °C), indicating good model accuracy across the model extent. Detailed model calibration results and longitudinal temperature profiles for each modeled stream within the study area were provided in Watershed Sciences (2012).

Water temperatures under current climatic, hydrologic and riparian conditions were substantially higher in the Upper Grande Ronde River basin (UGRB) (median *MWMT* across all model nodes = 24.4 °C) compared with the Catherine Creek basin (CCB) (median = 18.7 °C; Fig. 3). Simulated restoration of riparian vegetation substantially reduced the percentage of the stream network with peak summer water temperatures above 16 °C from 93% to 73% in the UGRB, and from 70% to 48% in the CCB (Fig. 4). Similarly, the proportion of habitat with *MWMT* exceeding 18 °C was predicted to decline from 86% to 61% in the UGRB and from 53% to 21.2% in the CCB following riparian restoration. Finally, the proportion of the stream network exceeding the incipient lethal limit of 25 °C declined from 40% to 6% in the UGRB, and from 6% to 0% in the CCB as a result of riparian reforestation. Despite these substantial potential reductions in water temperature, some areas in the lower mainstem Grande Ronde River and select tributaries were predicted to reach stressful peak temperatures even after riparian restoration (Fig. 4).

The relative temperature change resulting from riparian restoration was substantially higher in the UGRB compared with the CCB (Fig. 3). For example, the predicted change in median *MWMT* from the current condition to the PNV scenario was −5.5 °C in the UGRB, compared with −2.4 °C for the CCB. Similarly, the High, High/Med, and High/Med/Low priority scenarios reduced median *MWMT* by 2.9 °C, 4.1 °C, and 4.8 °C in the UGRB, and by 1.5 °C, 2.4 °C, and 2.4 °C in the CCB respectively.

Comparison of the current mainstem Grande Ronde River temperature profile with the four riparian restoration scenarios (scenarios 2—5) indicated that expected temperature reductions from riparian reforestation would be greatest in the upper to middle portion of the river (river km 86—32), but the influence of riparian restoration on water temperature diminished rapidly as the river entered the lower Grande Ronde Valley near river km 22 (Fig. 5). Simulated riparian restoration in high priority sites alone produced substantial reductions in *MWMT* in the mainstem Grande Ronde River up to 6.9 °C (median = 1.0 °C) compared with current

conditions, but these benefits diminished rapidly downstream of Beaver Creek (river km 53). Similarly, restoration of high and medium priority areas was predicted to reduce water temperatures up to 7.2 °C (median = 3.6 °C) below current. Temperature reductions from this scenario extended further downstream to about river km 40, after which the stream was predicted to warm rapidly to a level similar to current conditions. Complete riparian restoration throughout the UGRB (i.e., PNV scenario) could reduce median *MWMT* in the main stem by approximately 4.4 °C. However, post-restoration water temperatures in the lower portion of the river (i.e., below river km 32) were predicted to be quite high (>22 °C), suggesting that restoration of these very low priority areas would likely provide limited additional thermal benefit for salmonids in the mainstem Grande Ronde River.

Model simulations representing maximum vegetation growth at 25 year increments showed that the most rapid reductions in temperature occurred during the first 25 years, with incremental reductions in temperature gradually leveling off over time, with relatively little additional benefit occurring after year 75. For example, between year 0 and year 25, predicted median water temperature in the Upper Grande Ronde basin declined from 24.4 °C to 22.2 (−2.2 °C). In comparison, the decrease in median water temperature between year 75 and year 300 (PNV) was only −0.7 °C. By year 75, approximately 85% of the maximum temperature benefit was achieved, with relatively little benefit occurring thereafter.

Simulated narrowing of the river channel—assuming that riparian and climatic conditions remained constant—reduced median *MWMT* in the UGRB from 24.4 °C under current conditions to 22.2 °C (difference = −2.2 °C). Similarly, median *MWMT* in the CCB was predicted to decline from 18.3 °C under current conditions to 17.7 °C following channel narrowing (difference = −0.6 °C) (Fig. 3). A combination of basin-wide riparian restoration and channel narrowing (model scenario 7) was predicted to reduce median water temperatures by 6.5 °C in the UGRB compared with 3.0 °C in the CCB.

Projected increases in air temperature and reduced summer streamflow associated with climate change for the 2080s time period increased median *MWMT* by 2.7 °C in the UGRB and 1.5 °C in Catherine Creek (Fig. 3). However, simulated basin-wide restoration of riparian vegetation coincident with climate change impacts was estimated to decrease median *MWMT* by 1.9 °C and 1.7 °C in the UGRB and CCB respectively. Finally, a combination of climate change, vegetation restoration, and channel narrowing produced a net decrease in median water temperature of 3.5 °C in the UGRB and 1.8 °C in the CCB.

Median water temperature in the mainstem Grande Ronde River was projected to increase by approximately 3.4 °C above current conditions as a result of climate change, with maximum summer water temperatures exceeding the lethal limit for Chinook Salmon (i.e., 25 °C) across most of the river length (Fig. 6). However, basin-wide riparian restoration was predicted to offset these impacts and even reduce water temperature by as much as 3.4 °C (median = 0.4°) below the current condition (scenario 9), particularly in the middle and upper portions of the river upstream of
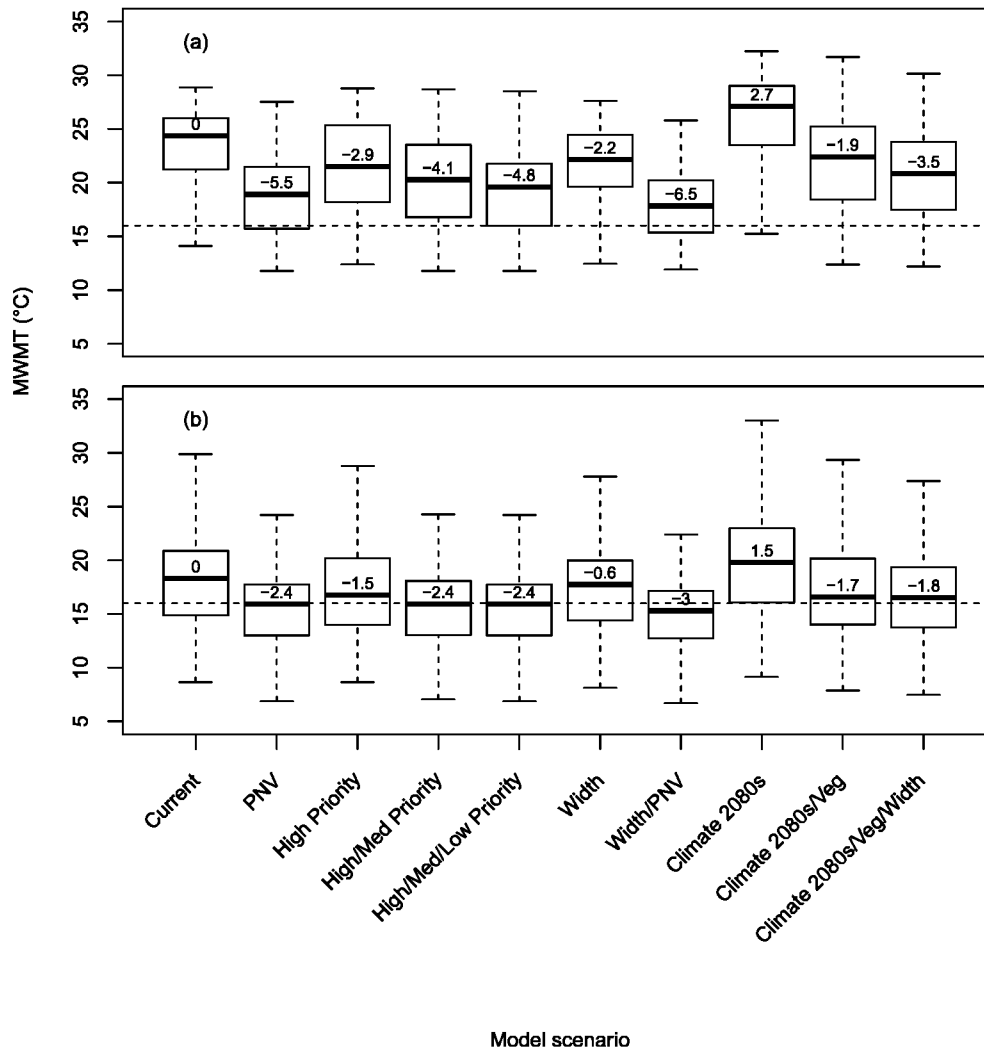
Fig. 3. Simulated maximum weekly maximum water temperatures (*MWMT*; °C) for each model scenario in (a) the Upper Grande Ronde River, and (b) Catherine Creek basins. Each box plot represents the distribution of *MWMT* values across all model nodes within the two focal watersheds including main stem and tributary locations. The numbers within each box represent the change in median temperature from current condition. The dashed red line indicates the Environmental Protection Agency's (EPA) temperature standard for core juvenile salmon rearing of 16 °C.

Beaver Creek. A combination of climate change, vegetation restoration, and channel narrowing (scenario 10) was predicted to reduce peak water temperatures in the mainstem Grande Ronde River by as much as 5.1 °C (median = 2.0 °C). These temperature reductions were limited primarily to the area upstream of Five Points Creek. Downstream of Five Points Creek, the predicted temperature profile for scenario 10 tracked closely with current conditions.

3.2. Fish abundance

The linear mixed effects model explained approximately 51% (adjusted R^2) of the variation in Chinook Salmon parr density. Temperature explained the greatest proportion of the model variation (31.5%), followed by redd density (14.7%), gradient (2.8%) and drainage area (1.8%). The temperature-density relationship was a piecewise function that was flat up to 18 °C, and then declined to near 0 at 28 °C (Fig. 7). All fixed-effect model terms were statistically significant at the $\alpha = 0.05$ level (p < 0.01). The random grouping factor (site) explained a negligible amount of the total variation in the data (site standard deviation < 0.001, residual

standard deviation = 1.761), but was included in the model to ensure that the model assumption of independence was satisfied. Diagnostic plots as well as formal tests of normality indicated that model assumptions were satisfied (Shapiro-Wilks Test, p < 0.05). Variance inflation factors (VIF) for independent variables were less than 3, indicating a low degree of collinearity among model covariates. The fit of the model to the data was only fair as evidenced by the somewhat low overall R^2 for the model and consequently, predictions to out-of-sample locations will be even less precise. However, because model errors were reasonably symmetric across the range of the data, we assumed that relative differences in predicted abundance among the different model scenarios are reasonably accurate. The final model used to predict fish abundance was given by:

$$\log(Density + 0.005) = \beta_0 + \beta_1 * \log(Area) + \beta_2 * Gradient \\ + \beta_3 * (MWMT - 18) \\ + \beta_4 * \log(Redds + 0.02), \quad (3)$$

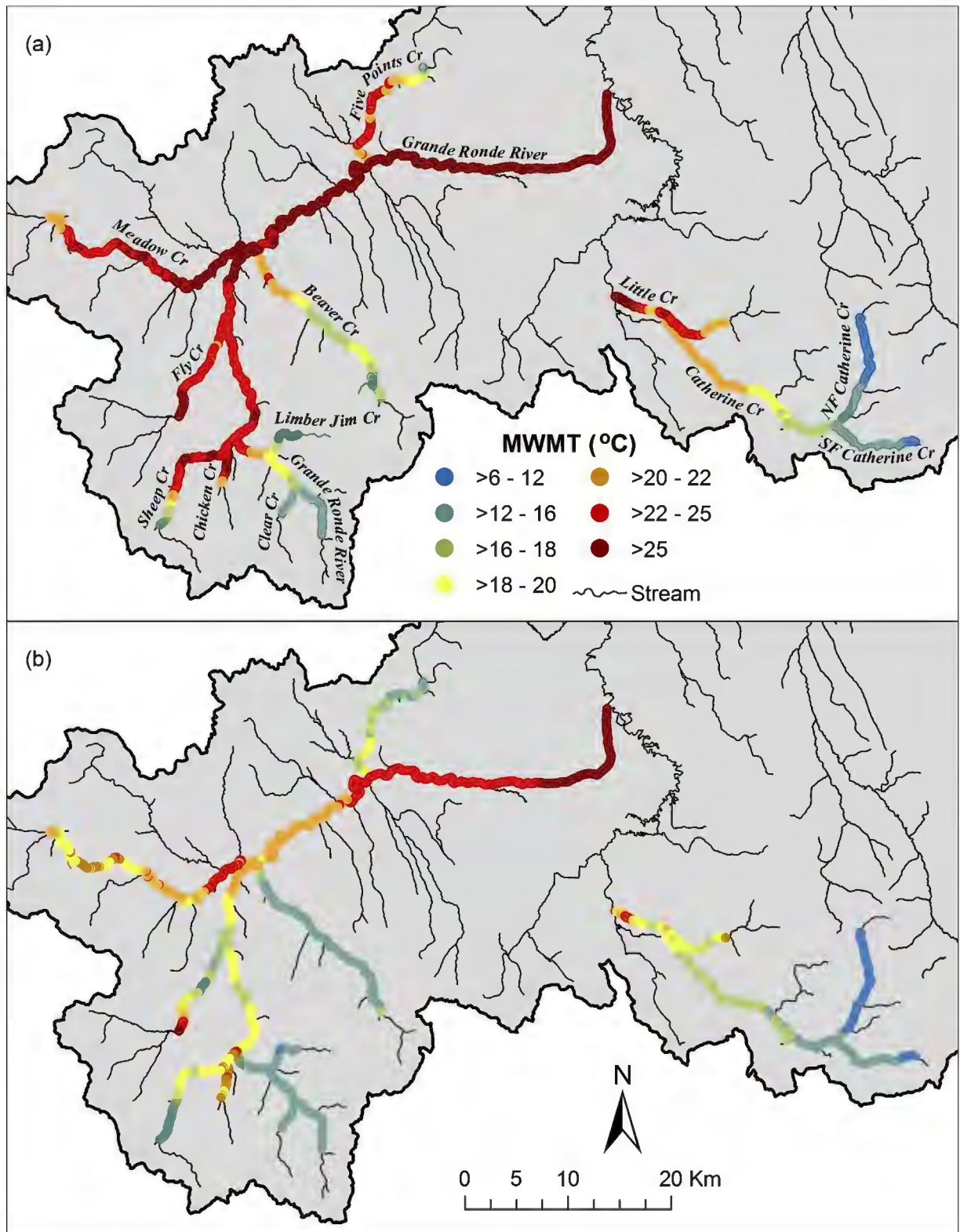where model coefficients (β_i) were given by:

Fig. 4. Map of simulated maximum weekly maximum water temperature (*MWMT*; °C) for (a) current conditions and (b) potential natural vegetation (PNV) conditions in the Upper Grande Ronde River and Catherine Creek basins.

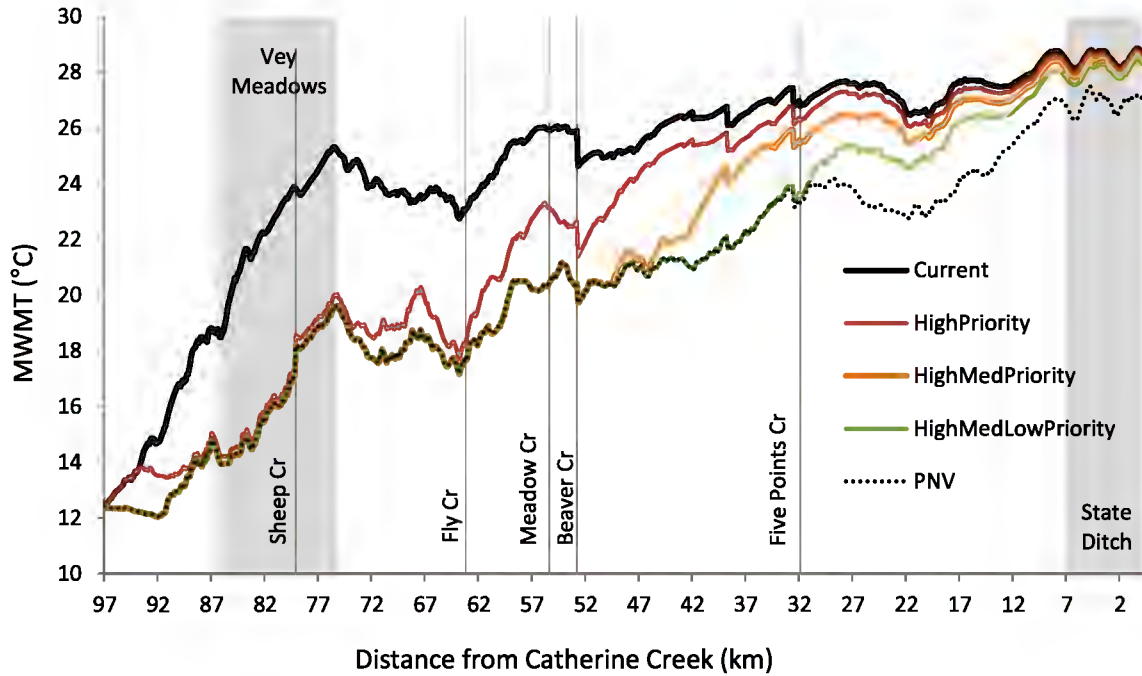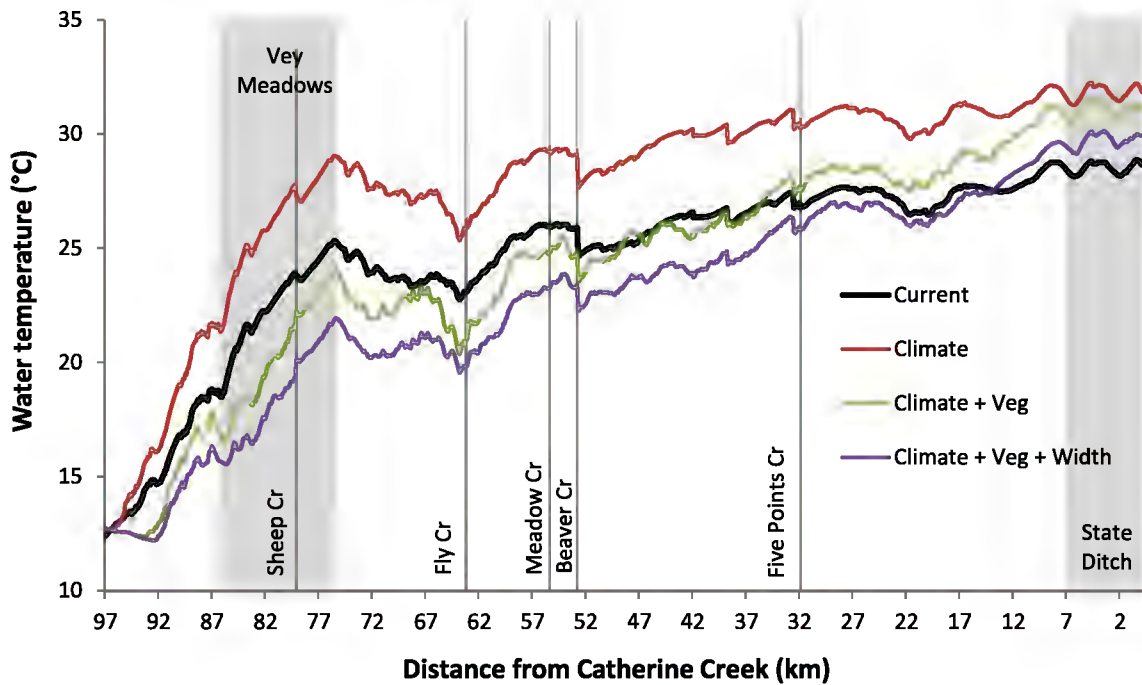$$\beta_0 = -2.0194(SE = 1.1259) \qquad\qquad \beta_1 = 0.7222(SE = 0.2084),$$

Fig. 5. Simulated maximum weekly maximum water temperature (*MWMT*; °C) in the mainstem Grande Ronde River from the headwaters to the Catherine Creek confluence under current conditions and four riparian restoration scenarios.

Fig. 6. Simulated maximum weekly maximum water temperature (*MWMT*; °C) in the mainstem Grande Ronde River from the headwaters to the Catherine Creek confluence for four model scenarios including current conditions, 2080s climate conditions, 2080's climate conditions plus riparian vegetation restoration, and 2080's climate conditions plus riparian and channel width restoration.

$$\beta_2 = -51.8642(SE = 17.8852),$$

$$\beta_3 = \begin{cases} 0, & MWMT \leq 18 \\ -0.2859 \ (SE = 0.0714), & MWMT > 18 \end{cases},$$

$$\beta_4 = 0.7127(SE = 0.1147).$$

Predicted abundance of Chinook Salmon summer parr under current conditions in the Upper Grande Ronde and Catherine Creek basins was approximately 46,000 and 55,000 respectively (Fig. 8). Basin-wide riparian reforestation in the absence of climate change
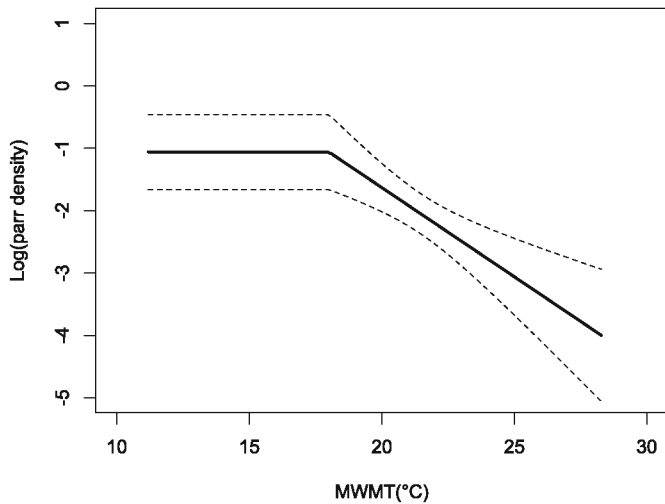
Fig. 7. Relationship between log (parr density (i.e., fish/m)) and maximum weekly maximum water temperature (*MWMT*; °C) estimated using a linear mixed-effects model. The dashed line represents the 95% confidence interval.

(scenario 2) could potentially increase abundance to 222,000 in the UGRB (377% increase) and 88,000 in the CCB (61% increase). Restoration of vegetation in high priority areas only was estimated to increase abundance to about 93,000 in the UGRB (100% increase), and 71,000 in the CCB (30% increase). Expanding vegetation restoration to include both high and medium priority areas could increase abundance to 166,000 (257% increase) and 84,000 (54% increase) in the UGRB and CCB respectively. Finally, restoration of high, medium, and low priority areas was estimated to increase abundance to 208,000 (348% increase) in the UGRB and 88,000 (61% increase) in the CCB. Interestingly, restoration of medium priority sites provided the greatest incremental increase in abundance in the UGRB, whereas restoration of high priority sites provided the greatest relative increase in abundance in the CCB. Riparian restoration in low priority areas provided little additional benefit in terms of total fish abundance in the CCB (7% increase over the High/Med scenario), but produced a substantial additional increase in fish abundance in the UGRB (91% increase over the High/Med scenario).

Simulated narrowing of the river channel produced a substantial increase in fish abundance, although the effect was relatively low compared with the expected benefits from riparian restoration. For example, fish abundance in the UGRB was predicted to increase by 57% as a result of channel narrowing, compared with an increase of 377% following riparian reforestation (Fig. 8). Similarly, channel narrowing was estimated to increase fish abundance by 22% in the CCB compared with a predicted increase of 61% resulting from riparian restoration. Combining channel width reductions with riparian reforestation produced the greatest predicted increases in fish abundance, with a potential increase of 590% in the UGRB and 67% in the CCB.

Projected water temperature increases resulting from climate change for the 2080s time period were predicted to reduce fish abundance by approximately 53% in the UGRB and 36% in Catherine Creek, assuming riparian vegetation cover and height remain similar to current conditions (Fig. 8). However, if riparian vegetation was restored basin-wide concurrently with these climate changes, we estimated that fish abundance could increase by 63% in the UGRB and 20% in the CCB. Additionally, if channel width reductions were combined with riparian restoration, we estimated that fish abundance could increase by as much as 114% in the UGRB and 37% in the CCB, despite the warming effects of climate change.

4. Discussion

4.1. Effect of scenarios on water temperature

The relatively large potential reductions in water temperature achievable through riparian restoration as demonstrated by our model results are generally consistent with findings from similar modeling assessments (Theurer et al., 1985; ODEQ, 2000; Sullivan and Rounds, 2004; Watanabe et al., 2005; Butcher et al., 2010) and with numerous field experiments throughout the Pacific Northwest that have demonstrated that forest harvesting can substantially increase stream temperatures, primarily by increasing the amount of solar radiation reaching the stream surface (Beschta et al., 1987; Moore et al., 2005). However, the magnitude of change in water temperature resulting from riparian restoration can vary considerably depending on other factors including streamflow, channel morphology, climate, existing vegetation, and anthropogenic stressors (e.g., grazing, timber harvest, dams) (Penaluna et al., 2015; Lynch et al., 2016). For example, the 4.4 °C median temperature reduction from riparian reforestation we predicted for the mainstem Upper Grande Ronde River was large compared with results from a similar simulation study in the Rogue River basin in Southwest Oregon, in which peak summer stream temperatures were predicted to decline by less than 1 °C following full riparian restoration (Crown et al., 2008). The lower temperature response to riparian restoration in the Rogue River appeared to be largely influenced by the Lost Creek Reservoir, which significantly increases summer base flow and reduces peak summer water temperatures. Similarly, a temperature modeling study in the North Fork Salmon River of Northern California showed that full riparian reforestation could reduce peak summer water temperatures by only 0.26 °C (Bond et al., 2015). In this case, temperature reductions from riparian restoration were likely limited by the existence of large conifer stands throughout much of the riparian zone under current conditions, and thus, a limited potential to increase riparian cover. On the other hand, simulated riparian restoration in the upper John Day River (above rkm 275), a nearby large tributary to the Columbia River with a similar history of habitat degradation and high water temperatures, reduced peak summer water temperatures by approximately 3.8 °C below the current condition (Butcher et al., 2010), a similar magnitude of reduction as predicted for the Grande Ronde River.

The greatest potential reductions in water temperature resulting from riparian restoration occurred in the upper to middle portion of the Upper Grande Ronde River (above Five Points Creek), particularly in areas that were designated as high and medium priority. These results lend credibility to the prioritization framework presented here and provide useful guidance for restoration practitioners seeking to cool water temperatures in the basin. Restoration practitioners have previously relied heavily on expert opinion in prioritizing restoration actions; however empirical results are preferred when available (Booth et al., 2016). However, despite these substantial potential cooling benefits from riparian restoration, we found that large portions of the stream network, particularly in the lower portion of the basin, would continue to exceed EPA temperature standards (i.e., 16 °C for "core" juvenile salmon rearing, and 18 °C for salmon migration and "non-core" juvenile rearing) even after restoration of riparian vegetation to its natural potential (Fig. 3). One reason for this may be that our model did not account for various other ecological factors that can contribute to cooling (e.g., hyporheic exchange, flow restoration). However, it is reasonable to assume that because of its arid climate, water temperatures were historically stressful to salmon during July and August in some portions of the Upper Grande Ronde River, particularly in the lower main stem where the river is wide and
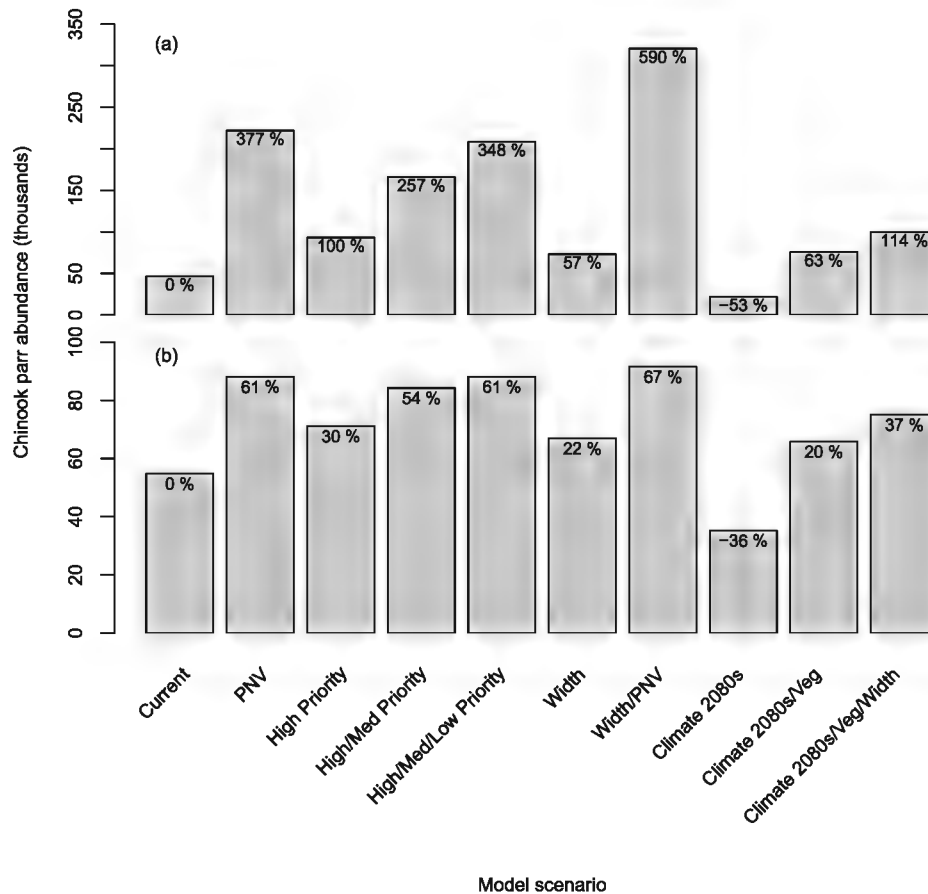
Fig. 8. Predicted abundance of Chinook Salmon summer parr for each model scenario in (a) the Upper Grande Ronde River, and (b) Catherine Creek basins. Numbers at the top of each bar indicate the percentage change in abundance from the current condition.

streamside vegetation is dominated by meadow and shrubland habitats with limited potential tree cover. This finding is congruent with temperature modeling results from the John Day River, which showed that water temperatures following restoration of riparian vegetation, channel morphology and streamflow were still well above biologically based temperature criteria for salmon across a large portion of the stream network (Butcher et al., 2010).

Model simulations demonstrated that channel narrowing (i.e., decreased width-to-depth ratio) can have an important cooling influence on water temperature in the Upper Grande Ronde and Catherine Creek basins, although thermal benefits associated with channel width were relatively small compared with the reductions in temperature achieved through riparian restoration (Fig. 3). Similar thermal responses to channel narrowing have been documented in other modeling analyses investigating land use impacts on water temperature (LeBlanc et al., 1997; ODEQ, 2000; Butcher et al., 2010). In the Upper Grande Ronde TMDL analysis, ODEQ also found that simulated channel width reductions in the mainstem Grande Ronde River provided a relatively small cooling benefit compared with vegetation restoration (ODEQ, 2000). In contrast, Butcher et al. (2010) found that reductions in channel width of 30% provided approximately equivalent reductions in water temperature compared with vegetation restoration in the upper 150 km of the John Day River, and substantially greater temperature reductions (i.e., approximately 2 °C below current) compared with vegetation restoration in the lower river where the channel is very wide and riparian shade potential is limited.

The simulated warming effect of climate change on water

temperature in the Upper Grande Ronde basin (median increase of 2.7 °C by 2080) and Catherine Creek (+1.5 °C) was generally consistent with other recent assessments of future climate change impacts on stream temperatures in the Pacific Northwest (Wu et al., 2012; Isaak et al., 2015) and in North America in general (Lynch et al., 2016), although the magnitude of change in water temperature varies depending on model assumptions, elevation, and geographic location. In a modeling study of climate change impacts on hydrology and temperature of Pacific Northwest rivers, Wu et al. (2012) predicted that climate change for the 2080s future scenario would increase average summer stream temperatures by 2.1 °C. Similarly, Isaak et al. (2015) predicted that mean August water temperatures in Pacific Northwest streams would increase by 2.8 °C on average by the 2080s. These increases correspond with—and even slightly exceed—expected climate-related changes in water temperature for rivers globally, with predicted increases in 95th percentile temperatures ranging from 1.0 to 2.2 °C for the years 2071–2100 (van Vliet et al., 2013).

Our model results demonstrated that restoration actions including riparian reforestation and channel narrowing could offset future climate-related increases in water temperature in the Grande Ronde basin, with net reductions in peak summer water temperature of 3.5 °C and 1.8 °C in the Upper Grande Ronde and Catherine Creek basins respectively. Similarly, Bond et al. (2015) found that climate-related warming in the North Fork Salmon River could be mitigated by full riparian reforestation for climate scenarios with a modest air temperature increase (+2 °C), but for scenarios with severe flow reduction and warming (71% flow

reduction, 6 °C air temperature increase), riparian reforestation could only reduce the predicted stream warming by half. Battin et al. (2007) predicted that full restoration of the Snohomish River basin in Western Washington, which included riparian reforestation, reduction of impervious surfaces, and improvements to in-stream complexity and floodplain connectivity, could offset climate warming and reduce average late summer (August 15-September 15) stream temperatures by 0.13–0.16 °C by the year 2050. However, under a more moderate restoration scenario, they predicted that water temperatures in year 2050 would increase by 0.03–0.04 °C above current temperatures.

Other factors beyond riparian vegetation and channel width can have an important influence on water temperature but were not included in our modeling analysis. For example, restoration actions such as channel reconstruction, levee removal, and construction of large woody debris jams have the potential to cool or buffer water temperatures by aggrading the stream bed, thereby increasing the degree of mixing between surface and subsurface water in the floodplain alluvium (i.e., hyporheic exchange) (Arrigoni et al., 2008; Beechie et al., 2013). In addition, flow restoration, which includes increasing in-stream flow by purchasing water rights, altering dam operations, or improving irrigation efficiency can substantially reduce water temperatures by increasing a stream's ability to withstand a given heat load without substantive change in water temperature (i.e., assimilative capacity) (Poole and Berman, 2001). Inclusion of such factors into future model scenarios could improve our understanding of the relative benefits of alternative restoration strategies.

Our model unrealistically assumes that—for the full riparian restoration scenario—the entire stream network could be restored to its natural potential. Currently, access to some private lands in the basin is restricted because of landowner denial and future access to this land is uncertain. In addition, some level of grazing impacts will likely persist due to its economic importance to landowners. Grazing by native ungulates like deer and elk may continue to be unnaturally high without a threshold abundance of natural predators (Ripple and Beschta, 2004). Survival of riparian plantings may also be impacted by factors such as desiccation, soil conditions, competition, animal damage, or channel incision, which could impact the likelihood that the riparian vegetation reaches its natural potential (Anderson and Graziano, 2002; Wall, 2011). Our model also unrealistically assumes that riparian restoration across the stream network occurs immediately, starting on day one of the model simulation period. In reality, tree planting typically occurs in a staggered fashion with the amount of riparian habitat restored being dictated by annual differences in funding and landowner permissions. These model uncertainties suggest that our full riparian restoration scenarios likely represent a best-case scenario in terms of expected thermal benefits from riparian restoration. As such, riparian restoration scenarios targeting only high and medium priority areas may be more realistic in that they assume only the highest priority portions of the basin would be restored to their full potential.

4.2. Effect of scenarios on fish abundance

The negative relationship we observed between juvenile Chinook Salmon density and water temperature is largely consistent with findings from similar field studies of salmonid populations throughout the Pacific Northwest (Ebersole et al., 2001; Welsh et al., 2001; Madriñán, 2008; Thompson et al., 2012). Potential increases in Chinook Salmon summer parr abundance up to 590% in the Upper Grande Ronde and 67% in Catherine Creek resulting from restoration of riparian vegetation and channel width are encouraging and highlight the importance of riparian shade—and to a

lesser extent channel width—for salmon productivity in these basins. Higher relative abundance increases in the Upper Grande Ronde compared with Catherine Creek are reflective of higher overall water temperatures and lower riparian shade in the Upper Grande Ronde, and consequently, a greater potential for water temperature improvements.

Climate change under current policy is predicted to accelerate extinction risk for endemic flora and fauna across the globe, including but not limited to fish (Urban, 2015). Of the studies that have focused on freshwater fish populations, the vast majority have concluded that climate change has significantly altered the distribution, phenology (e.g., migration timing), abundance, growth, recruitment, genetics and assemblage structure of many fish species, with the greatest impacts occurring in cold-water species like salmon and trout (Lynch et al., 2016). These findings are generally consistent with our results, which demonstrated a potential decline in juvenile salmon abundance of 53% in the Upper Grande Ronde and 36% in Catherine Creek due to climate-related water temperature increases.

Integrating climate change impacts with both riparian restoration and channel narrowing indicated that basin-wide restoration actions, if fully implemented immediately at a system level, could more than offset impacts from climate change, with net predicted increases in juvenile salmon abundance of 114% in the Upper Grande Ronde and 37% in Catherine Creek. In a similar modeling analysis of Chinook Salmon population response to habitat restoration and climate change in the Snohomish River basin in Western Washington, Battin et al. (2007) found that full habitat restoration could help mitigate the negative impacts of climate change and even allow salmon populations to increase in the face of climate change. Specifically, they found that full basin-wide restoration could limit declines in salmon populations to 5%, or could increase salmon populations by 19%, depending on the severity of the climate scenario selected.

We acknowledge that our model predicting juvenile fish abundance was relatively simplistic in that it does not include all important factors to which fish are known to respond (Jackson et al., 2001). We do however maintain that our approach represents a plausible relative fish response due to the well-supported effect of temperature on fish physiology, behavior, and distribution (Regier et al., 1990; Armour, 1991; McCullough, 1999). Our model did not incorporate density dependence explicitly in the form of a standard stock-recruitment function (i.e., Beverton-Holt or Ricker); however density dependence was implicitly accounted for by using redd abundance as an explanatory variable, and fish abundance values corresponded to average values observed during the study period. Although we focused on the juvenile rearing life stage, other salmon life stages (e.g., pre-spawn holding or egg incubation) can also be impacted by water temperature. We assumed that egg incubation, which is the most sensitive to high water temperature (optimal range 6–10 °C; EPA, 2003), is not significantly impacted by water temperature in the Grande Ronde basin because eggs incubate during fall and winter when temperatures are low. However, gamete viability in holding adults as well as survival of pre-spawn adults themselves can also be impaired by high water temperature (EPA, 2003). Interestingly, pre-spawn mortality data estimated from carcass recoveries in the Grande Ronde basin (Joseph Feldhaus, ODFW, pers. comm.), did not show a meaningful relationship with temperature and was therefore not included in our model. Utilizing the temperature results from this analysis within the context of a life-cycle model that properly accounts for density-dependent factors and temperature impacts on multiple life stages is an objective of ongoing research.

5. Conclusions

Results from our water temperature model indicated that intensive basin-wide restoration actions targeting both riparian vegetation and channel width could offset projected climate change impacts to salmon populations in the Upper Grande Ronde and Catherine Creek basins. A combination of riparian reforestation and channel narrowing was predicted to greatly reduce peak summer water temperatures in the study watersheds relative to current conditions, translating to large predicted increases in salmon abundance. However, significant portions of these watersheds—particularly in lower elevation reaches—continued to exceed stressful temperature limits for salmon growth and survival even after full riparian restoration, suggesting that alternative restoration strategies (e.g., increasing floodplain connectivity, streamflow restoration, and enhancement and protection of cold-water refuges) should also be implemented in order to maximize thermal benefits to threatened salmon populations.

These findings likely represent a best case scenario in terms of expected temperature reductions from riparian restoration because they are based on optimistic assumptions regarding the timing and spatial extent of future restoration actions. Given that a more realistic restoration scenario (e.g., high priority areas only) would result in more modest temperature improvements, combined with the rapid projected rise in water temperatures due to climate change, we emphasize the urgent need for a targeted and aggressive restoration strategy which includes riparian restoration as a key component. The temperature modeling and prioritization framework presented here should prove useful for restoration planners and practitioners seeking to improve habitat conditions for fish populations and other aquatic biota in temperature-impaired watersheds.

Acknowledgements

References

UWCIG (University of Washington Climate Impacts Group), 2012. Pacific Northwest Index (PNI). Accessed November 2015. http://www.cbr.washington.edu/status/pni.

Anderson, M., Graziano, G., 2002. Statewide Survey of Oregon Watershed Enhancement Board Riparian and Stream Enhancement Projects. Oregon Watershed Enhancement Board, Salem, Oregon.

Armour, C., 1991. Guidance for Evaluating and Recommending Temperature Regimes to Protect Fish. Fish and Wildlife Service. Biological Report 90 (22) (Instream Flow Information Paper 27).

Arrigoni, A.S., Poole, G.C., Mertes, L.A.K., O'Daniel, S.J., Woessner, W.W., Thomas, S.A., 2008. Buffered, lagged, or cooled? Disentangling hyporheic influences on temperature cycles in stream channels. Water Resour. Res. 44 (9), 1–13.

Barrett, J.W., 1978. Height Growth and Site Index Curves for Managed, Even-aged Stands of Ponderosa Pine in the Pacific Northwest. Research Paper PNW-232. US Department of Agriculture, Forest Service, Pacific Northwest Forest and Range Experiment Station, Portland, Oregon.

Battin, J., Wiley, M.W., Ruckelshaus, M.H., Palmer, R.N., Korb, E., Bartz, K.K., Imaki, H.,

2007. Projected impacts of climate change on salmon habitat restoration. Proc. Natl. Acad. Sci. 104 (16), 6720–6725.

Beechie, T., Imaki, H., 2014. Predicting natural channel patterns based on landscape and geomorphic controls in the Columbia River basin, USA: predicting Channel Patterns in the Columbia Basin. Water Resour. Res. 50 (1), 39–57.

Beechie, T., Imaki, H., Greene, J., Wade, A., Wu, H., Pess, G., Roni, P., Kimball, J., Stanford, J., Kiffney, P., Mantua, N., 2013. Restoring salmon habitat for a changing climate. River Res. Appl. 29, 939–960.

Belsky, A.J., Matzke, A., Uselman, S., 1999. Survey of livestock influences on stream and riparian ecosystems in the Western United States. J. Soil Water Conserv. 54 (1), 419–431.

Bernhardt, E.S., Palmer, M.A., Allan, J.D., Alexander, G., Barnas, K., Brooks, S., Carr, J., Clayton, S., Dahm, C., Follstad-Shah, J., Galat, D., Gloss, S., Goodwin, P., Hart, D., Hassett, B., Jenkinson, R., Katz, S., Kondolf, G.M., Lake, P.S., Lave, R., Meyer, J.L., O'Donnell, T.K., Pagano, L., Powell, B., Sudduth, E., 2005. Synthesizing U.S. river restoration efforts. Science 308 (5722), 636–637.

Beschta, R.L., Bilby, R.E., Brown, G.W., Holtby, L.B., Hofstra, T.D., 1987. Stream temperature and aquatic habitat: fisheries and forestry interactions. In: Salo, E., Cundy, T. (Eds.), Streamside Management: Forestry and Fishery Interactions. University of Washington Institute of Forest Resources, Seattle, Washington, pp. 191–232.

Bond, R.M., Stubblefield, A.P., Van Kirk, R.W., 2015. Sensitivity of summer stream temperatures to climate variability and riparian reforestation strategies. J. Hydrol. Reg. Stud. 4, 267–279.

Booth, D., Scholz, J., Beechie, T., Ralph, S., 2016. Integrating limiting-factors analysis with process-based restoration to improve recovery of endangered salmonids in the Pacific Northwest, USA. Water 8 (5), 174.

Boyd, M., Kasper, B., 2003. Analytical Methods for Dynamic Open Channel Heat and Mass Transfer: Methodology for the Heat Source Model Version 7.0. http://www.deq.state.or.us/wq/TMDLs/tools.htm.

BPA (Bonneville Power Administration), 2008. Administrator's Record of Decision, 2008 Columbia Basin Fish Accords. https://www.bpa.gov/news/pubs/PastRecordsofDecision/2008/MOA_ROD.pdf.

Breau, C., Cunjak, R.A., Peake, S.J., 2011. Behaviour during elevated water temperatures: can physiology explain movement of juvenile Atlantic salmon to cool water? J. Animal Ecol. 80 (4), 844–853.

Brierley, G.J., Fryirs, K.A., 2005. Geomorphology and River Management: Applications of the River Styles Framework. Blackwell Pub, Malden, Massachusetts.

Butcher, D., Crown, J., Brannan, K., Kishida, K., Hubler, S., 2010. John Day River Basin Total Maximum Daily Load (TMDL) and Water Quality Management Plan (WQMP). Oregon Department of Environmental Quality, Portland, Oregon.

Chen, Y.D., McCutcheon, S.C., Norton, D.J., Nutter, W.L., 1998. Stream temperature simulation of forested riparian areas: II. Model application. J. Environ. Eng. 124, 316–328.

Clendenen, G.W., 1977. Base-age Conversion and Site-index Equations for Engelmann Spruce Stands in the Central and Southern Rocky Mountains. Research Note Int-223. U.S. Department of Agriculture, Forest Service, Intermountain Forest and Range Experiment Station, Ogden, Utah.

Cochran, P.H., 1979. Site Index and Height Growth Curves for Managed, Even-aged Stands of Douglas-fir East of the Cascades in Oregon and Washington. Research Paper PNW-251. US Department of Agriculture, Forest Service, Pacific Northwest Forest and Range Experiment Station, Portland, Oregon.

Cochran, P.H., 1985. Site Index, Height Growth, Normal Yields, and Stocking Levels for Larch in Oregon and Washington. Research Note PNW-424. US Department of Agriculture, Forest Service, Pacific Northwest Forest and Range Experiment Station, Bend, Oregon.

Cooney, T., McClure, M., Baldwin, C., Carmichael, R., Hassemer, P., Howell, P., McCullough, D., et al., 2007. Viability Criteria for Application to Interior Columbia Basin Salmonid ESUs. Interior Columbia Basin Technical Recovery Team. https://www.nwfsc.noaa.gov/trt/trt_documents/ictrt_viability_criteria_reviewdraft_2007_body.pdf (Accessed 1 March 2016).

Crowe, E.A., Clausnitzer, R.R., 1997. Mid-montane Wetland Plant Associations of the Malheur, Umatilla and Wallowa-Whitman National Forests. Technical Paper R6-NR-ECOL-TP-22–97. U.S. Department of Agriculture, Forest Service, Pacific Northwest Region, Portland, Oregon.

Crowe, E.A., Kovalchik, B.L., Kerr, M., 2004. Riparian and Wetland Vegetation of Central and Eastern Oregon. Oregon State University, Portland, Oregon.

Crown, J., Meyers, B., Tugaw, H., Turner, D., 2008. Rogue River Basin Total Maximum Daily Load (TMDL). Oregon Department of Environmental Quality.

Dahms, W.G., 1975. Gross yield of central Oregon lodgepole pine. In: Baumgartner, D.M. (Ed.), Management of Lodgepole Pine Ecosystems: Symposium Proceedings. Washington State University, Pullman, Washington, pp. 208–232.

Ebbesmeyer, C.C., Strickland, R.M., 1995. Oyster Condition and Climate: Evidence from Willapa Bay. Publication WSG-MR 95–02, Washington Sea Grant Program. University of Washington, Seattle, Washington.

Ebersole, J.L., Liss, W.J., Frissell, C.A., 2001. Relationship between stream temperature, thermal refugia and rainbow trout Oncorhynchus mykiss abundance in arid-land streams in the northwestern United States. Ecol. Freshw. Fish 10 (1), 1–10.

EPA, 2003. EPA Region 10 Guidance for Pacific Northwest State and Tribal Temperature Water Quality Standards. U.S. Environmental Protection Agency, Region 10, Office of Water, Seattle, Washington.

Ficke, A.D., Myrick, C.A., Hansen, L.J., 2007. Potential impacts of global climate change on freshwater fisheries. Rev. Fish Biol. Fish. 17 (4), 581–613.

Ficklin, D.L., Barnhart, B.L., Knouft, J.H., Stewart, I.T., Maurer, E.P., Letsinger, S.L., Whittaker, G.W., 2014. Climate change and stream temperature projections in the Columbia River basin: habitat implications of spatial variation in hydrologic drivers. Hydrol. Earth Syst. Sci. 18, 4897–4912.

Herman, F.R., Curtis, R.O., DeMars, D.J., 1978. Height Growth and Site Index Estimates for Noble Fir in High-elevation Forests of the Oregon-Washington Cascades. Research Paper PNW-243. U.S. Department of Agriculture, Forest Service, Pacific Northwest Forest and Range Experiment Station, Portland, Oregon.

Isaak, D.J., Wenger, S.J., Peterson, E.E., Ver Hoef, J.M., Hostetler, S., Luce, C.H., Dunham, J.B., Kershner, J., Roper, B.B., Nagel, D., Horan, D., Chandler, G., Parkes, S., Wollrab, S., 2011. NorWeST: an Interagency Stream Temperature Database and Model for the Northwest United States. U.S. Fish and Wildlife Service, Great Northern Landscape Conservation Cooperative Grant. www.fs.fed.us/rm/boise/AWAE/projects/NorWeST.html.

Isaak, D.J., Wollrab, S., Horan, D., Chandler, G., 2012. Climate change effects on stream and river temperatures across the northwest U.S. from 1980–2009 and implications for salmonid fishes. Clim. Change 113 (2), 499–524.

Isaak, D., Wenger, S., Peterson, E., Ver Hoef, J., Luce, C., Hostetler, S., Dunham, J., Kershner, J., Roper, B., Nagel, D., Horan, D., Chandler, G., Parkes, S., Wollrab, S., 2015. Development and Application of NorWeST Stream Temperature Climate Scenarios for the Pacific Northwest. North Pacific Landscape Conservation Cooperative webinar. January 27.

ISAB (Independent Scientific Advisory Board)/ISRP(Independent Scientific Review Panel), 2016. Critical Uncertainties for the Columbia River Basin Fish and Wildlife Program. For the Northwest Power and Conservation Council, Portland, OR.

Jackson, D.A., Peres-Neto, P.R., Olden, J.D., 2001. What controls who is where in freshwater fish communities—the roles of biotic, abiotic, and spatial factors. Can. J. Fish. Aquati. Sci. 58 (1), 157–170.

Johnson, C.G., Clausnitzer, R.R., 1992. Plant Associations of the Blue and Ochoco Mountains. Technical Paper R6-ERW-TP-036–92. U.S. Department of Agriculture, Forest Service, Pacific Northwest Region, Portland, Oregon.

Johnson, C.G., Simon, S.A., 1987. Plant Associations of the Wallowa-Snake Province. Technical Paper R6-ECOL-TP-255A-86. U.S. Department of Agriculture, Forest Service, Pacific Northwest Region, Portland, Oregon.

Jonasson, B., Sedell, E., Banks, S.K., Garner, A.B., Horn, C., Bliesner, K.L., Dowdy, J.W., Drake, F.W., Favrot, S.D., Hay, J.M., McConnell, N.A., Ophoff, J.P., Power, B.C., Ruzycki, J.R., Carmichael, R.W., 2015. Investigations into the Life History of Naturally Produced Spring Chinook Salmon and Summer Steelhead in the Grande Ronde River Subbasin. Annual Report 2014, BPA Project # 1992-026-04. Oregon Department of Fish and Wildlife, La Grande, Oregon.

Kauffman, J.B., Krueger, W.C., 1984. Livestock impacts on riparian ecosystems and streamside management implications: a review. J. Range Manag. 37 (5), 430–438.

Kauffman, J.B., Krueger, W.C., Vavra, M., 1985. Ecology and Plant Communities of the Riparian Area Associated with Catherine Creek in Northeastern Oregon. Technical Bulletin 147. Oregon State University, Corvallis, Oregon.

LeBlanc, R.T., Brown, R.D., FitzGibbon, J.E., 1997. Modeling the effects of land use change on the water temperature in unregulated urban streams. J. Environ. Manag. 49 (4), 445–469.

Littell, J.S., Elsner, M.M., Mauger, G., Lutz, E., Hamlet, A.F., Salathé, E., 2011. Regional Climate and Hydrologic Change in the Northern US Rockies and Pacific Northwest: internally Consistent Projections of Future Climate for Resource Management. University of Washington College of the Environment, Seattle, Washington. Project Report of Climate Impacts Group.

Lynch, A.J., Myers, B.J.E., Chu, C., Eby, L.A., Falke, J.A., Kovach, R.P., Krabbenhoft, T.J., Kwak, T.J., Lyons, J., Paukert, C.P., Whitney, J.E., 2016. Climate change effects on north American inland fish populations and assemblages. Fisheries 41 (7), 346–361.

Madriñán, L.F., 2008. Biophysical Factors Driving the Distribution and Abundance of Redband/steelhead Trout (Oncorhynchus mykiss gairdneri) in the South Fork John Day River Basin, Oregon, USA. Ph.D. Thesis. Department of Fish and Wildlife, Oregon State University, Corvallis, Oregon.

McCullough, D.A., 1999. A Review and Synthesis of Effects of Alterations to the Water Temperature Regime on Freshwater Life Stages of Salmonids, with Special Reference to Chinook Salmon. EPA 910-R-99–010. U.S. Environmental Protection Agency, Region 10, Seattle, Washington.

McCullough, D.A., White, S., Justice, C., Blanchard, M., Lessard, R., Kelsey, D., Graves, D., Nowinski, J., 2015. Assessing the Status and Trends of Spring Chinook Habitat in the Upper Grande Ronde River and Catherine Creek. BPA Project # 2009-004-00. Columbia River Inter-Tribal Fish Commission, Portland, Oregon.

McCullough, D.A., White, S., Justice, C., Blanchard, M., Lessard, R., Kelsey, D., Graves, D., Nowinski, J., 2016. Assessing the Status and Trends of Spring Chinook Habitat in the Upper Grande Ronde River and Catherine Creek. BPA Project # 2009-004-00. Columbia River Inter-Tribal Fish Commission, Portland, Oregon.

Monserud, R.A., 1985. Applying Height Growth and Site Index Curves for Inland Douglas-fir. Research Paper Int-347. US Department of Agriculture, Forest Service, Intermountain Research Station, Ogden, Utah.

Moore, R.D., Spittlehouse, D.L., Story, A., 2005. Riparian microclimate and stream temperature response to forest harvesting: a review. J. Am. Water Resour. Assoc. 41 (4), 813–834.

Moore, K., Jones, K.K., Dambacher, J., Stein, C., 2008. Methods for Stream Habitat Surveys Aquatic Inventories Project. Conservation and Recovery Program. Oregon Department of Fish and Wildlife, Corvallis, Oregon.

Myrick, C.A., Cech, J.J., 2004. Temperature effects on juvenile anadromous salmonids in California's central valley: what don't we know? Rev. Fish Biol. Fish. 14 (1), 113–123.

NOAA (National Oceanic and Atmospheric Administration), 2008. Supplemental Comprehensive Analysis of the Federal Columbia River Power System and Mainstem Effects of the Upper Snake and Other Tributary Actions. NOAA Fisheries.

Nussbaum, A.F., 1996. Site Index Curves and Tables for British Columbia: Coastal Species. Land Management Handbook, Field Guide Insert 3, second ed. B.C. Ministry of Forests, Research Branch, Victoria, British Columbia.

ODEQ (Oregon Department of Environmental Quality), 2000. Upper Grande Ronde River Sub-Basin Total Maximum Daily Load (TMDL). Oregon Department of Environmental Quality, Water Quality Division, Portland, Oregon. http://waterquality.ODEQ.state.or.us/wq/.

Penaluna, B.E., Dunham, J.B., Railsback, S.F., Arismendi, I., Johnson, S.L., Bilby, R.E., Safeeq, M., Skaugset, A.E., 2015. Local variability mediates vulnerability of trout populations to land use and climate change. PLoS One 10 (8), e0135334.

Poole, G.C., Berman, C.H., 2001. An ecological perspective on in-stream temperature: natural heat dynamics and mechanisms of human-caused thermal degradation. Environ. Manag. 27 (6), 787–802.

Poole, G., Dunham, J., Hicks, M., Keenan, D., Lockwood, J., Materna, E., McCullough, D., Mebane, C., Risley, J., Sauter, S., Spalding, S., Sturdevant, D., 2001. Scientific Issues Relating to Temperature Criteria for Salmon, Trout, and Char Native to the Pacific Northwest. EPA 910-R-01–007. U.S. Environmental Protection Agency, Region 10, Seattle, Washington.

Principle Clerk of Surveys, General Land Office, 1855. Instructions to the Surveyors General of Public Lands of the United States for Those Surveying Districts Established in and since the Year 1850. Containing Also a Manual of Instructions to Regulate the Field Operations of Deputy Surveyors. A.O.P. Nicholson, Public Printer, Washington, District of Columbia.

Regier, H.A., Holmes, J.A., Pauly, D., 1990. Influence of temperature changes on aquatic ecosystems: an interpretation of empirical data. Trans. Am. Fish. Soc. 119, 374–389.

Ripple, W.J., Beschta, R.L., 2004. Wolves and the ecology of fear: can predation risk structure ecosystems? BioScience 54 (8), 755.

Simon, A., Rinaldi, M., 2006. Disturbance, stream incision, and channel evolution: the roles of excess transport capacity and boundary materials in controlling channel response. Geomorphology 79, 361–383.

Steele, R., Geier-Hayes, K., 1987. The Grand Fir/big Huckleberry Habitat Type in Central Idaho: Succession and Management. General Technical Report INT-228. U.S. Department of Agriculture, Forest Service, Intermountain Research Station, Ogden, Utah.

Steele, R., Geier-Hayes, K., 1989. The Douglas-fir/ninebark Habitat Type in Central Idaho: Succession and Management. General Technical Report INT-252. U.S. Department of Agriculture, Forest Service, Intermountain Research Station, Ogden, Utah.

Steele, R., Geier-Hayes, K., 1992. The Grand Fir/mountain Maple Habitat Type in Central Idaho: Succession and Management. General Technical Report INT-284. U.S. Department of Agriculture, Forest Service, Intermountain Research Station, Ogden, Utah.

Steele, R., Geier-Hayes, K., 1993. The Douglas-fir/pinegrass Habitat Type in Central Idaho: Succession and Management. General Technical Report INT-298. U.S. Department of Agriculture, Forest Service, Intermountain Research Station, Ogden, Utah.

Steele, R., Geier-Hayes, K., 1994. The Douglas-fir/white Spirea Habitat Type in Central Idaho: Succession and Management. General Technical Report INT-305. U.S. Department of Agriculture, Forest Service, Intermountain Research Station, Ogden, Utah.

Stevens, D.L., Olsen, A.R., 2004. Spatially balanced sampling of natural resources. Am. Stat. Assoc. 99 (465), 262–278.

Sullivan, A.B., Rounds, S.A., 2004. Modeling Streamflow and Water Temperature in the North Santiam and Santiam Rivers, Oregon, 2001-02. U.S. Geological Survey. U.S. Department of the Interior, Portland, Oregon.

Theurer, F.D., Lines, I., Nelson, T., 1985. Interaction between riparian vegetation, water temperature, and salmonid habitat in the Tucannon River. J. Am. Water Resour. Assoc. 21 (1), 53–64.

Thompson, L.C., Voss, J.L., Larsen, R.E., Tietje, W.D., Cooper, R.A., Moyle, P.B., 2012. Southern steelhead, hard woody debris, and temperature in a California central coast watershed. Trans. Am. Fish. Soc. 141 (2), 275–284.

Urban, M.C., 2015. Accelerating extinction risk from climate change. Science 348 (6234), 571–573.

USFS, 2015. Fire Effects Information System. U.S. Department of Agriculture, Forest Service, Rocky Mountain Research Station, Missoula Fire Sciences Laboratory (Producer). Accessed June 1, 2015. http://feis-crs.org/beta/.

UWCIG (University of Washington Climate Impacts Group), 2010. Hydrologic Climate Change Scenarios for the Pacific Northwest Columbia River Basin and Coastal Drainages. Accessed November 2015. http://www.hydro.washington.edu/2860/.

van Vliet, M.T.H., Franssen, W.H.P., Yearsley, J.R., Ludwig, F., Haddeland, I., Lettenmaier, D.P., Kabat, P., 2013. Global river discharge and water temperature under climate change. Glob. Environ. Change 23 (2), 450–464.

Wall, S.M., 2011. Efficacy of Riparian Revegetation Projects in the Inland Pacific Northwest. M.S. thesis. University of Montana, Missoula, Montana, p. 40.

Watanabe, M., Adams, R.M., Wu, J., Bolte, J.P., Cox, M.M., Johnson, S.L., Liss, W.J., Boggess, W.G., Ebersole, J.L., 2005. Toward efficient riparian restoration: integrating economic, physical, and biological models. J. Environ. Manag. 75 (2),

93–104.

Watershed Sciences, 2008. Deschutes River, Whychus Creek, and Tumalo Creek Temperature Modeling. Watershed Sciences, Inc. and MaxDepth Aquatics, Inc., Bend, OR (Prepared for State of Oregon Department of Environmental Quality).

Watershed Sciences, 2010. Airborne Thermal Infrared Remote Sensing, Upper Grande Ronde River Basin, Oregon. Prepared for the Columbia River Inter-tribal Fish Commission. Watershed Sciences, Inc., Corvallis, OR.

Watershed Sciences, 2012. Upper Grande Ronde River Basin Stream Temperature Model Expansion. Prepared for the Columbia River Inter-tribal Fish Commission. Watershed Sciences, Inc, Portland, Oregon.

Wells, A., 2006. Deep Canyon and Subalpine Riparian and Wetland Plant Associations of the Malheur, Umatilla, and Wallow-Whitman National Forest. General Technical Report PNW-GTR-682. U.S. Department of Agriculture, Forest Service, Pacific Northwest Research Station, Portland, Oregon.

Wells, A.F., Crowe, E., Blaha, R., 2015. Riparian Vegetation Mapping in the Grande Ronde Watershed, Oregon: Monitoring and Validation of Spring Chinook Habitat Recovery and Population Viability. Prepared for Columbia River Inter-Tribal Fish Commission by ABR, Inc. (Alaska Biological Research, Environmental Research & Services, Anchorage, AK) and Elizabeth Crowe, Fort Collins, Colorado.

Welsh, H.H., Hodgson, G.R., Harvey, B.C., Roche, M.F., 2001. Distribution of juvenile coho salmon in relation to water temperatures in tributaries of the Mattole River, California. N. Am. J. Fish. Manag. 21 (3), 464–470.

Whitney, J.E., Al-Chokhachy, R., Bunnell, D.B., Caldwell, C.A., Cooke, S.J., Eliason, E.J., Rogers, M., Lynch, A.J., Paukert, C.P., 2016. Physiological basis of climate change impacts on North American inland fishes. Fisheries 41 (7), 332–345.

Wu, H., Kimball, J.S., Elsner, M.M., Mantua, N., Adler, R.F., Stanford, J., 2012. Projected climate change impacts on the hydrology and temperature of Pacific Northwest rivers. Water Resour. Res. 48 (11).

Zuur, A.F., Ieno, E.N., Elphick, C.S., 2010. A protocol for data exploration to avoid common statistical problems: data exploration. Methods Ecol. Evol. 1 (1), 3–14.
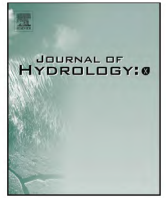
Research papers

Temperature buffering by groundwater in ecologically valuable lowland streams under current and future climate conditions

Vince P. Kaandorp [a,b,*], Pieter J. Doornenbal [a], Henk Kooi [a], Hans Peter Broers [c], Perry G.B. de Louw [a,d]

[a] Department of Subsurface and Groundwater Systems, Deltares, Utrecht, the Netherlands
[b] Department of Earth Sciences, Utrecht University, Utrecht, the Netherlands
[c] TNO Geological Survey of the Netherlands, Utrecht, the Netherlands
[d] Soil Physics and Land Management, Wageningen University, Wageningen, the Netherlands

ARTICLE INFO

ABSTRACT

Groundwater seepage influences the temperature of streams and rivers by providing a relatively cool input in summer and warm input in winter. Because of this, groundwater seepage can be a determining factor in the provision of suitable water temperatures for aquatic biota. Climate warming affects stream and groundwater temperatures, and changes the thermal characteristics of streams leading to the potential disappearance of habitats. In this study the importance of groundwater for the temperature of two Dutch lowland streams and its possible role in mitigating the effects of climate change was determined by combining field measurements and a modelling experiment. Stream temperature measurements using fibre optic cables (FO-DTS) and sampling of [222]Rn were done to map localized groundwater inflow. Several springs and seepage 'hot-spots' were located which buffered the water temperature in summer and winter. A stream temperature model was constructed and calibrated using the FO-DTS-measurements to quantify the energy fluxes acting on stream water. This way, the contribution to the stream thermal budget of direct solar radiation, air temperature and seepage were separated. The model was then used to simulate the effects of changes in shading, groundwater seepage and climate. Shading was shown to be an important control on summer temperature maxima. Groundwater seepage seemed to buffer the effect of climate warming, potentially making groundwater dominated streams more climate robust. Protecting groundwater resources in a changing climate is important for the survival of aquatic species in groundwater-fed systems, as groundwater seepage both sustains flow and buffers temperature extremes.

© 2019 The Authors. Published by Elsevier B.V. This is an open access article under the CC BY-NC-ND license (http://creativecommons.org/licenses/by-nc-nd/4.0/).

1. Introduction

Stream water temperature is an important factor influencing aquatic ecosystems as it affects species distribution, growth, metabolism and reproduction (Vannote and Sweeney, 1980), as well as oxygen concentrations, biological production and decomposition (Bowes et al., 2016; Haidekker and Hering, 2008; Hawkins et al., 1997; Ormerod, 2009; Rasmussen et al., 2011; Ward and Stanford, 1982; Ylla et al., 2014). Consequently, changes in stream temperature can act as a stressor on aquatic species (e.g. Piggott et al., 2015; Poole and Berman, 2001; Schülting et al., 2016). It is therefore not surprising that much research has been done on the effect of climate warming on stream temperature and aquatic

species (e.g. Eaton and Scheller, 1996; Guse et al., 2015; Isaak et al., 2018, 2015; Moss et al., 2003; Null et al., 2012). It is expected that in a warmer global climate the average and peak temperature of stream water will increase (Van Vliet et al., 2013; Watts et al., 2015; Webb and Nobilis, 2007).

Many studies on stream temperature have focused on the effect of air temperature, radiation and shading (e.g. Garner et al., 2017; Hannah et al., 2008; Macdonald et al., 2014; Westhoff et al., 2011). Due to these studies, it is now widely recognized that riparian shade reduces maximum stream temperatures in summer by blocking part of the incoming solar radiation (Dugdale et al., 2018; Sweeney and Newbold, 2014; Thomas et al., 2015), and therefore, that management practices like planting vegetation along streams can potentially mitigate the effect of climate warming (Kristensen et al., 2015; Nash et al., 2018; Thomas et al., 2015).

Groundwater temperature is influenced by the temperature of the infiltrating water and by the conduction of heat from the

---

* Corresponding author at: Department of Subsurface and Groundwater Systems, Deltares, Utrecht, the Netherlands.
E-mail address: Vince.Kaandorp@deltares.nl (V.P. Kaandorp).

surface. The impact of diurnal to seasonal variations of surface temperature dampens with depth. Downward from the surface, groundwater temperature, therefore, tends to approach the yearly average ground surface temperature (e.g. Bense and Kooi, 2004; de Louw et al., 2010; Vandenbohede et al., 2014). In areas with strong upward seepage, this moderate groundwater temperature is carried into streams. Therefore, groundwater seepage into streams is known to moderate summer and winter stream temperatures, and to create so called local *thermal refugia* (e.g. Hayashi and Rosenberry, 2002; Kaandorp et al., 2018b; Power et al., 1999) and *climate refugia* (e.g. Briggs et al., 2018b; Isaak et al., 2015; Meisner et al., 1988) for aquatic biota. Although the role of groundwater on stream temperatures is conceptually understood, its effect is often neglected or highly simplified in studies on stream temperature and almost never considered in stream temperature management. Therefore, the influence of groundwater on stream temperature and the subsequent response of aquatic ecology still requires more research.

The objective of this study is to determine the influence of groundwater on the temperature of two Dutch lowland streams and to get insight into its possible role in mitigating the effects of climate change. For this, both field measurements and a modelling experiment are done. Research questions are: a) what is the spatial variability of groundwater seepage to the streams, b) what is the spatial and temporal effect of groundwater seepage on stream temperature, c) how does the effect of groundwater inflow on stream temperature compare to the effect of air temperature and radiation (including shading), and d) what is the effect of groundwater on stream temperature in a warming climate?

We combine different field techniques such as Fibre Optic Distributed Temperature Sensing (FO-DTS) and measurements of the isotope ^{222}Rn to detect diffuse and localized groundwater inputs to the two Dutch lowland streams. FO-DTS is used to make high resolution temperature measurements, both in time and space (Selker et al., 2006). Compared to surface water, the temperature of groundwater is relatively constant throughout the year and as such lateral changes in stream water temperature can be used to locate groundwater seepage zones in specific moments in time (Briggs et al., 2012; Krause et al., 2012; Matheswaran et al., 2014b; Poulsen et al., 2015; Rosenberry et al., 2016; Sebok et al., 2013; Vandenbohede et al., 2014; Westhoff et al., 2007). The presence of the isotope ^{222}Rn in surface water also indicates recent seepage of groundwater, as it is rapidly removed in surface waters by radioactive decay and degassing. In addition to this field data, we construct a stream temperature model, which includes the effects of air temperature, radiation, shading and groundwater seepage. The model is used to analyze the behavior of the different processes affecting stream temperature. By applying different scenarios we derive the effect of climate change on stream thermal habitats and the mitigating effects of groundwater seepage.

2. Study area and methods

2.1. Study area

Field measurements were done in two lowland streams in the east of the Netherlands: the Springendalse Beek and the Elsbeek (Fig. 1). With catchments sizes of 4 km² and 11 km² respectively, these streams discharge to the Dinkel river. The area has a temperate marine climate with a mean annual air temperature of 9.6 °C and mean annual precipitation and evaporation of 850 and 560 mm per year respectively. The average discharge is 0.043 m³ s⁻¹ for the Springendalse Beek and 0.104 m³ s⁻¹ for the Elsbeek. The subsurface of the catchments consists of shallow aquifers (1–20 m thick) on top of clayey moraines. The streambed of

the streams consists of sand with occasionally some gravel. Details on the study catchments were described by Kaandorp et al. (2018b). A concise description of the studied stream stretches is given here.

The upstream catchment of the Springendalse Beek contains a few distinct spring areas and consists mainly of forest with some agricultural fields. The studied stream stretch extends 1500 m downstream from the stream origin (Fig. 1a). The upstream part has a relatively stable discharge, a stream width between 0.5 and 1.0 m and a water depth of a few centimetres. A small spring, a tributary, two seepage ponds and tributaries from a swamp discharge into the stream (Fig. 1a). The downstream part has a width of 1.0–1.5 m and a water depth of around 10 cm.

The Elsbeek predominantly consists of agricultural areas. The measured stream stretch extends from approximately 5000 to 6500 m downstream from the stream origin (Fig. 1b). The most upstream 200 m of the study stretch is straightened, flows through an agricultural area and has a width of about 1 m and a water depth of around 5 cm. Here the outflow of an agricultural ditch, which dries up during summer, joins the stream. This is followed by a stream stretch with a riparian forest and a pool-riffle sequence with pools up to 1 m deep and a width varying between 0.5 and 1.5 m. A stretch with a length of 150 m in the central part is again straightened and flows through an agricultural area with a width of around 1 m and a water depth of about 30 cm. After this an agricultural ditch joins the stream. The most downstream part of the studied stream stretch flows again through a forest, is shallow (∼3–10 cm) and has a width varying between 0.5 and 2.0 m. This part of the stream is deeply incised (1.0–1.5 m) into the landscape.

2.2. FO-DTS set-up

Stream temperatures were measured using an Oryx DTS (Sensornet USA) unit and CTC LSZH fibre-optic cables (TKF Connectivity Solutions, Netherlands). A cable with a length of 1300 m was positioned in the study stretch of the Springendalse Beek, from 200 m downstream from the stream origin (x = 200) to the end of the studied stream stretch (x = 1500) (Fig. 1). At x = 305 and x = 435, the cable was looped back and forth through a small spring directly next to the stream (x = 305), and in a side branch of the stream (x = 435), respectively (Fig. 1a). Approximately 1500 m of fibre optic cable was installed in the Elsbeek, covering the two forested stream stretches and two open areas (Fig. 1b). In both streams, the cable was installed on the streambed, and fixed using U shaped metal pegs. A double ended configuration was used with two calibration baths next to the Oxyx unit and a splice at the end of the fibre optic cable. By using the double ended setup corrections for splices and light attenuation in the fibre optic cable can be made (Hausner et al., 2011; Van De Giesen et al., 2012). For calibration, a coil of cable was placed in each isolated calibration bath which was equipped with a PT-100 temperature sensor and connected with the Oryx unit. Measurements were done for the whole months of August 2016 and January 2017 to capture both summer and winter temperature patterns. Each DTS measurement was done with a spatial resolution of 1.0 m and consisted of sequential measuring of 5 min through 2 channels, which were repeated either every half an hour (summer) or every hour (winter).

Because the DTS cable was placed on the streambed the measurements represent the temperature at the bottom of the stream, unless it was buried by sediments. Sediment was removed from the DTS cable several times, but it could not be prevented that during part of the measurement period some parts of the cable were buried by sediment. In the streambed the temperature variation present in the stream is attenuated with depth, and as such sedimentation leads to a temperature signal comparable to that of
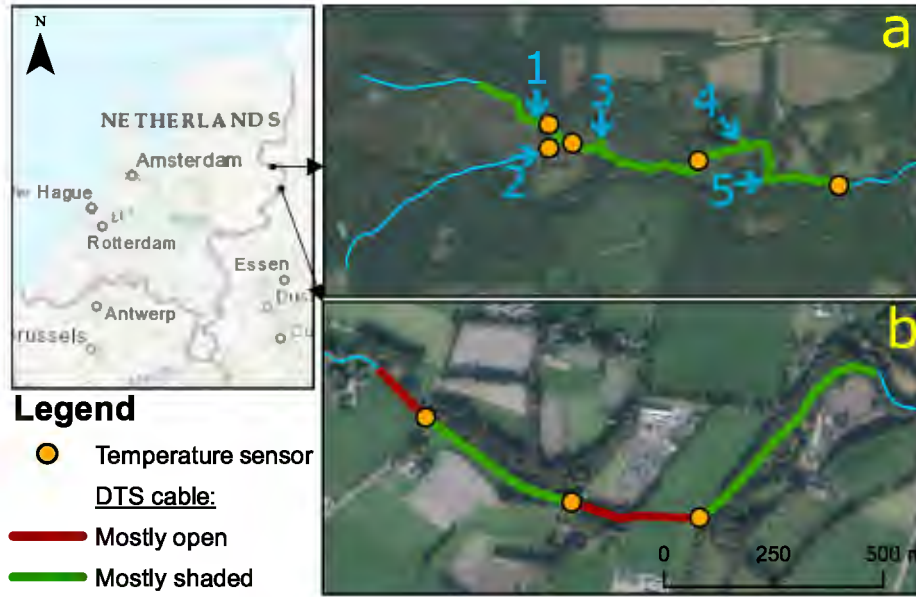
Fig. 1. Location of the fibre optic cables and temperature sensors in the Springendalse Beek (a) and Elsbeek (b). The numbered arrows 1 to 5 in panel a indicate inflow from a spring (1), tributary (2), small and large groundwater-fed ponds (3 and 4) and tributaries swamp (5).

groundwater seepage, such as a decrease in the standard deviation (SD) of the temperature (Sebok et al., 2015).

The DTS temperature measurements were calibrated using dispersion, slope and offset corrections which followed from the calibration baths. Further corrections for offsets were applied using Onset 12-Bit temperature smart sensors (S-TMB-M006) with HOBO data loggers (H21-001) which were installed just above the stream bed at 5 locations in the Springendalse Beek and 3 locations in the Elsbeek (Fig. 1). Comparison of the separate temperature sensors and the corrected DTS temperature measurements showed that stream temperatures could be measured with an accuracy of 0.19 °C on average. Temperatures were logged every 15 min and some of the loggers were supplied with an extra sensor to measure air temperature. Additional weather data was collected from nearby meteorological station Twenthe of the Royal Netherlands Meteorological Institute (KNMI).

2.3. Radon measurements

[222]Rn, an isotope released to the groundwater from aquifer material, was used as a tracer for groundwater in along-stream profiling (Cartwright et al., 2014; Cook et al., 2006; Genereux and Hemond, 1990). Samples were taken and measured immediately in the field using an Electronic Radon Detector (RAD7, Durridge). High radon values in streams were expected to be found only near locations with groundwater seepage because it rapidly decays (half-life of 3.8 days) and is released to the atmosphere due to degassing.

2.4. Stream temperature model

A stream temperature model (STM-GW) was built in Python using the xarray-simlab model framework (Bovy and McBain, 2017). The model is largely based on the model descriptions of Boyd and Kasper (2003) and Westhoff et al. (2007) and additionally simulates the interaction with groundwater in more detail (Fig. 2). In the model, all water fluxes (Q) are considered constant in time and only increase in the downstream direction due to groundwater and lateral inflow. The stream stretch is discretized into a 1D cell-centred grid and to prevent numerical diffusion a Courant number

of 1 is used. For this, the size of the stream cells fluctuates spatially with the flow velocity, which depends on the discharge, depth and stream width:

$$C = \frac{v_i * \Delta t}{\Delta x_i} = 1 \tag{1}$$

$$v_i = \frac{Q_i}{A_i} \tag{2}$$

$$\Delta x_i = \frac{Q_i}{A_i} \Delta t \tag{3}$$

where C is the Courant number [–], v_i is the flow velocity in cell i [m s^{-1}], Δt the time step [s] and Δx_i the cell size [m]. Q_i is the discharge at the downstream end of the cell [m s^{-1}] and A_i is the cross-sectional area [m^2] of the stream. The temperature in each cell is then calculated using:

$$T_i^{j+1} = \frac{T_i^j V_i + T_{GW}^j V_{GW} + T_{agri}^j V_{agri} + T_{pond}^j V_{pond}}{V_i + V_{GW} + V_{agri} + V_{pond}}$$
$$- \frac{v\Delta t}{\left(\frac{\Delta x_i + \Delta x_{i-1}}{2}\right)} \left(T_i^j - T_{i-1}^j\right) + \frac{R_i^j \Delta t}{A_i} \tag{4}$$

where T_i^{j+1} is the water temperature in the stream [°C] at grid cell i at the new time level j + 1, j denotes the old time level and i − 1 the grid cell upstream from cell i. The first term is the mixing term, the second term is the advection term and the third term is the temperature change due to the source/sink term. In a stream with no advection or energy source/sink but with only mixing from inflows (Fig. 2), the temperature is given by only by the mixing term:

$$T_i^{j+1} = \frac{T_i^j V_i + T_{GW}^j V_{GW} + T_{agri}^j V_{agri} + T_{pond}^j V_{pond}}{V_i + V_{GW} + V_{agri} + V_{pond}} \tag{5}$$

where T_i^j is the temperature [°C] and V_i the volume [m^3] of cell i at time j. V_{GW}, V_{agri} and V_{pond} are the volumes [m^3] of inflow per time step from groundwater, tributaries and seepage ponds respectively, and T_{GW}^j, T_{agri}^j and T_{pond}^j are their temperatures at time j. With only
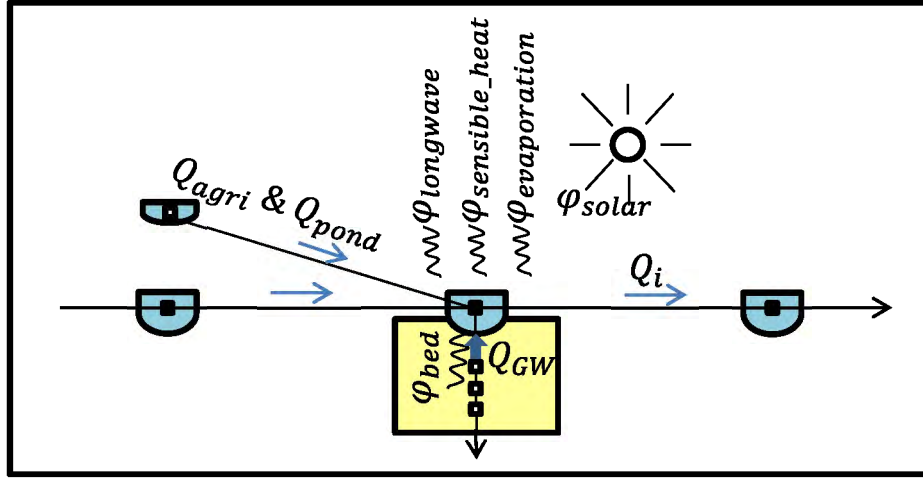
Fig. 2. Conceptualization of the STM-GW model. A stream cell can receive water from an upstream cell and from lateral inflow such as from tile drainage or seepage ponds. Each cell exchanges energy with the atmosphere by solar and longwave radiation, and latent and sensible heat flow. Each stream cell is connected to cells that represent the streambed to represent groundwater inflow and conductive heat exchange with the streambed.

advection, the stream temperature is given by the advection term (Eq. (4)):

$$T_i^{j+1} = T_i^j - \frac{v \Delta t}{\left(\frac{\Delta x_i + \Delta x_{i-1}}{2}\right)}(T_i^j - T_{i-1}^j) \qquad (6)$$

where $\frac{\Delta x_i + \Delta x_{i-1}}{2}$ is the average cell size between grid cell i and upstream cell i − 1 [m], which is needed because of the increase in cell size in the downstream direction. For simplicity dispersion is assumed to be negligible (e.g. Irvine et al., 2017; Rau et al., 2012). The temperature development of a stagnant body of water without inflow is determined by the source/sink term R (Eq. (4)), which includes all the energy fluxes that act on the water body:

$$R_i^j = \frac{B_i \varphi_{total\,i}^j}{\rho_w c_w} \qquad (7)$$

$$T_i^{j+1} = T_i^j + \frac{R_i^j \Delta t}{A_i} \qquad (8)$$

where B_i is the stream width [m] of cell i, c_w and ρ_w are the specific heat and density of the water and φ_{total} is the sum of all the energy fluxes per unit horizontal area [W m^{-2}].

φ_{total} is calculated for each cell for every time step and includes the various energy fluxes that influence stream temperature: solar radiation (φ_{solar}), longwave radiation ($\varphi_{longwave}$), latent heat flow ($\varphi_{evaporation}$), sensible heat flow ($\varphi_{sensible\_heat}$) and streambed conduction (φ_{bed}) (Fig. 2):

$$\varphi_{total} = \varphi_{solar} + \varphi_{longwave} + \varphi_{evaporation} + \varphi_{sensible\_heat} + \varphi_{bed} \qquad (9)$$

Solar radiation (φ_{solar}) [W m^{-2}] consists of both direct radiation and diffuse radiation which is described by fraction $D_{diffuse}$ of the incoming radiation (φ_{inRad}). A fraction D_f of the solar radiation penetrates the water and heats the streambed instead. Surface reflection coefficient R_{SS} corrects for reflection of solar radiation on the water surface and is based on the solar angle for direct radiation and is equal to 0.09 for diffuse radiation (Boyd and Kasper, 2003). Direct radiation is additionally corrected for shadow effects by shading factor C_S (Westhoff et al., 2007).

$$\varphi_{solar} = (1 - D_f)(\varphi_{direct} + \varphi_{diffuse}) \qquad (10)$$

$$\varphi_{direct} = C_s(1 - D_{diffuse})(1 - R_{SS})\varphi_{inRad} \qquad (11)$$

$$\varphi_{diffuse} = D_{diffuse}(1 - R_{SS})\varphi_{inRad} \qquad (12)$$

Longwave radiation ($\varphi_{longwave}$) [W m^{-2}] is the sum of the longwave radiation from clouds (atmospheric), back radiation from the water column and radiation emitted by the land cover (e.g. vegetation) (Boyd and Kasper, 2003):

$$\varphi_{longwave} = \varphi_{atmospheric} + \varphi_{back\_radiation} + \varphi_{land\_cover} \qquad (13)$$

$$\varphi_{atmospheric} = 0.96\varepsilon_{atm}\theta_{VTS}\sigma_{sb}(T_{air} + 273.2)^4 \qquad (14)$$

where ε_{atm} is the emissivity of the atmosphere [−], θ_{VTS} is the 'view to the sky' coefficient [−] and σ_{sb} is Stefan-Boltzmann constant [Wm^{-2} °C^{-1}].

$$\varepsilon_{atm} = 1.72 * \left(\frac{0.1 * e_a}{T_{air} + 273.2}\right)^{\frac{1}{7}} * (1 + 0.22 + C_L^2) \qquad (15)$$

where C_L is the cloudiness [−] and e_a is the actual vapour pressure [kPa].

$$e_a = \frac{H}{100}e_s \qquad (16)$$

where H is the relative humidity [%] and e_s is the saturation vapour pressure [kPa].

$$e_s = (6.1275e^{\left(\frac{17.27T_{air}}{237.3 + T_{air}}\right)} \qquad (17)$$

$$\varphi_{back\_radiation} = -0.96\sigma_{sb}(T + 273.2)^4 \qquad (18)$$

$$\varphi_{land\_cover} = 0.96(1 - \theta_{VTS})0.96\sigma_{sb}(T_{air} + 273.2)^4 \qquad (19)$$

Latent heat flow ($\varphi_{evaporation}$) [W m^{-2}] is calculated following the Penman equation for open water (Monteith, 1981):

$$\varphi_{evaporation} = -\rho_w L_e E \qquad (20)$$

where Le is the latent heat of evaporation [J kg^{-1}] and E is the Penman open water evaporation [m s^{-1}].

$$L_e = 1000(2501.4 + T) \qquad (21)$$

$$E = \frac{s\varphi_r}{\rho_w L_e(s + \gamma)} + \frac{c_{air}\rho_{air}(e_s - e_a)}{\rho_w L_e r_a(s + \gamma)} \qquad (22)$$

where s is the slope of the saturated vapour pressure curve at a given air temperature [kPa °C^{-1}], φ_r is the net radiation [W m^{-2}], γ is the psychrometric constant [kPa °C^{-1}] and r_a is the aerodynamic resistance [s m^{-1}].

$$\varphi_r = \varphi_{longwave} + \varphi_{solar} \tag{23}$$

$$r_a = \frac{245}{0.54 v_{wind} + 0.5} \tag{24}$$

where v_{wind} is the wind velocity [m s^{-1}].

$$s = \frac{4100 e_s}{(237 + T)^2} \tag{25}$$

The equation for sensible heat flow ($\varphi_{sensible\_heat}$) [W m^{-2}] is given by Boyd and Kasper (2003):

$$\varphi_{sensible\_heat} = B_r \varphi_{evaporation} \tag{26}$$

where Br is the Bowen ratio [–] given by:

$$B_r = 6.1 * 10^{-4} P_A \frac{T - T_{air}}{e_s^w - e_a^w} \tag{27}$$

where P_A is the adiabatic atmospheric pressure [kPa], e_s^w and e_a^w are the saturated and actual vapour pressure using the stream temperature [kPa].

$$e_a^w = \frac{H}{100} e_s^w \tag{28}$$

$$e_s^w = 0.61275 e^{\left(\frac{17.27 T}{237.3 + T}\right)} \tag{29}$$

$$P_A = 101.3 - 0.1055 z \tag{30}$$

where z is the elevation [m] at which humidity and air temperature were measured.

Heat Exchange between the streambed and the stream φ_{bed} [W m^{-2}] is computed by combining each stream cell with a vertical 1D streambed model (Boyd and Kasper, 2003):

$$\varphi_{bed} = -k \frac{T - T_{streambed}}{\frac{\Delta z}{2}} \tag{31}$$

Where k is the thermal conductivity of the combined water and soil matrix [J m^{-1} s^{-1} °C^{-1}], T is the water temperature in the stream [°C], $T_{streambed}$ is the temperature of the upper streambed cell of the streambed model [°C] and Δz is the thickness of the topmost cell [m]. Temperatures in the vertical 1D streambed model are solved using the advection-diffusion heat equation, with an upwind and a central difference solution for advection and diffusion respectively and a fixed cell size:

$$T_{iz}^{j+1} = T_{iz}^j + \frac{\Delta t}{c \rho} \left(\frac{k}{\Delta z^2} \left(T_{iz-1}^j - 2T_{iz}^j + T_{iz+1}^j \right) \right.$$
$$\left. - \frac{v_z c_w \rho_w}{\Delta z} \left(T_{iz-1}^j - T_{iz}^j \right) \right) + \frac{R_{bed}}{\Delta z} \tag{32}$$

where T_{iz}^{j+1} is the groundwater temperature [°C] at grid cell iz at the new time level j + 1, j denotes the old time level and iz − 1 the grid cell above cell i, v_z is the vertical groundwater flux (specific discharge) [m s^{-1}], c and ρ are the specific heat and density of the combined water and soil matrix, and R_{bed} is a source/sink term which only applies to the top model layer which represents the streambed. This layer exchanges energy with the stream water and is heated by the fraction D_f of the solar radiation (φ_{solar}) reaching the streambed. The source/sink term R_{bed} is given by:

$$R_{bed} = -\varphi_{bed} + \varphi_{solar} \frac{D_f}{1 - D_f} \tag{33}$$

The lower boundary of the model has a fixed temperature to represent a stable aquifer temperature at depth and the upper cell of the streambed model represents the stream and has a temperature that is updated every time step. Heat from streambed friction is considered to be negligible.

2.5. Model parameterization

The model was set-up for a length of 1500 m divided into 45 cells based on the flow velocity (Eq. (3)), and with characteristics similar to the Springendalse Beek such as springs, tributaries and groundwater-fed ponds. The model was run with a time step of 90 s for a total of three months: June and July 2016 to spin-up the model to get rid of artificial features inherited from the simple initial condition, and August 2016 for analysis. The vertical streambed models consisted of cells of 0.05 m and had a constant temperature boundary equal to the mean annual air temperature at a depth of 5 m. This depth could potentially be too shallow to have no seasonal temperature variations and we therefore ran a model test with the boundary at a depth of 10 m, but this did not result in a significant difference in stream temperature. The first cell was fed by seepage and an extra discharge component with the same temperature as the seepage in that cell, so that this discharge could be calibrated without getting unrealistic seepage rates through the small streambed area in the model cell. Air temperature, humidity, cloud cover and solar radiation were measured at nearby meteorological station Twenthe by the Dutch Meteorological Institute. The values that were used for thermal physical properties of the sediments were reported by Anibas et al. (2011) for another lowland stream with a sandy streambed and a wind velocity of 0.1 m s^{-1} was taken from Westhoff et al. (2007), representing the wind-sheltered location of the stream in a dense forest with abundant plants growing in and around the stream.

2.6. Scenario modelling

Different scenarios were run with the calibrated model (Table 3). The effect of climate warming was tested by raising the air temperature by two degrees in scenario 1a, while keeping the temperature of the deeper groundwater the same. Because the increase in air temperature is expected to also increase the temperature of the groundwater (e.g. Menberg et al., 2014; Taylor and Stefan, 2009), in scenario 1b both the air and groundwater temperature were increased by 2 °C. The importance of groundwater was tested by running the model with 50% more and 50% less groundwater seepage in the stream (scenarios 2 and 3). The effect of shading was evaluated by removing shading from a small part of the modelled stream (scenario 4) and by removing shading from the whole catchment (scenario 5).

3. Results

3.1. FO-DTS temperature measurements

3.1.1. Springendalse Beek

Fig. 3 displays results of temperature measurements in the Springendalse Beek in summer and winter. In summer, the absolute temperature slightly increases in the downstream direction (Fig. 3b) and the daily temperature amplitude tends to go up when there are no lateral inflows. Low temperatures between 10.3 and 15.0 °C close to the spring area (x = 200) indicate a strong influence of groundwater inflow. Downstream of the spring, the inflow of groundwater is less, and stream temperature is more influenced by atmospheric processes; measured temperatures vary between 12.3 and 18.8 °C at x = 1450 (Fig. 3b). In winter, the effect of groundwater seepage also is clearly visible in the DTS measurements. Upstream the stream water has a relatively high temperature in winter (5.0–9.6 °C), while temperatures decrease downstream (2.1–6.6 °C) (Fig. 3e–g). The mean and average daily standard deviation (SD) were also derived from the DTS data in order to locate groundwater seepage zones, using the fact that
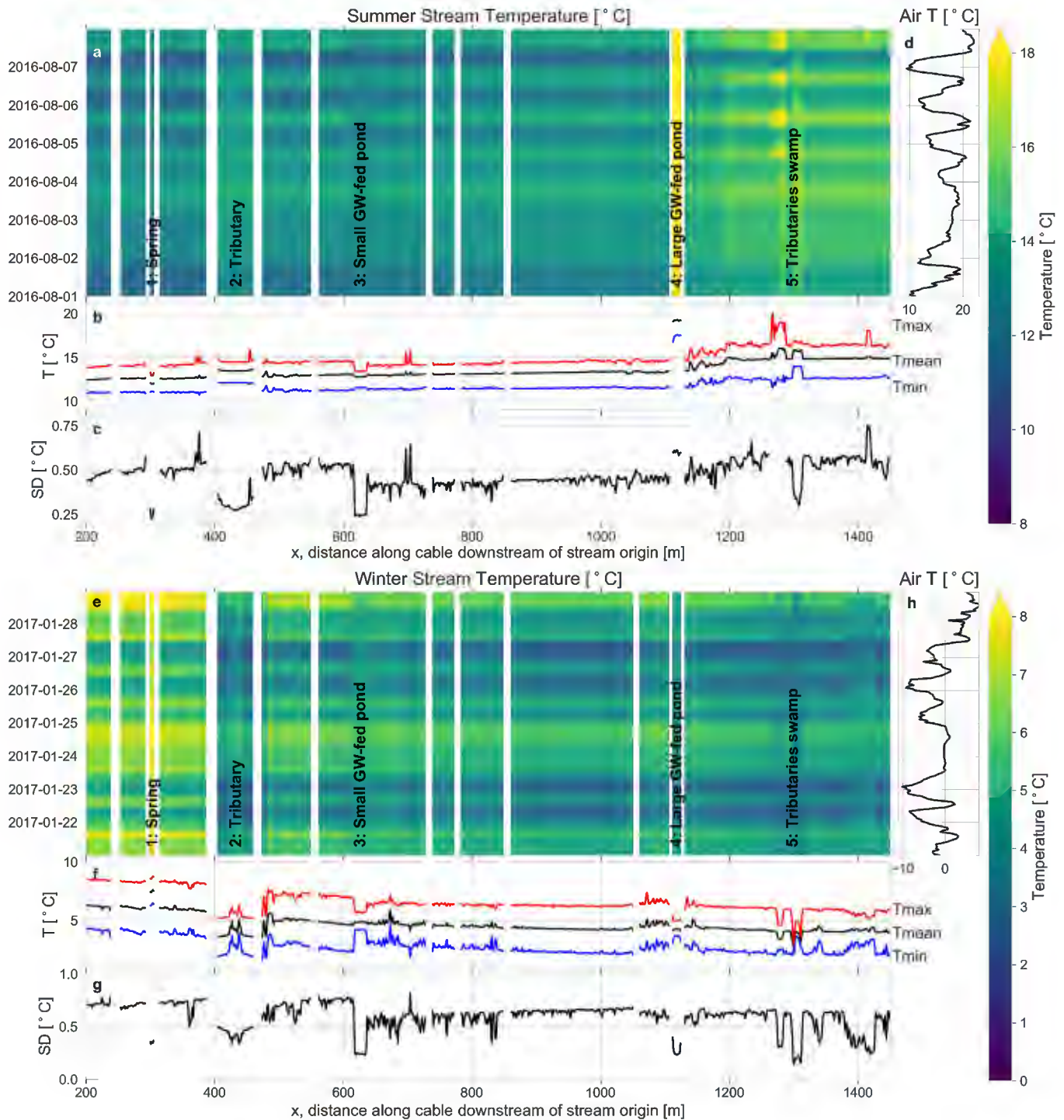
Fig. 3. Temperatures in the Springendalse Beek measured in a summer week (panels a–c) and in a winter week (panels e–g). Note that the legend colours are different between panels a and e. Streamflow is from left to right and the air temperature at a nearby meteorological station is given in panels d and h for the summer and winter period respectively. Maximum, average daily mean and minimum temperatures during the shown periods are given in panels b and f, and the average daily standard deviation in panels c and g. Thermal anomalies appear as warmer or colder vertical bands in panels a and e, of which locations 1–5 are indicated and listed in Table 1. Locations where the cable was known to be exposed to the air are filtered out and appear as white vertical lines. (For interpretation of the references to colour in this figure legend, the reader is referred to the web version of this article.)

groundwater has less temperature variation and thus the SD is lowered at locations with seepage (e.g. Hare et al., 2015; Lowry et al., 2007; Matheswaran et al., 2014a; Rosenberry et al., 2016). See for instance at x = 630 and Table 1, which summarizes the data for some specific locations. Upstream in the Springendalse Beek the SD is around 0.5 °C both in summer and winter, and in the

downstream direction increases in summer to around 1 °C and remains approximately stable at 0.5 °C in winter.

Table 1 lists characteristics of thermal anomalies associated with specific hydrological features such as tributaries and springs. At location 1 (Fig. 3) the cable was looped through the outflow of a small spring which had a lower summer and higher winter

Table 1
Features in the Springendalse Beek with distinct thermal characteristics.

Location	Location along cable [m]	Feature	Summer		Winter		Observations
			Mean	SD	Mean	SD	
Upstream	200	–	12.6	0.75	6.3	1.02	
1	305	Spring	12.1	0.47	7.5	0.53	Sand volcanoes, loose sediment
2	435	Tributary	13.5	0.53	3.9	0.82	
3	630	Small GW-fed pond	12.8	0.43	4.9	0.36	Year-round discharge
4	1120	Large GW-fed pond	19.2	0.88	4.3	0.29	Year-round discharge
5	1300	Tributaries swamp	15.9	0.69	2.5	0.21	
Downstream	1430	–	15.0	0.88	3.9	0.94	

temperature than the water in the stream (Table 1) as a result of the stable temperature of groundwater seepage. The outflow of a small groundwater-fed pond at location 3 had this same thermal groundwater characteristics of lower summer and higher winter temperatures than the stream water. In addition, the stream temperature at x = 350, 650, 1100 and 1400 m had similar characteristics as the spring (1) and the small groundwater-fed pond (3): the up- to downstream summer warming and winter cooling was dampened and SD values were lower than expected (Fig. 3). This suggests that significant seepage occurs at these locations. The outflow of a larger groundwater-fed pond at 4 had high summer temperatures and a high SD (Table 1), which is different from the small groundwater-fed pond and suggests a smaller groundwater influence on the temperature. This is potentially due to a longer residence time in the larger pond: although fed by groundwater, the larger volume of the pond results in a larger residence time of the water which slowly loses the groundwater thermal signal. Contrary to the groundwater indicative thermal signals, a tributary stream at location 2 (Fig. 3) had relatively high summer and low winter temperatures (Table 1), and the same holds for the outflow of a swamp through two small tributaries at location 5. The discharge of both

these inflows is fed by an agricultural area, where it derives from drains (shallow groundwater) and is influenced by atmospheric processes while flowing towards the Springendalse Beek.

Besides effects from groundwater seepage, effects of air temperature and rainfall are also visible in the DTS-measurements. For instance, a sharp increase in stream temperature occurred between August 1st and 2nd (Fig. 3a) and is the result of input from precipitation during a rainstorm. In addition, monitoring artefacts are shown, for instance around x = 1280 where a temperature increase is seen from August 4th as a result of the cable becoming exposed to air due to lowering of the water level.

3.1.2. Elsbeek

The measured stream stretch in the Elsbeek is located further downstream from the stream origin than the measured stretch in the Springendalse Beek (approximately 5000 vs 200 m). The measured temperature of the Elsbeek slightly decreases in the downstream direction before increasing between x = 750 and 900 and finally decreasing again towards the most downstream measured point (Fig. 4a, b). This pattern is also clearly visible in the SD (Fig. 4c), which is lower at locations with a lower temperature.
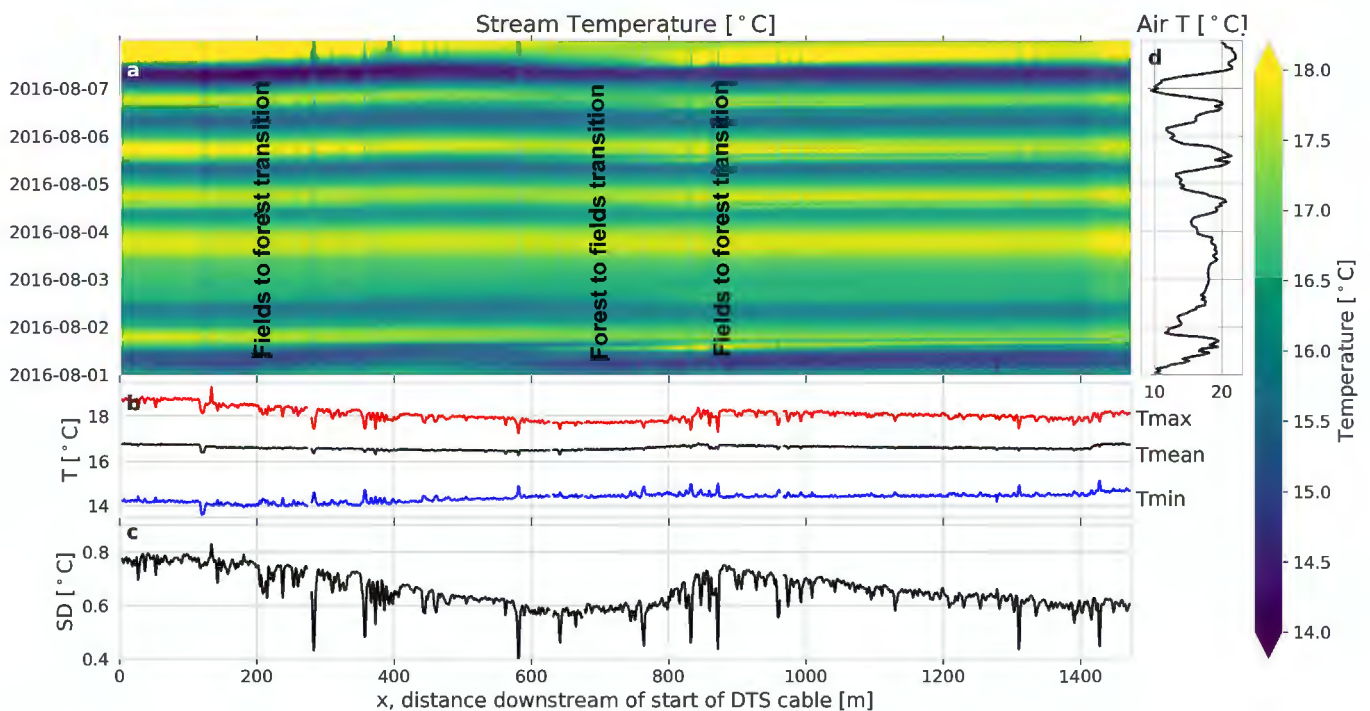

Fig. 4. Temperatures in the Elsbeek measured in a summer week (panel a). Streamflow is from left to right and the air temperature at a nearby meteorological station is given in panel d. Maximum, average daily mean and minimum temperatures during the shown period are given in panel b and the average daily standard deviation in panel c. Thermal anomalies appear as warmer or colder vertical bands in panel a.

The parts of the stream with decreasing temperatures coincide with the locations of (riparian) forests while the stretches with increasing temperatures are located in agricultural fields. The temperature measurements show several negative spikes in maximum temperature and SD (Fig. 4). While this appears similar to the characteristics of seepage, these locations have a minimum temperature significantly above the average groundwater temperature of around 11 °C. Instead of seepage, visual inspections showed that at these locations the DTS cable is either located on the bottom of (stagnant) pools or buried by sediment.

3.2. ^{222}Rn measurements

The ^{222}Rn concentration in groundwater was measured both at piezometers within our catchment which showed concentrations between 3210 and 5800 Bq m^{-3} and at the spring which showed concentrations of 733 and 3730 Bq m^{-3} (Fig. 5). The low spring concentration of 733 Bq m^{-3} might be influenced by recent precipitation or by some decay in the spring area, as the other radon concentrations of 3000 Bq m^{-3} and higher are in line with the concentrations found for groundwater in other studies in the Netherlands, including well fields in the region of our catchment (Kwakman and Versteegh, 2016; Yu et al., 2019). The ^{222}Rn activity in the stream water in the most upstream part of the Springendalse Beek catchment is between 104 and 1240 Bq m^{-3} while more downstream ^{222}Rn concentrations are below 500 Bq m^{-3} (Fig. 5), showing a decrease in groundwater influence in the downstream direction. The small groundwater-fed pond has a mean Radon level of 1388 Bq/m^3 (n = 4) indicating a large relative influence of recent groundwater seepage. The concentrations in the large pond have an average of 177 Bq m^{-3} (n = 3; Fig. 5) indicating only a small influence of recent seepage.
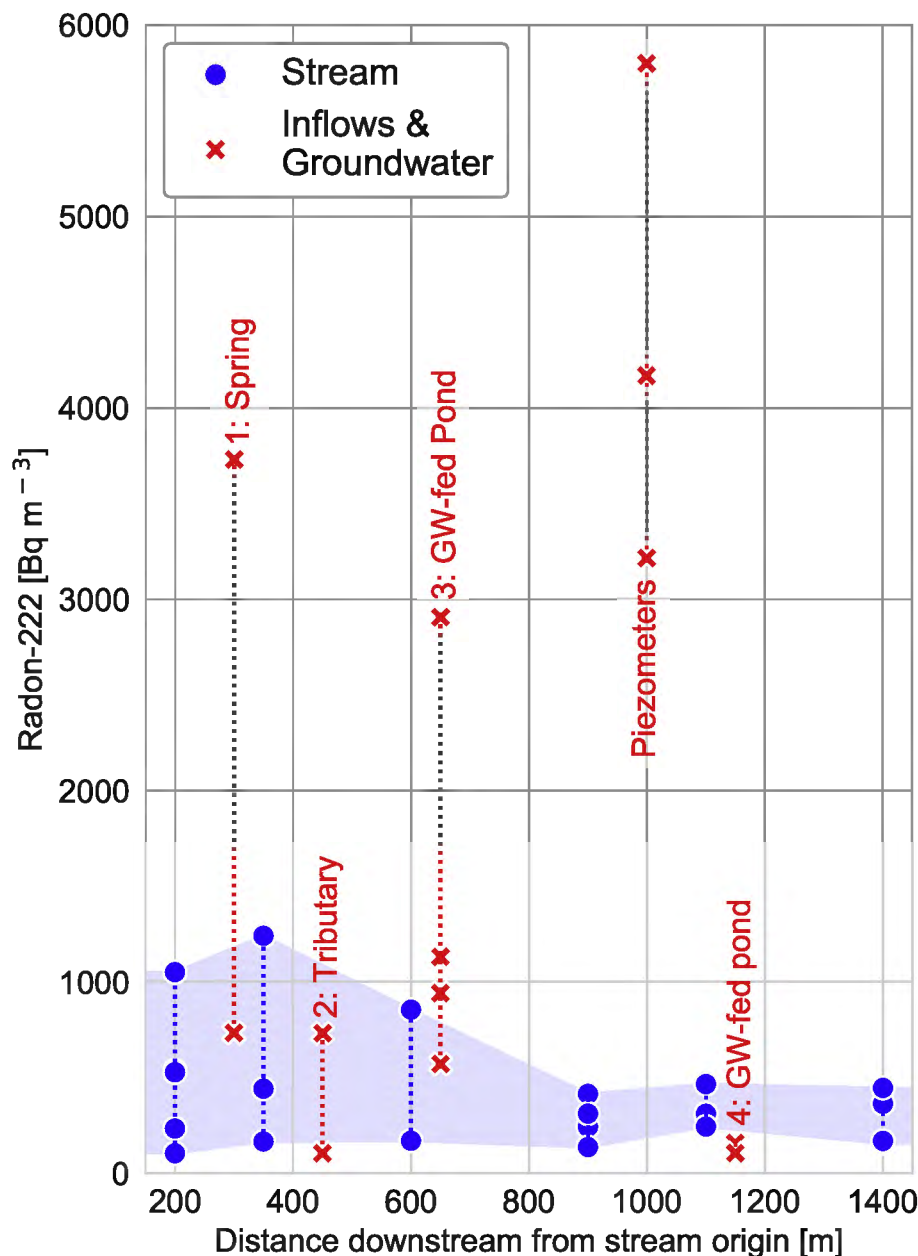

Fig. 5. Measurements of ^{222}Rn taken during 6 field campaigns in the catchment of the Springendalse Beek: of stream water (blue circles) and of inflows towards the stream (Table 1) and piezometers (red crosses). (For interpretation of the references to colour in this figure legend, the reader is referred to the web version of this article.)

Table 2
Calibrated model parameters.

Parameter	Description	Value	Reference
H [%]	Humidity 2016–2017	23–100	KNMI, Twenthe station
T_{air} [°C]	Air temperature 2016–2017	−10.1 to 34.1	KNMI, Twenthe station
φ_{inRad} [W m^{-2}]	Solar radiation 2016–2017	0.0–952.8	KNMI, Twenthe station
Δt [s]	Time step	90	Chosen
Δx [m]	Length of stream reservoir	Variable along x-axis	Based on Courant number = 1
Δz [m]	Length of soil reservoir	0.05	Chosen
B [m]	Stream width	0.60–1.50	Estimated
Z [m]	Stream depth	0.03–0.07	Estimated
Q [m^2 s^{-1}]	Stream discharge	0.05–0.34	Estimated
v_z [mm d^{-1}]	Groundwater flux	0.05–1.20	Estimated
T_{deepGW} [°C]	Temperature of lower z boundary	11.0	Estimated
$D_{diffuse}$ [−]	Fraction of diffuse solar radiation	0.0	Estimated
Df [−]	Fraction of solar radiation reaching the streambed	0.5	Estimated
R_{SS} [−]	Surface reflection	Based on solar angle	Boyd and Kasper (2003)
C_s [%]	Shading factor	5–20	Estimated
C_L [−]	Cloudiness	0–1	KNMI, Twenthe station
θ_{VTS} [−]	View to the sky coefficient	0.6	Estimated
σ_{sb} [Wm^{-2} °C^{-1}]	Stefan-Boltzmann constant	5.67 * 10^{-8}	–
v_{wind} [m s^{-1}]	Wind velocity	0.1	Westhoff et al. (2007)
γ [kPa °C^{-1}]	Psychrometric constant	0.66	Westhoff et al. (2007)
ρ_a [kg m^{-3}]	Density of air	1.2	–
ρ_w [kg m^{-3}]	Density of water	1000	–
ρ_{sed} [kg m^{-3}]	Density of the saturated sediment	1965	Anibas et al. (2011), Dujardin et al. (2014)
c_{air} [J kg^{-1} °C^{-1}]	Specific heat capacity of air	1004	–
c_w [J kg^{-1} °C^{-1}]	Specific heat capacity of water	4182	–
c_{sed} [J kg^{-1} °C^{-1}]	Specific heat capacity of the saturated sediment	1365	Anibas et al. (2011), Dujardin et al. (2014)
k_w	Thermal conductivity of water	0.6	–
k_{sed}	Thermal conductivity of the saturated sediment	1.833	Anibas et al. (2011), Dujardin et al. (2014)

3.3. Model calibration

The manual calibration was done step-wise and an overview of the model parameters is shown in Table 2. The model is most sensitive to the parameters θ_{VTS}, $D_{Diffuse}$, upstream starting Q and the width of the stream, and therefore focus was on these parameters during calibration. Discharge from groundwater seepage and lateral inflow, stream width and depth and shading varied along the stream length and were estimated using our knowledge of the field sites and were then further calibrated (Fig. 6). The initial temperature of the stream and the streambed were set to 10 and 11 °C respectively. Calibration of D_f and $D_{diffuse}$ resulted in values of 0.5 and 0.0 respectively. Lateral inflow from an agricultural stream was added to the model at x = 435. The temperature of this inflow represented discharge from a tile drained area (seepage from 1 m depth). The two seepage ponds in the Springendalse Beek were located at locations x = 650 and 1150 m in the model. The pond sizes, depths, shading and seepage rates were also calibrated with the DTS measurements. Their depths were 1.5 and 1.0 m and their surface areas 900 and 3000 m^2 respectively. The pond at
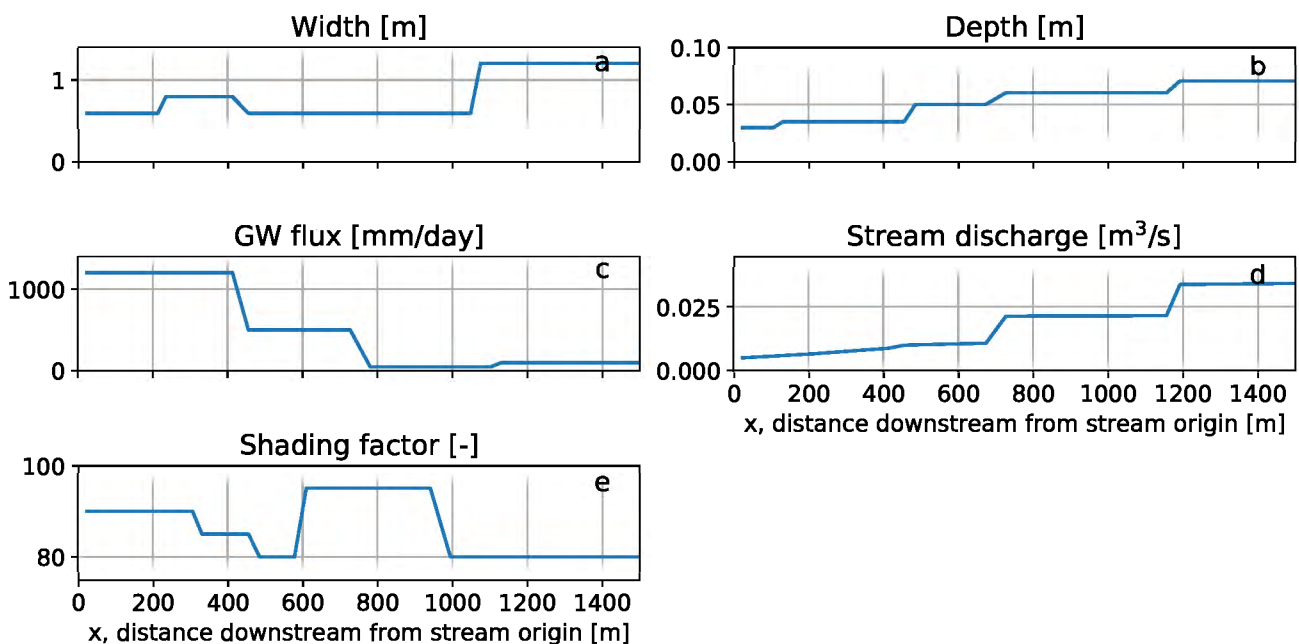

Fig. 6. Calibrated stream width (a) and depth (b), groundwater seepage rates (c), discharge (d) and shading factor (e) in the model, representing the Springendalse Beek.

650 m had a calibrated seepage rate of 1000 mm per day and was 90% shaded. The pond at 1150 m had a calibrated seepage rate of 350 mm per day and was not shaded with a shading factor of only 10%.

3.4. Modelled temperature distribution along the stream

The calibrated STM-GW model, using the parameters listed in Table 2, shows a reasonable fit with the observed DTS data from the Springendalse Beek (Fig. 7), especially considering that the model does not include local heterogeneity in e.g. water depth and air temperature. Both the diurnal temperature variation in the up-and downstream temperature are represented well by the model, although the simulated temperature upstream is slightly underestimated (Fig. 7b). Fig. 7c shows the modelled result for two night and two days (2 AM and 2 PM), for a warmer day (Day 1) and colder day (Day 2). The temperature pattern from up- to downstream on these days is simulated adequately by the model including the modelled features such as the spring and tributary spring. Especially the temperature step resulting from the tributary stream at x = 450 and the inflow of water from the seepage ponds (x = 700 and x = 1200) lead to clear temperature steps in the model, that were also observed in the DTS measurements (Fig. 7c).

Using the model, we were able to investigate the theoretical importance of the different processes affecting the stream temperature. For comparison with the other energy fluxes, the heat energy provided by seepage [W m^{-2}] was calculated using:

$$E_{seepage} = \Delta T v_z c_w \rho_w \qquad (34)$$

where ΔT is the temperature difference between the stream and seeping groundwater, which means that Eq. (34) gives the energy

flux compared to the current stream water temperature and is thus an *apparent* rather than an absolute heat flux, as explained by Kurylyk et al. (2016). Fig. 8 shows the modelled energy fluxes to and from the stream on August 6, 2016. The energy flux from seepage is mostly negative because seepage of groundwater often leads to cooling on summer days. The higher seepage rates given to the upstream part of the model are also shown in the energy fluxes (Fig. 8a and c): higher seepage rates lead to more cooling of the stream both through the advective flux and through increased streambed conduction. The negative energy fluxes from both bed conduction and seepage increase during the day, because stream water is heated and the temperature difference between seepage and stream water increases. The flux from solar radiation naturally has a day-night fluctuation and is lower at locations with shading. Sensible heat flow is dependent on the difference between stream water and air temperature (Eq. (27)) and therefore shows a day-night pattern as well. It decreases in the downstream direction, as the difference between stream water and air temperature decreases due to the heating or cooling of the stream water in the downstream direction by atmospheric processes.

3.5. Scenario modelling

From the base run (Fig. 7), several model parameters were changed to simulate different scenarios to get a better understanding of the possible future changes resulting from climate change and the role of groundwater in this. Table 3 shows the upstream (x = 200) and downstream (x = 1450) average, minimum and maximum stream temperature for the calibrated base run and five different scenarios.
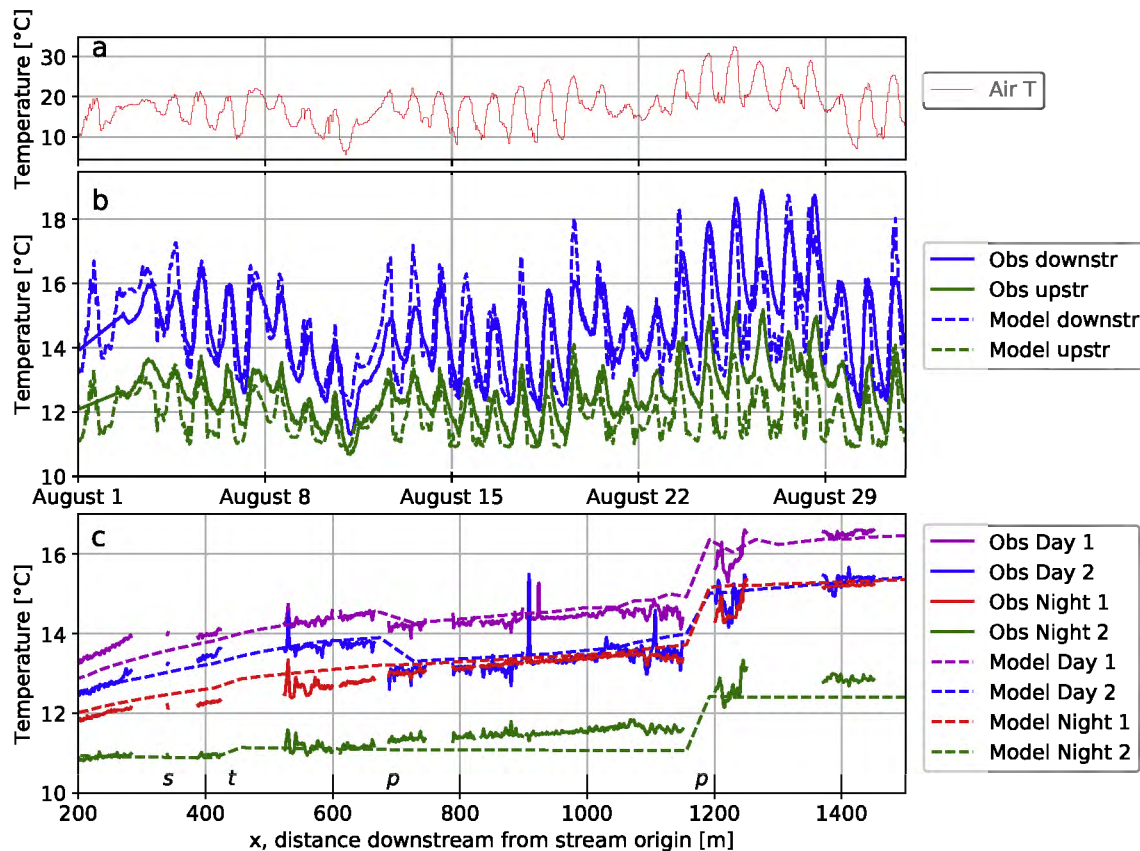

Fig. 7. Fit between the calibrated model and measurements taken in the Springendalse Beek in August 2016. Panel a shows the air temperature, panel b shows the fit for both up- (x = 200) and downstream (x = 1450) and panel c shows the fit for 2 day and 2 night measurements. The letters at the bottom of panel c indicate the location of a spring (s), a tributary (t) and ponds (p).
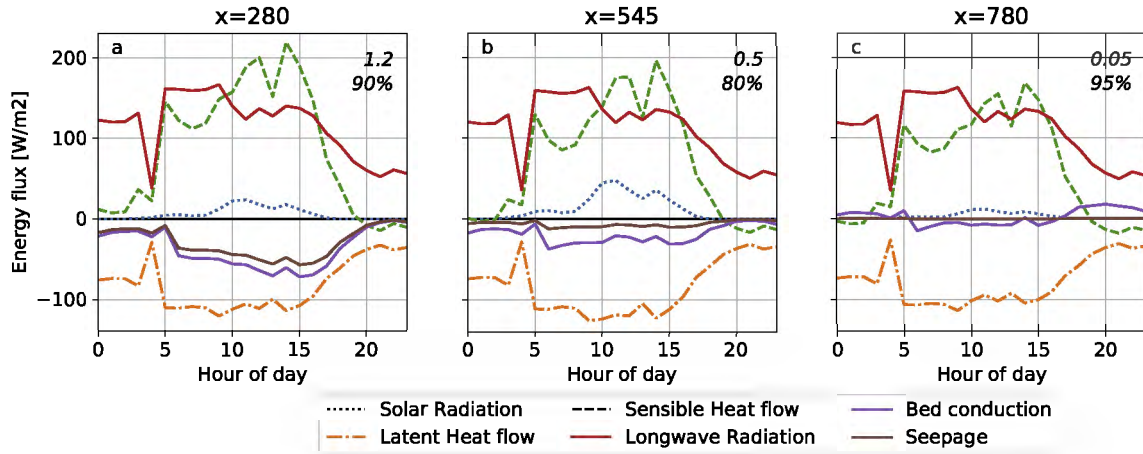
Fig. 8. Modelled energy fluxes to (positive) and from (negative) the stream at 3 different locations on August 6th 2016. The seepage rate (m d⁻¹) and percentage of shading are indicated at the top right of the figures: panels a, b and c show locations with a high, medium and low seepage rate respectively.

Table 3
Results of the scenario modelling: statistics for the month August 2016.

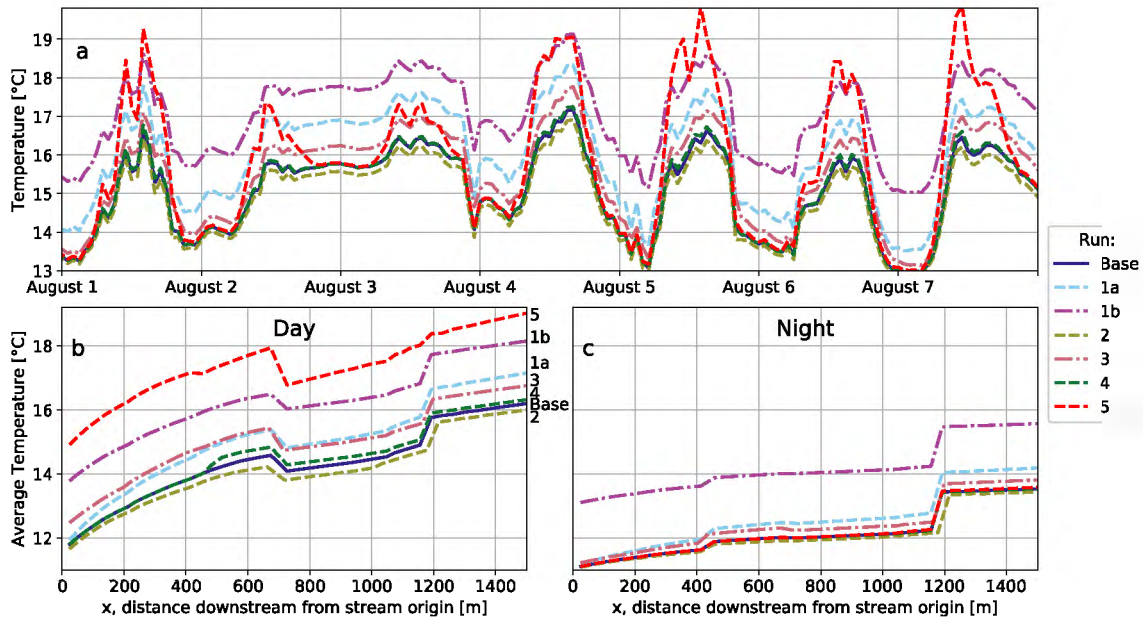| Scenario		Upstream temperature [°C]			Downstream temperature [°C]		
		Average	Min	Max	Average	Min	Max
0	Base run	12.0	10.9	14.3	14.6	12.2	18.7
		Temperature change from base run [°C]:					
1a	T + 2 °C, GWlower_boundary + 0 °C	0.3	0.0	0.5	0.8	0.2	1.0
1b	T + 2 °C, GWlower_boundary + 2 °C	1.9	2.0	1.8	2.0	2.0	1.9
2	50% more GW in stream	−0.1	0.0	−0.3	−0.1	−0.1	−0.2
3	50% less GW in stream	0.3	0.0	0.8	0.4	0.0	0.7
4	No shading between x = 450–500	0.0	0.0	0.0	0.1	0.0	0.2
5	No shading	1.2	0.0	5.0	1.1	0.0	4.3

Fig. 9. Result of the modelled scenarios listed in Table 3. Panel a shows the downstream (x = 1450) temperature simulated in the different scenario runs for the whole of August 2016. Panels b and c show the simulated mean day and night temperature (August 2016) from up to downstream.

An increase in air temperature in scenarios 1a and 1b resulted in an increase in water temperature (Fig. 9a). In scenario 1a a stable groundwater temperature buffers the increase in water temperature compared to scenario 1b, where the stream temperature increased by approximately the same amount as the air and groundwater temperature (Table 3, Fig. 9a). The upstream temperature is hardly affected by an increase in air temperature because it is located close to the upstream stream spring. Especially the night temperature both up- and downstream seems to be almost fully determined by the groundwater temperature, as the 2 °C increase

of the lower boundary in scenario 1b leads to a similar increase of the minimum temperature both upstream and downstream. Scenarios 2 and 3 show the effect of an increase or decrease of groundwater seepage in the stream: an increase of seepage resulted in lower maximum temperatures while a decrease resulted in higher maximum temperatures (Table 3). The removal of shading between x = 450 and 500 had a local effect on this new non-shaded part where temperature increased by 0.4 °C (Fig. 9b), and had only a slight effect on the maximum temperature downstream (+0.1 °C). In scenario 5, where shading was removed from the whole stream, daytime temperatures strongly increased, approximately the same or more as in scenario 1b. However, night temperatures stayed the same since the effect of shading is depleted when there is no solar radiation (Fig. 9).

4. Discussion

4.1. Mapping local and diffuse groundwater seepage

4.1.1. Springendalse Beek

The stream temperature and ^{222}Rn measurement in the Springendalse Beek reflected the stream to be highly influenced by groundwater, as was expected from the fact that several springs exist in this particular catchment (van der Aa et al., 1999). The stream had both local and diffuse seepage locations. Two local seepage spots were identified from the temperature measurements: a spring and groundwater-fed pond (locations 1 and 3; Table 1). The ^{222}Rn measurements and other field observations such as sand volcanoes, loose sediments, abundant presence of macrofauna and year-round discharge confirmed the presence of seepage at these features (Fig. 5). Small hotspots of diffuse seepage (maximum length a few meters) were located at 4 locations (around x = 350, 650, 1100 and 1400), indicated by lower SD values and a dampening of the warming in summer and cooling in winter in the downstream direction. However, the hotspots were not clearly visible in the ^{222}Rn measurements, probably because their flux was too small compared to river discharge to influence ^{222}Rn downstream. The observed increase in discharge in the downstream direction indicates that low rates of diffuse seepage are occurring in the catchment, but this could not be shown in the measurements, as small fluxes cannot be located adequately using DTS (e.g. Krause et al., 2012) or ^{222}Rn measurements. Substantial variations in time were found between the ^{222}Rn measurements, which could be related to changes in exchange with the atmosphere due to wind and turbulence (e.g. Cartwright et al., 2014; Cook, 2013; Genereux and Hemond, 1992; Wallin et al., 2011) or to changing flow velocities and discharge leading to a change in decay time.

The outflow of the small pond and the measured groundwater (spring and piezometers) have a clear groundwater ^{222}Rn signal which is much higher than the ^{222}Rn values measured in the outflow of the large groundwater-fed pond (Fig. 5). It was expected that both ponds would show a clear groundwater signal because both have a year-round discharge but no inflow of surface water and therefore must have a significant input of groundwater. The ^{222}Rn concentration at the large pond is the lowest measured in the catchment and was at some occasions difficult to detect (Fig. 5). The difference in ^{222}Rn between the ponds suggests that the residence time of water in the large pond is much larger than in the small pond, allowing for more decay of Radon and a change in the thermal signature. With a half-life time of 3.8 days and ignoring degassing for simplicity, seeping groundwater with a ^{222}Rn concentration of 3500 Bq m^{-3} (as measured in the piezometers and spring) would take approximately 5 days to reach the average level of 1400 Bq m^{-3} found in the small pond but 19 days

to reach the average level of 117 Bq m^{-3} found in the large pond. Relating the residence time with the volume and discharge in the pond is done using:

$$T = \frac{V}{N} \tag{35}$$

where T is the characteristic time [days], V is the volume [L] and N is the (groundwater) recharge [L s^{-1}] (e.g. van Ommen, 1986). The outflow of the pond can be assumed to equal the groundwater discharge towards the ponds and was measured at 4 vs 3 L s^{-1} for the large and small pond respectively. With estimated volumes of 5000 and 1300 m^3 respectively, the characteristic residence time is estimated to be 15 and 5 days, and thus close to the estimations of 19 and 5 days using ^{222}Rn. The slight deviation found for the large pond could result from an underestimation of pond volume, but also from ignoring the atmospheric exchange of radon, which would also lead to a decrease in the estimated residence time. However, we assume atmospheric exchange to be a much slower process than radioactive decay in the ponds, especially because they contain stagnant water, are located in a forest and thus sheltered from wind and contain abundant water plants that prohibit the presence of waves or turbulence that would promote the atmospheric exchange. As atmospheric exchange would then be governed by diffusion from deeper water to the pond surface, this effect was assumed to be negligible relative to the effect of the radioactive decay with a half-life time of 3.8 days (e.g. Dimova et al., 2013; Dulaiova and Burnett, 2006; Emerson and Broecker, 1973; Zappa et al., 2003). The longer residence time in the large pond than in the small pond results in more warming in summer (Table 1), especially since the large pond is barely shaded.

4.1.2. Elsbeek

It was not possible to locate groundwater seepage in the Elsbeek using the FO-DTS measurements. An increase in streamflow and the presence of iron oxide precipitation along banks show that diffuse seepage does occur in the catchment but apparently these fluxes are not large enough to create a distinguishable temperature signal. Patterns in the measured temperature were attributed to morphological and riparian differences. Several thermal anomalies were found but were caused by the burial of sediment and presence of pools. In addition, the temperature and SD along the stream seem to have a good correlation with the sequence of open-shaded-open-shaded stream stretches (Fig. 4).

4.2. DTS-measurements in a heterogeneous stream system

Similar to the conclusions of Matheswaran et al. (2014a), the standard deviation of diurnal temperatures was found to be best suitable for locating groundwater seepage in summer, while the mean temperature appeared useful for winter measurements. Several difficulties appeared in analysis of the DTS measurements. First, the DTS cable and streambed may be warmed up by direct solar radiation (Neilson et al., 2010), although we did not find evidence for this. Second, sedimentation of the DTS cable led to a similar signal as seepage, which was also found by e.g. Karan et al. (2017). Sediment functions as insolation of the cable which therefore shows a buffered temperature signal. To separate the temperature effect of sedimentation, Sebok et al. (2015) used parallel DTS cables which allowed them to detect sedimentation and scouring. Hilgersom et al. (2016) were able to distinguish sedimentation by applying a 3D DTS devise, although this seems only practical for lab or small field areas. Third, we aimed to place the cable in the centre of the stream but because of that may have missed seepage occurring only on certain sides of the stream, as recent studies have shown the large heterogeneity in shallow subsurface

temperatures, groundwater flow paths and seepage (e.g. Gilmore et al., 2016; Kennedy et al., 2009; Rosenberry et al., 2016).

Lastly, measurements from the Elsbeek suggested that stratification of water temperatures (Neilson et al., 2010) is occurring in pools (Fig. 4), also leading to a temperature signal similar to that of seepage. These pools in the Elsbeek are deep (~1 m) compared to the low streamflow in summer (can go to zero in dry periods). Because the fibre-optic cable is placed on the streambed, the temperature of the water at the bottom of a pool is measured. Because more energy is needed to heat the water mass in a pool, the temperature reacts more slowly on changes and thus pools present a buffered temperature signal, similar to the effect of groundwater seepage. The temperature at the pool bottom can significantly differ from the temperature of the surface as thermal layering can occur in deeper pools, where solar radiation does not heat the entire water column (Sebok et al., 2013). Pools do not necessary greatly influence the temperature of streams, as this stratification can only occur if the water flowing into the pool stays at the surface and continues to flow in the downward direction, with limited mixing with the water in the pool. Sedimentation of the cable at the bottom of the pool may also occur, further buffering the measured temperature signal.

4.3. The buffering capacity of shading and stream morphology

Compared to other studies (e.g. Harrington et al., 2017), the effect of direct solar radiation on the temperature of our study stream is relatively low and the other fluxes relatively high (Fig. 8). Direct solar radiation does not affect stream temperatures as much as the other atmospheric energy fluxes because of the high shading of the Springendalse Beek. In addition, the other energy fluxes are relatively high because the temperature difference between the stream water and air is large, increasing e.g. longwave radiation (Equation (19)). As expected, shading reduced maximum stream temperatures (Table 3, Fig. 9). However, shading has a large impact on the temperature of the stream: without shading, the water temperature would increase in summer by ~4 °C (scenario 5). Removing shading from a small stream stretch (50 m) affected the maximum temperature even 1 km downstream (scenario 4; Fig. 9b). Garner et al. (2014) argued that while shading seems to cause cooling of stream water, the discrepancy between the water temperature in open and shaded stretches is caused by the fact that in shaded parts water is less heated and daytime heating therefore lags behind compared to non-shaded parts. This could also explain the observed temperature variation between open and shaded parts in the Elsbeek, where temperatures increase in the non-shaded parts and decrease in the shaded parts (Fig. 4).

In addition to shading, the stream temperature is also influenced by the water depth. A shallow stream warms up faster, but also has a higher flow velocity than locations with pools allowing less time for warming of the water. The temperature measured in the Elsbeek showed that the temperature at the bottom of deeper pools was buffered and had less extreme temperature peaks than the surrounding stream sections because the larger body of water at these locations was able to adsorb more heat than shallow stream sections.

4.4. Temperature buffering by groundwater

Our temperature measurements showed that groundwater provides relatively cool water in summer and warm water in winter (Figs. 4 and 5), which was especially clear in springs (Table 1). Separating the energy fluxes of seepage from the other processes using the model (Fig. 8) showed that the importance of groundwater for stream temperature depends on the temperature difference between the surface- and groundwater. For instance, the buffering

capacity of seepage increases during a summer day as the stream gets heated and the temperature difference increases (Fig. 8). The scenarios showed that the increase in stream temperature resulting from decreased seepage (scenario 3) is larger than the decrease in temperature following from increased seepage (scenario 2). This is not only due to the change in the amount of groundwater versus the volume of stream water, but also follows from the fact that with higher groundwater fluxes the temperature of seepage is more similar to the deeper groundwater than with low seepage rates, because less time is available for downward conduction of heat. Higher seepage fluxes thus increase the temperature gradient in the streambed, and therefore increase the buffering capacity of groundwater both through the advective flux and through increased streambed conduction (Caissie and Luce, 2017).

Recent studies showed the importance of 'source depth' of seepage for the temperature signal that is transported by groundwater to surface waters (Briggs et al., 2018a, 2018b; Kurylyk et al., 2015). The temperature of shallow groundwater is influenced by the seasonality at the surface, and as such the buffering capacity of this groundwater is lower than that of deeper groundwater. Thus, groundwater seepage may hold a (lagged and attenuated) seasonal temperature signal, resulting from either the groundwater flow path and transferred from infiltration zones (Briggs et al., 2018b, 2018a; Kurylyk et al., 2015) or from heat conduction from the streambed at the seepage zone (Caissie and Luce, 2017). Our study did include the second process of heat conduction at seepage zones (Eq. (32)), which is especially important if seepage velocities are slower and deep flow paths are dominant. However, with the methods in our study we were not able to consider the first process of source depth, which is especially important when groundwater velocities are high and/or travel times short, which is known to be the case for at least part of the seepage in these catchments (Kaandorp et al., 2018a).

We found that the spring and two groundwater-fed ponds discharge groundwater towards the stream, but with different residence times from the moment of seepage till the moment of discharge to the stream. This leads to a clear difference in the temperature effect on the stream, which is listed in Table 4. Because the water discharging through the spring only takes little time to join the stream, its temperature in winter is always higher than the stream water (Fig. 3). As residence time increases, the water is more influenced by atmospheric processes such as sensible heat flow and it changes temperature compared to the stream water. For instance, the large groundwater-fed pond has an estimated residence time between 15 and 19 days and in winter discharges water towards the stream which is both colder on average and during the day (maximum) than the water in the stream.

4.5. Climate warming

Scenarios 1a and 1b, in which air temperatures where increased in both scenarios and groundwater temperatures only in scenario 1b, showed how the buffering capacity of groundwater highly depends on the temperature increase of groundwater in a changing climate. Much is still unknown about the exact response of the temperature of groundwater to climate change (e.g. Menberg et al., 2014; Watts et al., 2015). Kurylyk et al. (2015) simulated the temperature of shallow groundwater during several climate change scenarios. They showed for instance a case where 50 years after an instantaneous increase in the air temperature of 2.0 °C the temperature of groundwater at a recharge location in a sandy aquifer had increased by 1.9 °C at a depth of 5 m and by 1.6 °C at a depth of 20 m. Because it is expected that the increase in the groundwater temperature will always lag behind on the increase of the air temperature (e.g. Kurylyk et al., 2013), the temperature difference between the two increases in a warming climate,

Table 4
Comparison of features with point groundwater seepage.

		Spring	Small GW-fed pond	Large GW-fed pond
Location		1	3	4
Location along cable		305 m	630 m	1120 m
Residence time/time since seepage		0–1 days	5 days	15–19 days
Temperature in winter relative to stream temperature	Minimum	↑	↑	↑
	Average	↑	↑	↓
	Maximum	↑	↓	↓

depending on the depth where groundwater is flowing. This would lead to a relative increase in the buffering capacity of groundwater compared to the current climate and thus partly buffers the effect of climate warming in groundwater dominated streams.

Climate change might not lead to a consistent year-round increase in temperatures, but instead lead to a different temperature increase in summer than in winter, which will also affect the buffering capacity of groundwater on stream temperature. In our study area, part of the streamflow is derived from deeper groundwater (Kaandorp et al., 2018a) and the temperature of this deeper groundwater depends on the average temperature increase, not seasonality as seasonal signals are dampened with depth. Therefore, if summer temperatures increase more than winter temperatures (e.g. by 3 °C and 1 °C respectively) and the groundwater temperature increases by the average (e.g. 2 °C), the temperature difference between the stream and groundwater changes. In this example the thermal buffering by groundwater is increased both in summer and winter compared to in the current climate. However, if the reverse happens and winter temperatures increase more than summer temperatures, the buffering capacity of groundwater decreases. Furthermore, climate change also leads to changes in cloudiness and humidity, affecting direct solar radiation and latent heat flow and thus both stream and groundwater temperatures (Taylor and Stefan, 2009). We conclude that the effect of climate warming on groundwater temperatures is extremely complex and can have large spatial heterogeneity due to differences in e.g. recharge rates (Kurylyk et al., 2014) and geohydrological settings.

4.6. Implications for groundwater-dependent streams and ecology

The temperature of groundwater is likely to be lower than maximum air temperatures in summer and thus in most climate warming scenarios seepage buffers temperature peaks. In addition, groundwater dominated streams have a lower risk of drying up than other streams and rivers, and are therefore able to support the survival of species during drought. Springs especially, can deliver a thermal signal most related to groundwater towards the stream due to their local high flow velocities, which does not allow much time for downward heat conduction. Groundwater-fed streams are less vulnerable to climate change thanks to these less intense temperature and discharge extremes.

However, the thermal refugia created by groundwater seepage are still threatened by climate warming, as many species living at these locations are more susceptible to changes in temperatures than species that are already adapted to more variable water temperatures (e.g. Hazelwood and Hazelwood, 1985; van den Hoek and Verdonschot, 2001). If future temperatures rise, the input flux of groundwater might not be high enough to ensure the required low temperature certain species need to survive (e.g. Kurylyk et al., 2014). The high groundwater input into the Springendalse Beek allows for the presence of spring and spring stream species (Verdonschot, 1990) and a high amount of rare species (van Walsum et al., 2002). This, together with the high amount of shad-

ing makes this stream a special case especially for the Netherlands and worth protecting.

5. Conclusions

Several measurement techniques were combined with a stream temperature model in order to study the importance of groundwater on the temperature of lowland streams. Using DTS measurements, localized seepage was mapped in two Dutch streams, which was confirmed by sampling of ^{222}Rn. We have seen that groundwater seepage is able to buffer the temperature of stream and provide thermal and climate refugia by lowering maximum temperatures. Seasonality in seepage temperatures can be caused by shallow and fast flow paths from infiltration areas or by heat conduction in seepage zones with slow groundwater velocities. Our measurements suggest that while air temperature and shading generally have a large influence on stream temperature, the presence of significant seepage can be crucial in the occurrence of thermal refugia. The effect of groundwater may be even more important in a warming climate, although this depends on the exact change in air temperature and its seasonality. We conclude that groundwater dominated streams are potentially more climate resilient than streams without a significant contribution from seepage. It seems possible to make use of groundwater in reducing summer temperature maximums, as an alternative or additionally to the creation of (riparian) shading. For instance, reducing the pumping of groundwater can increase groundwater levels and seepage. More research effort is needed on the exact consequence of climate change on the temperature of groundwater and therefore of seepage, as this is still mostly unclear and depends on many (local) factors. We conclude with the statement that groundwater seepage is a crucial factor to include the study and management of lowland stream temperatures and ecology.

Declaration of interests

The authors declared that there is no conflict of interest.

References

Anibas, C., Buis, K., Verhoeven, R., Meire, P., Batelaan, O., 2011. A simple thermal mapping method for seasonal spatial patterns of groundwater-surface water interaction. J. Hydrol. 397, 93–104. https://doi.org/10.1016/j.jhydrol.2010.11.036.

Benoit Bovy, & Geordie McBain. (2017, November 20). benbovy/xarray-simlab: 0.1.1 (Version 0.1.1). Zenodo. https://doi.org/10.5281/zenodo.1063391.

Bense, V.F., Kooi, H., 2004. Temporal and spatial variations of shallow subsurface temperature as a record of lateral variations in groundwater flow. J. Geophys. Res. B: Solid Earth 109, 1–13. https://doi.org/10.1029/2003JB002782.

Bowes, M.J., Loewenthal, M., Read, D.S., Hutchins, M.G., Prudhomme, C., Armstrong, L.K., Harman, S.A., Wickham, H.D., Gozzard, E., Carvalho, L., 2016. Identifying multiple stressor controls on phytoplankton dynamics in the River Thames (UK) using high-frequency water quality data. Sci. Total Environ. 569–570, 1489–1499. https://doi.org/10.1016/j.scitotenv.2016.06.239.

Boyd, M., Kasper, B., 2003. Analytical methods for dynamic open channel heat and mass transfer: methodology for the heat source. Model Version 7, 204.

Briggs, M.A., Johnson, Z.C., Snyder, C.D., Hitt, N.P., Kurylyk, B.L., Lautz, L., Irvine, D.J., Hurley, S.T., Lane, J.W., 2018a. Inferring watershed hydraulics and cold-water habitat persistence using multi-year air and stream temperature signals. Sci. Total Environ. 636, 1117–1127. https://doi.org/10.1016/j.scitotenv.2018.04.344.

Briggs, M.A., Lane, J.W., Snyder, C.D., White, E.A., Johnson, Z.C., Nelms, D.L., Hitt, N.P., 2018b. Shallow bedrock limits groundwater seepage-based headwater climate refugia. Limnologica 68, 142–156. https://doi.org/10.1016/j.limno.2017.02.005.

Briggs, M.A., Lautz, L.K., McKenzie, J.M., Gordon, R.P., Hare, D.K., 2012. Using high-resolution distributed temperature sensing to quantify spatial and temporal variability in vertical hyporheic flux. Water Resour. Res. 48, 1–16. https://doi.org/10.1029/2011WR011227.

Caissie, D., Luce, C., 2017. Quantifying streambed advection and conduction heat fluxes. Water Resour. Res. 53, 1595–1624. https://doi.org/10.1002/2016WR019813.

Cartwright, I., Hofmann, H., Gilfedder, B., Smyth, B., 2014. Understanding parafluvial exchange and degassing to better quantify groundwater inflows using ^{222}Rn: the King River, southeast Australia. Chem. Geol. 380, 48–60. https://doi.org/10.1016/j.chemgeo.2014.04.009.

Cook, P.G., 2013. Estimating groundwater discharge to rivers from river chemistry surveys. Hydrol. Process. 27, 3694–3707. https://doi.org/10.1002/hyp.9493.

Cook, P.G., Lamontagne, S., Berhane, D., Clark, J.F., 2006. Quantifying groundwater discharge to Cockburn River, southeastern Australia, using dissolved gas tracers 222Rn and SF6. Water Resour. Res. 42. https://doi.org/10.1029/2006WR004921.

de Louw, P.G.B., Oude Essink, G.H.P., Stuyfzand, P.J., van der Zee, S.E.A.T.M., 2010. Upward groundwater flow in boils as the dominant mechanism of salinization in deep polders, The Netherlands. J. Hydrol. 394, 494–506. https://doi.org/10.1016/j.jhydrol.2010.10.009.

Dimova, N.T., Burnett, W.C., Chanton, J.P., Elizabeth, J., 2013. Application of radon-222 to investigate groundwater discharge into small shallow lakes. J. Hydrol. 486, 112–122. https://doi.org/10.1016/j.jhydrol.2013.01.043.

Dugdale, S.J., Malcolm, I.A., Kantola, K., Hannah, D.M., 2018. Stream temperature under contrasting riparian forest cover: understanding thermal dynamics and heat exchange processes. Sci. Total Environ. 610–611, 1375–1389. https://doi.org/10.1016/j.scitotenv.2017.08.198.

Dujardin, J., Anibas, C., Bronders, J., Jamin, P., Hamonts, K., Dejonghe, W., Brouyère, S., Batelaan, O., 2014. Combining flux estimation techniques to improve characterization of groundwater–surface-water interaction in the Zenne River, Belgium. Hydrogeol. J. 1657–1668. https://doi.org/10.1007/s10040-014-1159-4.

Dulaiova, H., Burnett, W.C., 2006. Radon loss across the water-air interface (Gulf of Thailand) estimated, 33, 1–4. https://doi.org/10.1029/2005GL025023.

Eaton, J.G., Scheller, R.M., 1996. Effects of climate warming on fish thermal habitat in streams of the United States. Limnol. Oceanogr. 41, 1109–1115. https://doi.org/10.4319/lo.1996.41.5.1109.

Emerson, S., Broecker, W., 1973. Gas-exchange rates in a small lake as determined by the radon method. J. Fish. Res. Board Canada 30, 1475–1484.

Garner, G., Malcolm, I.A., Sadler, J.P., Hannah, D.M., 2017. The role of riparian vegetation density, channel orientation and water velocity in determining river temperature dynamics. J. Hydrol. 553, 471–485. https://doi.org/10.1016/j.jhydrol.2017.03.024.

Garner, G., Malcolm, I.A., Sadler, J.P., Hannah, D.M., 2014. What causes cooling water temperature gradients in a forested stream reach? Hydrol. Earth Syst. Sci. 18, 5361–5376. https://doi.org/10.5194/hess-18-5361-2014.

Genereux, D.P., Hemond, H.F., 1992. Determination of gas exchange rate constants for a small stream on walker branch watershed, Tennessee. Water Resour. Res. 28, 2365–2374.

Genereux, D.P., Hemond, H.F., 1990. Naturally occurring radon 222 as a tracer for streamflow generation: steady state methodology and field Example. Water Resour. Res. 26, 3065–3075. https://doi.org/10.1029/WR026i012p03065.

Gilmore, T.E., Genereux, D.P., Solomon, D.K., Solder, J.E., 2016. Groundwater transit time distribution and mean from streambed sampling in an agricultural coastal plain watershed, North Carolina, USA. Water Resour. Res., 2025–2044 https://doi.org/10.1002/2015WR017600.Received.

Guse, B., Kail, J., Radinger, J., Schröder, M., Kiesel, J., Hering, D., Wolter, C.F., Fohrer, N., 2015. Eco-hydrologic model cascades: Simulating land use and climate change impacts on hydrology, hydraulics and habitats for fish and macroinvertebrates. Sci. Total Environ. 533, 542–556. https://doi.org/10.1016/j.scitotenv.2015.05.078.

Haidekker, A., Hering, D., 2008. Relationship between benthic insects (Ephemeroptera, Plecoptera, Coleoptera, Trichoptera) and temperature in small and medium-sized streams in Germany: a multivariate study. Aquat. Ecol. 42, 463–481. https://doi.org/10.1007/s10452-007-9097-z.

Hannah, D.M., Malcolm, I.A., Soulsby, C., Youngson, A.F., 2008. A comparison of forest and moorland stream microclimate, heat exchanges and thermal dynamics. Hydrol. Process. 22, 919–940. https://doi.org/10.1002/hyp.

Hare, D.K., Briggs, M.A., Rosenberry, D.O., Boutt, D.F., Lane, J.W., 2015. A comparison of thermal infrared to fiber-optic distributed temperature sensing for evaluation of groundwater discharge to surface water. J. Hydrol. 530, 153–166. https://doi.org/10.1016/j.jhydrol.2015.09.059.

Harrington, J.S., Hayashi, M., Kurylyk, B.L., 2017. Influence of a rock glacier spring on the stream energy budget and cold - water refuge in an alpine stream. Hydrol. Process. 31, 4719–4733. https://doi.org/10.1002/hyp.11391.

Hausner, M.B., Suarez, F., Glander, K.E., Van De Giesen, N.C., Selker, J.S., Tyler, S.W., 2011. Calibrating single-ended fiber-optic raman spectra distributed temperature sensing data. Sensors 11, 10859–10879. https://doi.org/10.3390/s111110859.

Hawkins, C.P., Hogue, J.N., Decker, L.M., Feminella, J.W., 1997. Channel Morphology, Water Temperature, and Assemblage Structure of Stream Insects.

Hayashi, M., Rosenberry, D.O., 2002. Effects of ground water exchange on the hydrology and ecology of surface water. Ground Water 40, 309–316.

Hazelwood, D.H., Hazelwood, S.E., 1985. The effect of temperature on oxygen consumption in four species of freshwater fairy shrimp Crustacea Anostraca. Freshw. Invertebr. Biol. 4, 133–137.

Hilgersom, K.P., Van De Giesen, N.C., de Louw, P.G.B., Zijlema, M., 2016. Three-dimensional dense distributed temperature sensing for measuring layered thermohaline systems. Water Resour. Res. 52, 6656–6670. https://doi.org/10.1029/2008WR006912.M.

Irvine, D.J., Briggs, M.A., Lautz, L.K., Gordon, R.P., Mckenzie, J.M., 2017. Using diurnal temperature signals to infer vertical groundwater-surface water exchange. Ground Water 55, 10–26. https://doi.org/10.1111/gwat.12459.

Isaak, D.J., Luce, C., Horan, D.L., Chandler, G.L., Wollrab, S.P., Nagel, D.E., 2018. Global warming of salmon and trout Rivers in the Northwestern U. S.: road to ruin or path through purgatory? 566–587. https://doi.org/10.1002/tafs.10059.

Isaak, D.J., Young, M.K., Nagel, D.E., Horan, D.L., Groce, M.C., 2015. The cold-water climate shield: Delineating refugia for preserving salmonid fishes through the 21st century. Global Change Biol. 21, 2540–2553. https://doi.org/10.1111/gcb.12879.

Kaandorp, V.P., de Louw, P.G.B., van der Velde, Y., Broers, H.P., 2018a. Transient groundwater travel time distributions and age-ranked storage-discharge relationships of three lowland catchments. Water Resour. Res. 1–18. https://doi.org/10.1029/2017WR022461.

Kaandorp, V.P., Molina-Navarro, E., Andersen, H.E., Bloomfield, J.P., Kuijper, M.J.M., de Louw, P.G.B., 2018b. A conceptual model for the analysis of multi-stressors in linked groundwater–surface water systems. Sci. Total Environ. 627, 880–895. https://doi.org/10.1016/j.scitotenv.2018.01.259.

Karan, S., Sebok, E., Engesgaard, P., 2017. Air/water/sediment temperature contrasts in small streams to identify groundwater seepage locations. Hydrol. Process. 31, 1258–1270. https://doi.org/10.1002/hyp.11094.

Kennedy, C.D., Genereux, D.P., Corbett, D.R., Mitasova, H., 2009. Spatial and temporal dynamics of coupled groundwater and nitrogen fluxes through a streambed in an agricultural watershed. Water Resour. Res. 45, 1–18. https://doi.org/10.1029/2008WR007397.

Krause, S., Blume, T., Cassidy, N.J., 2012. Investigating patterns and controls of groundwater up-welling in a lowland river by combining Fibre-optic Distributed Temperature Sensing with observations of vertical hydraulic gradients. Hydrol. Earth Syst. Sci. 16, 1775–1792. https://doi.org/10.5194/hess-16-1775-2012.

Kristensen, P.B., Kristensen, E.A., Riis, T., Alnoee, A.B., Larsen, S.E., Vervier, P., Baattrup-Pedersen, A., 2015. Riparian forest as a management tool for moderating future thermal conditions of lowland temperate streams. Inl. Waters 5, 27–38. https://doi.org/10.5268/IW-5.1.751.

Kurylyk, B.L., MacQuarrie, K.T.B., Caissie, D., McKenzie, J.M., 2015. Shallow groundwater thermal sensitivity to climate change and land cover disturbances: derivation of analytical expressions and implications for stream temperature modeling. Hydrol. Earth Syst. Sci. 19, 2469–2489. https://doi.org/10.5194/hess-19-2469-2015.

Kurylyk, B.L., MacQuarrie, K.T.B., Voss, C.I., 2014. Climate change impacts on the temperature and magnitude of groundwater discharge from shallow, unconfined aquifers. Water Resour. Res. 50, 3253–3274. https://doi.org/10.1002/2013WR014588.

Kurylyk, B.L., Moore, R.D., Macquarrie, K.T.B., 2016. Scientific briefing: quantifying streambed heat advection associated with groundwater – surface water interactions. Hydrol. Process. 30, 987–992. https://doi.org/10.1002/hyp.10709.

Kurylyk, B.L., Bourque, C.P.-A., Macquarrie, K.T.B., 2013. Potential surface temperature and shallow groundwater temperature response to climate change: an example from a small forested catchment in east-central NB

(Canada). Hydrol. Earth Syst. Sci. 17, 2701–2716. https://doi.org/10.5194/hess-17-2701-2013.

Kwakman, J.F.M., Versteegh, P.J.M., 2016. Radon-222 in ground water and finished drinking water in the Dutch provinces Overijssel and Limburg. Bilthoven.

Lowry, C.S., Walker, J.F., Hunt, R.J., Anderson, M.P., 2007. Identifying spatial variability of groundwater discharge in a wetland stream using a distributed temperature sensor. Water Resour. Res. 43. https://doi.org/10.1029/2007WR006145.

Macdonald, R.J., Boon, S., Byrne, J.M., Silins, U., 2014. A comparison of surface and subsurface controls on summer temperature in a headwater stream. Hydrol. Process. 28, 2338–2347. https://doi.org/10.1002/hyp.9756.

Matheswaran, K., Blemmer, M., Rosbjerg, D., Boegh, E., 2014a. Seasonal variations in groundwater upwelling zones in a Danish lowland stream analyzed using Distributed Temperature Sensing (DTS). Hydrol. Process. 28, 1422–1435. https://doi.org/10.1002/hyp.9690.

Matheswaran, K., Blemmer, M., Thorn, P., Rosbjerg, D., Boegh, E., 2014b. Investigation of stream temperature response to non-uniform groundwater discharge in a Danish lowland stream. River Res. Appl. https://doi.org/10.1002/rra.2792.

Meisner, J.D., Rosenfeld, J.S., Regier, H.A., 1988. The role of groundwater in the impact of climate warming on stream salmonines. Fisheries 13, 2–8. https://doi.org/10.1577/1548-8446(1988)013<0002:TROGIT>2.0.CO;2.

Menberg, K., Blum, P., Kurylyk, B.L., Bayer, P., 2014. Observed groundwater temperature response to recent climate change. Hydrol. Earth Syst. Sci. 18, 4453–4466. https://doi.org/10.5194/hess-18-4453-2014.

Monteith, J.L., 1981. Evaporation and surface temperature. Quart. J. R. Meteorol. Soc. 107, 1–27.

Moss, B., Mckee, D., Atkinson, D., Collings, S.E., Eaton, J.W., Gill, A.B., Harvey, I., Hatton, K., Heyes, T., Wilson, D., 2003. How important is climate? Effects of warming, nutrient addition and fish on phytoplankton in shallow lake microcosms. J. Appl. Ecol. 40, 782–792. https://doi.org/10.1046/j.1365-2664.2003.00839.x.

Nash, C.S., Selker, J.S., Grant, G.E., Lewis, S.L., Noël, P., 2018. A physical framework for evaluating net effects of wet meadow restoration on late-summer streamflow. Ecohydrology 11. https://doi.org/10.1002/eco.1953.

Neilson, B.T., Hatch, C.E., Ban, H., Tyler, S.W., 2010. Solar radiative heating of fiber-optic cables used to monitor temperatures in water. Water Resour. Res. 46, 1–17. https://doi.org/10.1029/2009WR008354.

Null, S.E., Viers, J.H., Deas, M.L., Tanaka, S.K., Mount, J.F., 2012. Stream temperature sensitivity to climate warming in California's Sierra Nevada: impacts to coldwater habitat. Clim. Change 116, 149–170. https://doi.org/10.1007/s10584-012-0459-8.

Ormerod, S.J., 2009. Climate change, river conservation and the adaptation challenge. Aquat. Conserv. Mar. Freshwater Ecosyst. 613, 609–613. https://doi.org/10.1002/aqc.

Piggott, J.J., Townsend, C.R., Matthaei, C.D., 2015. Climate warming and agricultural stressors interact to determine stream macroinvertebrate community dynamics. Global Change Biol. 21, 1887–1906. https://doi.org/10.1111/gcb.12861.

Poole, G.C., Berman, C.H., 2001. An ecological perspective on in-stream temperature: natural heat dynamics and mechanisms of human-caused thermal degradation. Environ. Manage. 27, 787–802. https://doi.org/10.1007/s002670010188.

Poulsen, J.R., Sebok, E., Duque, C., Tetzlaff, D., Engesgaard, P.K., 2015. Detecting groundwater discharge dynamics from point-to-catchment scale in a lowland stream: combining hydraulic and tracer methods. Hydrol. Earth Syst. Sci. 19, 1871–1886. https://doi.org/10.5194/hess-19-1871-2015.

Power, G., Brown, R.S., Imhof, J.G., 1999. Groundwater and fish – insights from northern North America. Hydrol. Process. 422, 401–422.

Rasmussen, J.J., Baattrup-Pedersen, A., Riis, T., Friberg, N., 2011. Stream ecosystem properties and processes along a temperature gradient. Aquat. Ecol. 45, 231–242. https://doi.org/10.1007/s10452-010-9349-1.

Rau, G.C., Andersen, M.S., Acworth, R.I., 2012. Experimental investigation of the thermal dispersivity term and its significance in the heat transport equation for flow in sediments. Water Resour. Res. 48, 1–21. https://doi.org/10.1029/2011WR011038.

Rosenberry, D.O., Briggs, M.A., Delin, G., Hare, D.K., 2016. Combined use of thermal methods and seepage meters to efficiently locate, quantify, and monitor focused groundwater discharge to a sand-bed stream. Water Resour. Res. 52, 4486–4503. https://doi.org/10.1002/2016WR018808.

Schülting, L., Feld, C.K., Graf, W., 2016. Effects of hydro- and thermopeaking on benthic macroinvertebrate drift. Sci. Total Environ. https://doi.org/10.1016/j.scitotenv.2016.08.022.

Sebok, E., Duque, C., Engesgaard, P., Boegh, E., 2015. Application of distributed temperature sensing for coupled mapping of sedimentation processes and spatio-temporal variability of groundwater discharge in soft-bedded streams. Hydrol. Process. 29, 3408–3422. https://doi.org/10.1002/hyp.10455.

Sebok, E., Duque, C., Kazmierczak, J., Engesgaard, P.K., Nilsson, B., Karan, S., Frandsen, M., 2013. High-resolution distributed temperature sensing to detect seasonal groundwater discharge into Lake Vaeng. Denmark. Water Resour. Res. 49, 5355–5368. https://doi.org/10.1002/wrcr.20436.

Selker, J.S., Thévenaz, L., Huwald, H., Mallet, A., Luxemburg, W., Van De Giesen, N.C., Stejskal, M., Zeman, J., Westhoff, M.C., Parlange, M.B., 2006. Distributed fiber-optic temperature sensing for hydrologic systems. Water Resour. Res. 42, 1–8. https://doi.org/10.1029/2006WR005326.

Sweeney, B.W., Newbold, J.D., 2014. Streamside forest buffer width needed to protect stream water quality, habitat, and organisms: a literature review. J. Am. Water Resour. Assoc. 50, 560–584. https://doi.org/10.1111/jawr.12203.

Taylor, C.A., Stefan, H.G., 2009. Shallow groundwater temperature response to climate change and urbanization. J. Hydrol. 375, 601–612. https://doi.org/10.1016/j.jhydrol.2009.07.009.

Thomas, S.M., Griffiths, S.W., Ormerod, S.J., 2015. Adapting streams for climate change using riparian broadleaf trees and its consequences for stream salmonids. Freshw. Biol. 60, 64–77. https://doi.org/10.1111/fwb.12467.

Van De Giesen, N.C., Steele-Dunne, S.C., Jansen, J., Hoes, O., Hausner, M.B., Tyler, S.W., Selker, J.S., 2012. Double-ended calibration of fiber-optic raman spectra distributed temperature sensing data. Sensors (Switzerland) 12, 5471–5485. https://doi.org/10.3390/s120505471.

van den Hoek, T.H., Verdonschot, P.F.M., 2001. De invloed van veranderingen in temperatuur op beek- macrofauna. Wageningen.

van der Aa, N.G.F.M., Goes, B.J.M., de Louw, P.G.B., den Otter, C., Reckman, J.W.T.M., Stuurman, R.J., 1999. Ecohydrologische Systeemanalyse. Springendalse Beek, Delft.

van Ommen, H.C., 1986. Influence of diffuse sources of contamination on the quality of outflowing groundwater including non-equilibrium adsorption and decomposition. J. Hydrol. 88, 79–95.

Van Vliet, M.T.H., Franssen, W.H.P., Yearsley, J.R., Ludwig, F., Haddeland, I., Lettenmaier, D.P., Kabat, P., 2013. Global river discharge and water temperature under climate change. Glob. Environ. Chang. 23, 450–464. https://doi.org/10.1016/j.gloenvcha.2012.11.002.

van Walsum, P.E.V., Verdonschot, P.F.M., Runhaar, J., 2002. Effects of climate and land-use change on lowland stream ecosystems. Wageningen.

Vandenbohede, A., de Louw, P.G.B., Doornenbal, P.J., 2014. Characterizing preferential groundwater discharge through boils using temperature. J. Hydrol. 510, 372–384. https://doi.org/10.1016/j.jhydrol.2014.01.006.

Vannote, R.L., Sweeney, B.W., 1980. Geographic analysis of thermal equilibria: a conceptual model for evaluating the effect of natural and modified thermal regimes on aquatic insect communities 115, 667–695.

Verdonschot, P.F.M., 1990. Ecological characterization of surface waters in the province of Overijssel, The Netherlands. Thesis 255.

Wallin, M.B., Öquist, M.G., Buffam, I., Billett, M.F., Nisell, J., Bishop, K.H., 2011. Spatiotemporal variability of the gas transfer coefficient (K CO$_2$) in boreal streams: Implications for large scale estimates of CO$_2$ evasion. Glob. Biochem. Cycles 25, 1–14. https://doi.org/10.1029/2010GB003975.

Ward, J. V., Stanford, J.A., 1982. Evolutionary Ecology of Aquatic Insects, 97–117.

Watts, G., Battarbee, R.W., Bloomfield, J.P., Crossman, J., Daccache, A., Durance, I., Elliott, J.A., Garner, G., Hannaford, J., Hannah, D.M., Hess, T., Jackson, C.R., Kay, A.L., Kernan, M., Knox, J., Mackay, J., Monteith, D.T., Ormerod, S.J., Rance, J., Stuart, M.E., Wade, A.J., Wade, S.D., Weatherhead, K., Whitehead, P.G., Wilby, R.L., 2015. Climate change and water in the UK – past changes and future prospects. Prog. Phys. Geogr. 39, 6–28. https://doi.org/10.1177/0309133314542957.

Webb, B.W., Nobilis, F., 2007. Long-term changes in river temperature and the influence of climatic and hydrological factors. Hydrol. Sci. J. 52, 74–85. https://doi.org/10.1623/hysj.52.1.74.

Westhoff, M.C., Bogaard, T.A., Savenije, H.H.G., 2011. Quantifying spatial and temporal discharge dynamics of an event in a first order stream, using distributed temperature sensing. Hydrol. Earth Syst. Sci. 15, 1945–1957. https://doi.org/10.5194/hess-15-1945-2011.

Westhoff, M.C., Savenije, H.H.G., Luxemburg, W.M.J., Stelling, G.S., Van De, N.C., Selker, J.S., Pfister, L., Uhlenbrook, S., 2007. A distributed stream temperature model using high resolution temperature observations. Hydrol. Earth Syst. Sci. 11, 1469–1480.

Yu, L. Rozemeijer, J.C., van der Velde, Y., van Breukelen, B.M., Ouboter, M., Broers, H.P., 2019. Urban hydrogeology: transport routes and mixing of water and solutes in a groundwater influenced urban lowland catchment. Manuscript submitted for publication.

Ylla, I., Canhoto, C., Romaní, A.M., 2014. Effects of warming on stream biofilm organic matter use capabilities. Microb. Ecol. 68, 132–145. https://doi.org/10.1007/s00248-014-0406-5.

Zappa, C.J., Raymond, P.A., Terray, E.A., McGillis, W.R., 2003. Variation in surface turbulence and the gas transfer velocity over a tidal cycle in a macro-tidal estuary. Estuaries 26, 1401–1415.